EVALUATION OF THE IMPACT OF URBAN SPRAWL DYNAMICS ON ECOSYSTEM SERVICES IN SELECTED METROPOLITAN AREAS IN TOGO AND GHANA

By

TOSSOUKPE, Adjowa Yéwa
PhD/SPS/FT/2021/13010

WEST AFRICAN SCIENCE SERVICE CENTRE ON
CLIMATE CHANGE AND ADAPTED LAND USE
CLIMATE CHANGE AND HUMAN HABITAT
FEDERAL UNIVERSITY OF TECHNOLOGY
MINNA

JULY, 2025

EVALUATION OF THE IMPACT OF URBAN SPRAWL DYNAMICS ON ECOSYSTEM SERVICES IN SELECTED METROPOLITAN AREAS IN TOGO AND GHANA

By

TOSSOUKPE, Adjowa Yéwa
PhD/SPS/FT/2021/13010

A THESIS SUBMITTED TO THE POSTGRADUATE SCHOOL, FEDERAL UNIVERSITY OF TECHNOLOGY, MINNA, NIGERIA IN PARTIAL FULFILMENT OF THE REQUIREMENTS FOR THE AWARD OF THE DEGREE OF DOCTOR OF PHILOSOPHY (PhD) IN CLIMATE CHANGE AND HUMAN HABITAT

JULY, 2025

DECLARATION

I hereby declare that this thesis titled: "**Evaluation of the impact of urban sprawl dynamics on ecosystem services in selected metropolitan areas in Togo and Ghana**" is a collection of my original research work and it has not been presented for any other qualification anywhere. Information from other sources (published or unpublished) has been duly acknowledged.

TOSSOUKPE Adjowa Yéwa
PhD/SPS/FT/2021/13010
Federal University of Technology Minna,
Niger State

Signature/Date

CERTIFICATION

The thesis, titled: "**Evaluation of the impact of urban sprawl dynamics on ecosystem services in selected metropolitan areas in Togo and Ghana**" by: Adjowa Yéwa TOSSOUKPE (PhD/SPS/FT/2021/13010) meets the regulations governing the awards of the degree of PhD of the Federal University of Technology, Minna and it is approved for its contribution to scientific knowledge and literary presentation.

PROF. J. J. DUKIYA ---------------------------
Major Supervisor Signature & Date

DR. FOUSSENI FOLEGA ------14/11/2025---------
Co-Supervisor Signature & Date

DR. MICHAEL THIEL ------14/11/2025---------
Co-Supervisor Signature & Date

PROF. A. A. OKHIMAMHE ----------------------------
DIRECTOR OF WASCAL, Signature & Date
CLIMATE CHANGE & HUMAN HABITAT

PROF. A. N. SAIDU ----------------------------
DEAN OF POSTGRADUATE SCHOOL Signature & Date

DEDICATION

I dedicated this work to the loving memory of my late father Mr. TOSSOUKPE Yawo Kasségné Imorou, whose unwavering support, encouragement, and wisdom have been a guiding light throughout my life. His strength and values continue to inspire me every day. Though he is no longer here, his presence remains deeply felt in every step of this journey.

ACKNOWLEDGMENTS

I would like to express my deepest gratitude to God almighty for his guidance and protection throughout this journey. Despite the many challenges I encountered, His presence has been a source of strength and inspiration, enabling me to persevere and overcome obstacles.

My sincere gratitude goes to the German Federal Ministry of Education and Research (BMBF) for providing the scholarship through the West African Science Service Centre on Climate Change and Adapted Land Use (WASCAL). This support enabled the successful completion of this research. I'm profoundly thankful to my supervisors, Prof. Jaiye Dukiya, Dr. Fousseni Folega and Dr. Michael Thiel. Their expert guidance, insightful feedback, and constant support have been valuable in shaping this work. Your encouragement and belief in my abilities motivated me to strive for excellence and I'm truly grateful for your mentorship.

I would also like to extend my heartfelt appreciation to Prof. Appollonia Aimiosino Okhimamhe, the director of WASCAL CC&HH, for her dedication to fostering an enriching academic environment and her commitment to students' success, which has greatly enhanced my educational experience. Her inspiring leadership truly makes a difference. I would also like to thank the staff of WASCAL CC & HH for their dedication and assistance.

To my internal reviewers, I extend my heartfelt thanks for the time you dedicated to evaluating this work and for your valuable input, which has greatly contributed to its improvement.

I would like to express my sincere appreciation to Prof. Daouda Kone, Director of WASCAL Capacity Building, Mrs. Selasi A. Weto, and Prof. Benjamin Lamptey for their assistance during my data collection in Greater Accra, Ghana. Your support has been instrumental in the success of my research, and I am deeply thankful for your contributions.

I would like also like to sincerely thank the Earth Observation Research Cluster at the Institute of Geography and Geology, University of Würzburg, Germany, for their technical support.

To my dear Dr. Saratu Usman Ibrahim, former Deputy Director of WASCAL CC&HH, thank you for your motherly love and care that you have shown me throughout my journey. Your support has been invaluable, and I am truly grateful for your guidance.

Additionally, I wish to express my gratitude to Prof. Komi Agboka and staff members of WASCAL Togo for your support and encouragement that have made a significant impact on my academic journey.

I would also like to extend my heartfelt thanks to Dr. kossi B. Amegnaglo, Dr. Badabate Diwediga, and Dr. Leonard K. M. Agbodan for their invaluable guidance and support throughout my research, may God bless you all.

To my amazing and tireless mother, Mrs. Dare Davi, thank you for your unconditional love and support. Your sacrifices and encouragement have been the foundation of my achievements. I am eternally grateful for the values you instilled in me and for always believing in my potential. I would also like to express my gratitude to my siblings, especially my brother Marc Tossoukpe, and my sister Modoukpe Tossoukpe, for their constant support and encouragement.

I would like to extend my heartfelt gratitude to Mr. Stéphane Attigossou for his constant presence and support. I am truly grateful. May God bless you and your family.

My sincere appreciation goes to Mr. Biova Hounou and his wife, Mrs. Obidon Gadzezo, for their selfless assistance during my data collection in Greater Accra, Ghana. I also wish to express my gratitude to Dr. Essossimna Magamana and Mr. Kobadega Samah for their encouragement throughout this journey.

Finally, I wish to acknowledge all my colleagues, and everyone who has contributed to this journey. Your kindness, support, and constructive feedback have been valuable. Thank you all from the bottom of my heart.

ABSTRACT

Urbanisation and population growth in West Africa have led to significant changes in land use and land cover (LULC), raising environmental concerns. In view of this, the study evaluated the impact of urban sprawl on ecosystem services in the District Autonome du Grand Lome (DAGL) and Greater Accra Metropolitan Area (GAMA) from 1986 to 2023 and from 1991 to 2023 respectively, using geospatial techniques; the Google Earth Engine platform and InVEST model. The findings indicate a decline in the verdant landscape, with forested areas in DAGL declined from 24 % in 1986 to 3 % by 2023, and from 34 % in 1991 to 2 % in 2023 in GAMA. Grasslands also saw significant reductions, while built up areas expanded dramatically rising from 18 % to 62 % in DAGL and from 10 % to 70 % in GAMA. The Urban Expansion Intensity Index (UEII) reflects rapid urban growth, with DAGL at 1.19 % and GAMA at 1.88 %. Directional analyses revealed that urban expansion predominantly occurs towards the north-west in DAGL and both north-east and north-west in GAMA. In DAGL the total carbon storage significantly declined from 3,604,852 Mg of C in 1986 to 1,367,113 Mg of C by 2023. The most substantial loss in carbon storage was between 2001 and 2015. Similarly, in the GAMA, carbon storage dropped from 16,574,522 Mg of C in 1991 to 4,120,702 Mg of C by 2023, with major decrease between 2002 and 2017. More so, in DAGL, the runoff retention index has remained low, fluctuating between 2.00 % in 1986 and 2.43 % in 2001, before dropping to 2.01 % by 2023 with total runoff retention decreasing from 29,098,483 m³ in 1986 to 17,908,270 m³ in 2023. In contrast, in GAMA region had a higher runoff retention index of 14.75 % in 1991, and decreased to 9.66 % by 2023. Despite this initial advantage, total runoff retention also declined significantly from 85,027,128 m³ in 1991 to 57,500,096 m³ in 2023. The study also revealed a decrease in cooling capacity from 0.60 % in 2001 to 0.30 % in 2023 in DAGL with direct correlation with the average temperature increase from 26°C in 2001 to 29.5°C in 2023. In the same vein, cooling capacity declined from 0.65 % in 2002 to 0.25 % in 2023 in GAMA with average temperatures rising from 25.5°C in 2002 to 29.0°C in 2023. Going by all these negative impacts of urban sprawl in both cities, it is therefore recommended that vertical and mixed land use development with integrated ecological preservation approaches, should take pre-eminence over horizontal development to achieve eco-development and more resilient urban future.

TABLE OF CONTENTS

Title Page		i
Declaration		ii
Certification		iii
Dedication		iv
Acknowledgments		v
Abstract		viii
Table of Contents		ix
List of Tables		xiv
List of Figures		xvii
List of Appendices		xix
List of Abbreviations		xx
CHAPTER ONE		**1**
1.0	**INTRODUCTION**	**1**
1.1	Background to the Study	1
1.2	Statement of the Research Problem	3
1.3	Aim and Objectives of the Study	4
1.4	Justification for the Study	5
1.6	Scope and Limitation	7
1.6.1	Scope of the study	7

1.6.2 Limitation of the study 8

CHAPTER TWO **9**

2.0 LITERATURE REVIEW **9**

2.1 Conceptual Framework 9

2.1.1 Ecosystem Services (ESs) 9

2.1.2 Urban sustainability framework (USF) 10

2.1.3 Millennium ecosystem assessment framework 11

2.1.4 Common International Classification of Ecosystem Services (CICES) 12

2.2 Theoretical Framework 13

2.2.1 Concentric zone theory 13

2.2.3 Urban ecological footprints 14

2.3 Review of Related Studies 15

2.3.1 Drivers of urban expansion 15

2.3.2 Urban development dynamics and ecosystem services 17

2.3.2.1 Google earth engine (GEE) in environmental monitoring 18

2.3.2.2 The random forest (RF) classifier 20

2.3.3 Ecosystem services distribution and analysis for sustainable city planning and planning and development 21

2.3.3.1 Different models for ecosystem services analyses 22

2.3.3.2 Environmental challenges in DAGL 24

2.3.3.3	*Environmental challenges in GAMA*	25
2.3.4	Relationship between urban Sprawl, metropolitan city development, and Ecosystem Services	27
2.3.5	Examples from other regions / countries	29
2.3.6	The Overview and key issues of the study	31
2.3.6.1	*Overview*	31
2.3.6.2	*Discussion of the key issues*	32
CHAPTER THREE		**35**
3.0	**MATERIALS AND METHODS**	**35**
1.5	Description of the Study Area	35
1.5.1	Study location and it's environment	35
1.5.2	Climate	36
1.5.3	Soil, vegetation and hydrology	37
1.5.4	Population trend	39
1.5.5	Socio-economic activities	41
3.1	Materials	42
3.1.1	Data type	42
3.1.1.1	*Remote sensing data*	42
3.1.1.2	*Ground data*	43
3.1.1.3	*Climate data*	43

3.1.1.4	*Data from literature*	44
3.2	Methods	44
3.2.1	Spatial and temporal changes in the sprawl of urban areas and change in LULC in DAGL and GAMA	44
3.2.1.1	*Land cover mapping*	44
3.2.1.2	*Urban expansion analysis*	50
3.2.1.3	*Urban sprawl quantification*	51
3.2.2	Distribution and variation in the provision of selected ecosystem services in DAGL and GAMA	52
3.2.2.1	*Structure of the model*	52
3.2.2.2	*Model description*	53
3.2.3	Evaluate the relationship between urban expansion and ecosystem service degradation in DAGL and GAMA	59
CHAPTER FOUR		**61**
4.0	**RESULTS AND DISCUSSION**	**61**
4.1	Results	61
4.1.1	Spatial and temporal changes in the sprawl of urban areas and the change in land use and land cover in DAGL and GAMA	61
4.1.1.1	*Land use and land cover (LULC) change in the metropolitan areas*	61
4.1.1.2	*Accuracy assessment*	72
4.1.1.3	*Urban expansion dynamics and sprawl*	74

4.1.2	Distribution and variation in the provision of selected ecosystem services in DAGL and GAMA	85
4.1.2.1	*Carbon storage and sequestration analysis*	85
4.1.2.1	*Urban cooling and heat mitigation*	90
4.1.2.1	*Flood risk mitigation*	92
4.1.3	Relationship between urban expansion and ecosystem service provision in the selected metropolitan areas DAGL and GAMA	94
4.1.3.1	*Pearson correlation*	94
4.1.3.2	*Geographical weighted regression (GWR)*	96
4.2	Discussion	101
4.3	Major Findings	109
CHAPTER FIVE		**110**
5.0	**CONCLUSION AND RECOMMENDATIONS**	**110**
5.1	Conclusion	110
5.2	Recommendations	111
5.2.1	Recommendations on policy improvement	111
5.2.2	Recommendations on performance improvement	112
5.3	Contributions to Knowledge	113
REFERENCES		**114**
APPENDICES		**130**

LIST OF TABLES

Table		Page
2.1	Description of ESs categorised based on CICES classification	13
3.1	Populations and population density in DAGL and GAMA	40
3.2	Summary of the remote sensing dataset used for land use and land cover mapping in the study	43
3.3	Description of land use and land cover classes	47
3.4	Carbon pool table for DAGL	55
3.5	Carbon pool table for GAMA	55
4.1	Land use and land cover transition matrix from 1986 to 2001 in DAGL in percentage	64
4.2	Land use and land cover transition matrix from 2001 to 2015 in DAGL in percentage	64
4.3	Land use and land cover transition matrix from 2015 to 2023 in DAGL in percentage	65
4.4	Area coverage, Absolute change and Average annual rate of change for DAGL	67
4.5	Land use and land cover transition matrix from 1991 to 2002 in GAMA in percentage	68
4.6	Land use and land cover transition matrix from 2002 to 2017 in GAMA in percentage	69
4.7	Land use and land cover transition matrix from 2017 to 2023 in GAMA in percentage	69

4.8 Area coverage, Absolute change and Annual rate of change for GAMA 71

4.9 Accuracy assessment of different years for DAGL 73

4.10 Accuracy assessment of different years for GAMA 74

4.11 The built-up area in different quadrants-wise direction and UEII value from 1986 to 2023 in DAGL 77

4.12 The built-up area in different quadrants-wise direction and UEII value from 1991 to 2023 in GAMA 79

4.13 Built-up area coverage per buffer per direction in DAGL in 1986 80

4.14 Built-up area coverage per buffer per direction in DAGL in 2001 80

4.15 Built-up area coverage per buffer per direction in DAGL in 2015 81

4.16 Built-up area coverage per buffer per direction in DAGL in 2023 81

4.17 Built-up area coverage per buffer per direction in GAMA in 1991 82

4.18 Built-up area coverage per buffer per direction in GAMA in 2002 82

4.19 Built-up area coverage per buffer per direction in GAMAin 2017 83

4.20 Built-up area coverage per buffer per direction in GAMA in 2023 84

4.21 Carbon stored and sequestered in DAGL and GAMA and carbon stored per LULC type 88

4.22 Average cooling capacity and average temperature over DAGL and GAMA 91

4.23 Runoff retention value in DAGL and GAMA 93

4.24 GWR analysis results for DAGL 98

4.25 GWR analysis results for GAMA 100

LIST OF FIGURES

Figure		Page
2.1	Relation between the methods and the outcome dimensions for sustainability	11
2.2	Millennium Ecosystem Assessment Conceptual Framework	12
3.1	The Study Area	35
3.2	Umbrothermal diagram of DAGL from 1992 to 2022	36
3.3	Umbrothermal diagram of GAMA from 1992 to 2022	37
3.4	Population growth in DAGL and GAMA	41
3.5	Flow chart of the research methodology	46
3.6	InVEST model interface	53
4.1	Land use and land cover map of DAGL and GAMA	62
4.2	Land Use and Land Cover change in DAGL in 1986, 2001, 2015, and 2023	62
4.3	Land Use and Land Cover change in GAMA in 1991, 2002, 2017, and 2023	66
4.4	Density of built-up area over DAGL and GAMA	75
4.5	Spatial orientation of urban expansion with gradient-direction in DAGL	76
4.6	Spatial orientation of urban expansion with gradient-direction in GAMA	78
4.7	Carbon storage map in DAGL and GAMA	86

4.8	Carbon storage per LULC type over DAGL and GAMA	87
4.9	Carbon sequestration per LULC type over DAGL	89
4.10	Carbon sequestration per LULC type over GAMA	90
4.11	Heat mitigation index in DAGL and GAMA	90
4.12	Runoff retention in DAGL and GAMA	92
4.13	The correlation matrix for DAGL	95
4.14	The correlation matrix for GAMA	96

LIST OF APPENDICES

Appendix		Page
A	Ecosystem services models	130
B	Ecosystem services models “continuation”	131
C	Maps with ground truth for LULC classification	132
D	Biophysical parameters used for the InVEST urban cooling model	132
E	Additional parameters submitted to the InVEST Urban cooling model for DAGL	133
F	Additional parameters submitted to the InVEST Urban cooling model for GAMA	133
G	Curve numbers for a combination of LULC types and Hydrological soil group used in InVEST urban flood mitigation model	133
H	User, producer accuracies, commission and omission errors for the different classified images for DAGL	134
I	User, producer accuracies, commission and omission errors for the different classified images for GAMA	135

LIST OF ABBREVIATIONS

AFOLU	Agriculture, Forestry, and Other Land Uses.
CART	Classification and Regression Trees
CICES	Common International Classification of Ecosystem Services
CN	Curve Number
DAGL	District Autonome du Grand Lome
ESs	Ecosystem services
GAMA	Greater Accra Metropolitan Area
GEE	Google Earth Engine
GIS	Geographic Information System
GPSC	Global Platform on Sustainable Cities
HMI	Heat Mitigation Index
HSG	Hydrological Soil Group
InVEST	Integrated Valuation of Ecosystem Services and Trade-offs
IPCC	Intergovernmental Panel on Climate Change
LULC	Land Use and Land Cover
NDVI	Normalised Difference Vegetation Index
NDBI	Normalised Difference Built-Up Index
NDWI	Normalised Difference Water Index
RF	Random Forest

RS	Remote Sensing
SCS-CN	Soil Conservation Service – Curve Number
UEII	Urban Expansion Intensity Index
WRM	Water Resource Management

CHAPTER ONE

1.0 INTRODUCTION

1.1 Background to the Study

Urban sprawl is a significant consequence of rapid urbanisation, characterised by the outward expansion of cities into the surrounding rural areas and defined by low-density development patterns, which often result in various environmental challenges (Dabie, 2015). It involves significant land consumption with the conversion of natural landscapes, open space, natural vegetation, and agriculture land into urban areas. This phenomenon is driven by a combination of factors that includes population growth, migration, economic opportunities, and inadequate urban planning (Ingwani *et al*., 2024). Such changes have profound implications for ecosystem processes and services that are essential for human well-being and urban resilience (Seto *et al*., 2012; Zhai *et al*., 2021; ECA/AfDB, 2022). Consequently, these transformations seriously threaten the sustainable development of cities (Hou *et al*., 2024).

Urban expansion and urbanisation have been shown to lead to a decline in Ecosystem Services (ESs). Urban expansion and urbanisation have been shown to lead to a decline in Ecosystem Services (ESs) globally. In north American cities like Atlanta, urban sprawl exacerbates ecosystem service degradation through increased impervious surfaces and habitat fragmentation, disrupting hydrological functions (Sun *et al*., 2018). In Ethiopia, Addis Ababa's rapid urbanisation caused an expansion of built-up areas, displacing croplands and green spaces, resulting in annual ecosystem service value losses (Hailu *et al*., 2024). To understand urban sprawl dynamics, it is essential to evaluate various elements such as land use changes, population density shifts, and the transformation of natural habitats into built environments (Dupras and Alam, 2015; Dupras *et al*., 2016;

Aswal *et al*., 2018; Korah *et al*., 2024). In both District Autonome du Grand Lomé (DAGL) and Greater Accra Metropolitan Area (GAMA), rapid urban growth has led to increased impervious surfaces and habitat loss, disrupting ecological processes and diminishing biodiversity (Asabere *et al*., 2020; Somadjago *et al*., 2020; Amouzoukpo, 2021; Devendran and Banon, 2022). The evaluation of these trends can be conducted through remote sensing and Geographic Information Systems (GIS), which allow for detailed analysis of Land Use and Land Cover changes over time. This quantitative approach provides insights into how urban expansion correlates with environmental degradation and the decline of ecosystem services.

The necessity for evaluating urban sprawl trends is underscored by the growing recognition of ecosystem services' critical role in urban resilience and sustainability. As cities continue to expand, understanding how urban sprawl affects vital services becomes increasingly important. The degradation of these services not only affects local environments but also has broader implications for human well-being and climate resilience (Kafy *et al*., 2022). Therefore, a comprehensive evaluation of urban sprawl dynamics is essential for informing effective policies that mitigate adverse environmental impacts while promoting sustainable urban development. Despite existing research on urbanisation in West Africa, there is a notable gap in understanding the specific impacts of urban sprawl on ecosystem services at a localised level. Previous studies have often focused on broader regional analyses or economic dimensions without adequately addressing ecological consequences.

In DAGL and GAMA, there is limited knowledge about how urban sprawl specifically affects critical ecosystem services such as carbon storage, flood risk control, and urban cooling. This knowledge gap highlights the need for research that connects urban planning with ecological sustainability, particularly as rapid urbanisation threatens vital ecosystems in these ecologically sensitive areas. Understanding the influence of urban sprawl on ecosystem resilience is essential for developing adaptive strategies and informing sustainable urban planning practices in Togo and Ghana.

1.2 Statement of the Research Problem

Urban expansion would align with sustainable development principles, balancing population growth with environmental conservation. Urban planning would prioritise controlled spatial growth, integrating green infrastructure to maintain ecosystem services while ensuring equitable access to housing and economic opportunities. Moreover, prioritise natural habitat preservation to prevent fragmentation and biodiversity loss, ultimately reducing environmental degradation and fostering resilient cities.

Both DAGL and GAMA, which are the largest and most populated cities in Togo and Ghana respectively, are experiencing rapid population increase primarily driven by urban migration and natural population growth. They face significant challenges from this rapid urbanisation, resulting in insecure tenure systems; unregulated land markets, inadequate housing, environmental degradation as well as waste disposal problems, among others (Seto *et al*., 2012; Patra *et al*., 2018; Devendran and Banon, 2022; ECA/AfDB, 2022). The spatial growth of DAGL and GAMA stems from economic opportunities, housing demand, and horizontal construction, yet proceeds without soil assessments, and without following any urban development plans (Aholou, 2008; Guézéré, 2011; Biakouye, 2014; Sorsy *et al*., 2023). This unregulated expansion, fuelled by rural migration towards economic hubs (Amouzoukpo, 2021; Agbemedi, 2022), has eroded vegetation cover, prioritising built-up areas over ecological preservation. For instance, in DAGL, municipalities like Adetikope and Agoènyivé exhibit declining plant diversity due to modern construction and agricultural land conversion, while Adetikope's surge in development intensifies environmental pressures (Takili *et al*., 2020; Amouzoukpo, 2021). Similarly, Bawa (2017) highlighted the replacement of farmland with infrastructure, threatening food security and agricultural sustainability. In GAMA, urbanisation has fragmented natural habitats through increased built-up land, reducing green spaces (Asabere *et al*., 2020; Puplampu and Boafo, 2021).

The implications of such changes are critical, as the loss of plant diversity not only disrupts ecosystem functions but also diminishes the resilience of communities facing climate change. However, studies on the implications of these changes for ecosystem services in these metropolitan areas are limited. The gaps our study aimed to fill.

The current situation raises critical questions such as:

i. What is the trend in urban expansion and Land Use and Land Cover change in DAGL and GAMA?

ii. What is the distribution and variation of the selected ecosystem services in DAGL and GAMA?

iii. To what extent does urban sprawl correlate with ecosystem service degradation, in these metropolitan areas?

1.3 Aim and Objectives of the Study

This study aims at evaluating the impact of urban sprawl development on ecosystem services in Togo and Ghana towards the achievement of sustainable urban development in both countries. Based on the aim of the study, the specific objectives are to:

i. assess the spatial and temporal changes in the expansion of urban areas and the change in Land Use and Land Cover from 1986 to 2023 in DAGL and GAMA.

ii. examine the distribution and variation in the provision of the selected ecosystem services from 1986 to 2023 in DAGL and GAMA.

iii. analyse the relationship between urban sprawl development and ecosystem service degradation in DAGL and GAMA metropolitan areas.

1.4 Justification for the Study

Ecosystems provide a range of services that fulfil human needs and also contribute to environmental sustainability. This study would make important contributions to the scientific understanding of urban-ecosystem interactions in West Africa while providing practical guidance for managing the impacts of urban expansion on ecosystem services in these rapidly growing metropolitan areas.

While Togo and Ghana have established laws and policies to regulate urban expansion and protect natural resources such as Togo's Decree N° 67_228 on town planning, Togo's National Housing Strategy, Ghana's Land Use and Spatial Planning Act, 2016, and Ghana's National Housing policy, their effectiveness in addressing the challenges of rapid urbanisation are often limited. Both countries struggle with the realities of informal settlements, prevalent in urban areas like DAGL and GAMA. In Togo, there is a disconnect between urban policies and how land is actually used by the population. This disconnects leads to uncontrolled development, largely driven by customary landowners who operate without effective state oversight. As a result, housing shortages worsen, and structural imbalances are exacerbated. Similarly, in the Greater Accra Metropolitan Area (GAMA), the Strategic Plan highlights that the natural environment cannot support continued urban growth without proper planning and management of land use.

The outcomes of this study will provide policymakers with critical insights into the tangible effects of urban sprawl, highlighting the urgent need for sustainable urban planning practices to mitigate its impacts on ecosystem services. As urban expansion poses significant threats to food security, habitat conservation, human health, biodiversity, and carbon sequestration (Seto *et al*., 2012; Güneralp *et al*., 2018), the findings will enable decision makers to identify areas for targeted interventions and prioritise conservation efforts. The findings will guide urban planning and management strategies, helping to mitigate the adverse effects of urban sprawl on ecosystems in rapidly growing West African cities, particularly in the context of climate change, thereby to empower planners and decision makers to make informed choices regarding land use, infrastructure development, and environmental protection.

The results of this research will provide essential insights for urban planners and environmental managers working towards the achievement of Sustainable Development Goal (SDG) targets such as make cities and human settlements inclusive, safe, resilient and sustainable by the reduction of the adverse per capita environmental effects of cities (Goal 11), take urgent action to combat climate change and its impacts by integrating climate change measures into urban planning and development (Goal 13), protect, restore, and promote sustainable use of terrestrial ecosystems, and reverse land degradation and loss of biodiversity (Goal 15). The outcomes are expected to enhance understanding of the relationship between environmental health and poverty alleviation, as vulnerable populations often rely heavily on ecosystem services for their basic needs. Furthermore, the study will strengthen the capacity of environmental institutions in Togo and Ghana to mitigate environmental degradation and adapt to climate change, ultimately contributing to more effective land use policies and infrastructure planning that prioritise sustainability and resilience.

The impact of urban development on ecosystem services, which are vital for human survival and the preservation of natural resources in both urban and peri-urban environments, is a critical area of study. The current research will provide a pathway for further research on urban sustainability and ecosystem protection, offering relevant insights for future urban and ecosystem modelling.

The insights from this research are expected to enhance scientific knowledge on the relationship between urbanisation, land use change, and ecosystem services. It may serve as a model for similar studies in other regions, facilitating comparative analyses and the development of broader theories. Additionally, the insights gained could inform the design of future research projects while identifying knowledge gaps that warrant further investigation, ultimately guiding policymakers in making informed decisions that promote sustainable urban development and effective environmental management.

1.5 Scope and Limitation

1.5.1 Scope of the study

The study focuses on the period 1986 and 2023 for DAGL and 1991 to 2023 for GAMA to evaluate the impact of urban sprawl on ecosystem services, justified by the rapid population growth and urban expansion in African cities over the last three decades (Hope, 1998; Sylla, 2021). The selected timeframes align with census periods in both countries and account for data quality issues, such as the lack of quality imagery before 1991 for GAMA. This research specifically examines critical ecosystem services like carbon storage, flood risk control, and urban cooling, which are vital for residents' health and security amid climate change. By analysing the dynamics of urban sprawl and its effects on these services, the study aims to provide insights that inform sustainable urban planning practices to mitigate adverse impacts and enhance resilience against climate change.

1.5.2 Limitation of the study

This study is limited by differences in the temporal datasets between DAGL and GAMA, which may affect the continuity, consistency, and comprehensiveness of the data analysis. More so, the irregular satellite image coverage could lead to overlooked intermediate changes. However, these limitations do not significantly impact the main findings of the study. Instead, they provide important considerations for future research in these areas.

CHAPTER TWO

2.0 LITERATURE REVIEW

2.1 Conceptual Framework

Urban sprawl is a multifaceted phenomenon that refers to the uncontrolled expansion of urban areas into rural landscapes, often characterised by low-density development, excessive consumption of land and separation of land uses (Sinha, 2018). This process is driven by various factors, including population growth, economic opportunities, and inadequate urban planning (Mosammam *et al*., 2016). The consequences of urban sprawl extend beyond land use changes; it significantly impact ecosystem services (Ess), which are the benefits that humans derive from natural ecosystems (Seto *et al*., 2012; Zhai *et al.*, 2021). The dynamics of urban sprawl and its implications for ecosystem services are crucial for achieving sustainable urban development, especially in rapidly urbanising regions like West Africa.

2.1.1 Ecosystem services (ESs)

Ecosystem services are critical benefits provided by natural ecosystems that support human well-being and environmental health. These services are typically categorised into three main types based on the CICES classification: Provisioning, Regulating and Maintenance, and Cultural Services (Haines-Young and Potschin, 2018). Urban sprawl significantly disrupts these services through habitat fragmentation and resource overexploitation. In metropolitan regions such as DAGL and GAMA, ecosystem services are under increasing pressure from rapid urbanisation. The destruction of green spaces for housing and infrastructure development not only threatens biodiversity but also limits essential services, with effects on human life and urban resilience (Leha *et al*., 2013). The integration of ecosystem service assessments into urban planning is essential for overcoming these challenges and ensuring sustainable city development.

2.1.2 Urban sustainability framework (USF)

The Urban Sustainability Framework (USF) was created by the Global Platform for Sustainable Cities (GPSC) managed by the World Bank in partnership with the Global Environment Facility (GEF) in 2018. The Urban Sustainability Framework (USF) provides a comprehensive approach to managing the growth and development of urban areas while maintaining environmental integrity and improving the quality of life for urban residents. A city is sustainable by using two important methods such as (1) good governance and integrated urban planning processes and (2) sound management of city finances to ensure financial sustainability with outcomes called dimensions. The four dimensions in this framework are: (1) robust economic growth, prosperity, and competitiveness across all parts of the city; (2) protection and conservation of ecosystems and natural resources into perpetuity; (3) mitigation of greenhouse gas (GHG) emissions while fostering overall city resilience; and (4) inclusiveness and liability, mainly through the reduction of city poverty levels and inequality (Figure 2.1).

The environment provides food, water, and other essential commodities. Healthy ecosystems regulate the climate and attenuate the effects of extreme weather events, while improving residents' quality of life and well-being. The expansion of the city must be carefully managed to preserve natural habitats, agricultural resources, and the ecosystem services they provide. The dimension 2 of this framework especially focuses on ecosystems and biodiversity conservation and restoration within and beyond the city boundaries, air quality maintenance, water resource management, solid waste management and consumption and production patterns. Such approach promotes a holistic and integrated method of addressing the environmental, social, and economic challenges associated with rapid urbanisation.

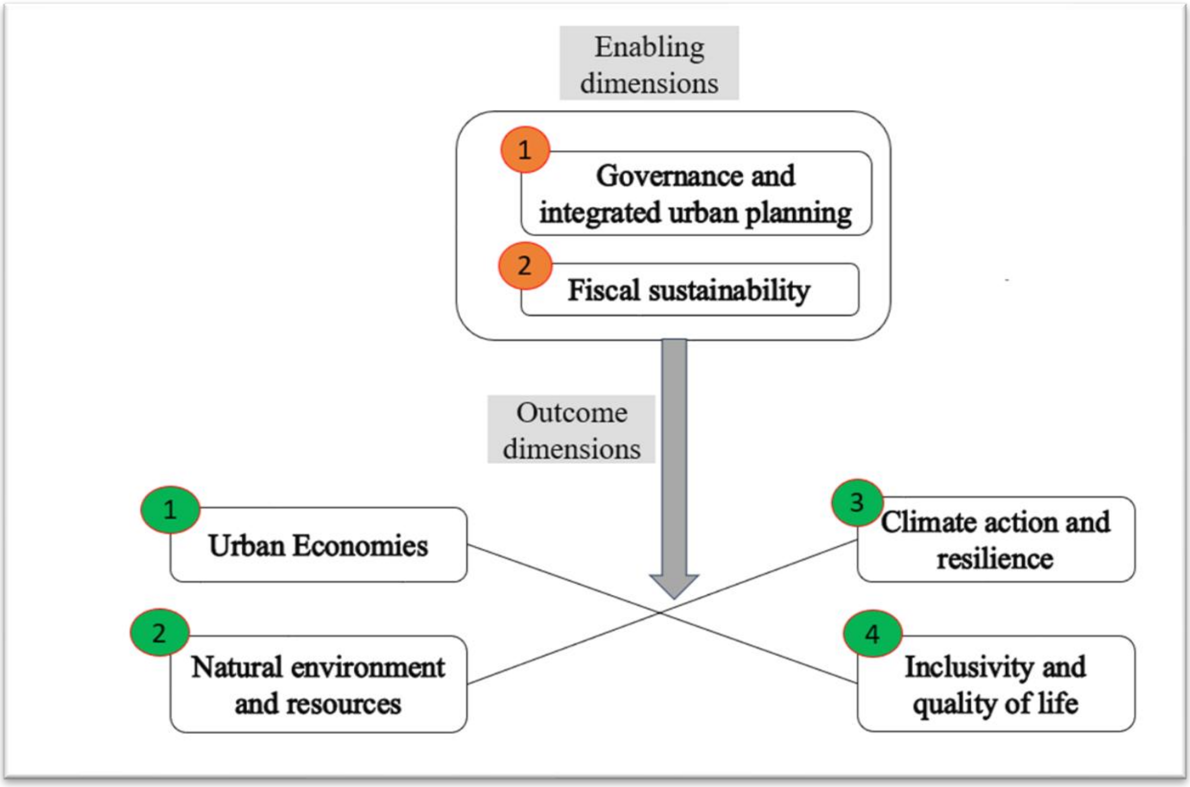

Figure 2.1: Relation between the methods and the outcome dimensions for sustainability

Source: (World Bank, 2018)

2.1.3 Millennium ecosystem assessment framework

The MEA (Millennium Ecosystem Assessment Framework) conceptual framework (MEA, 2005) (Figure 2.2) assumes a complex interaction between humans and other parts of ecosystems, leading directly and indirectly to changes in ecosystems and environment that result in changes in human well-being. Additionally, many environmental factors alter the human condition, and impact ecosystems. The production of various services from coastal ecosystems, wetlands, protected biotopes, and agricultural land is impacted both directly and indirectly, leading to changes in ecosystem services that subsequently affect the livelihoods of local residents.

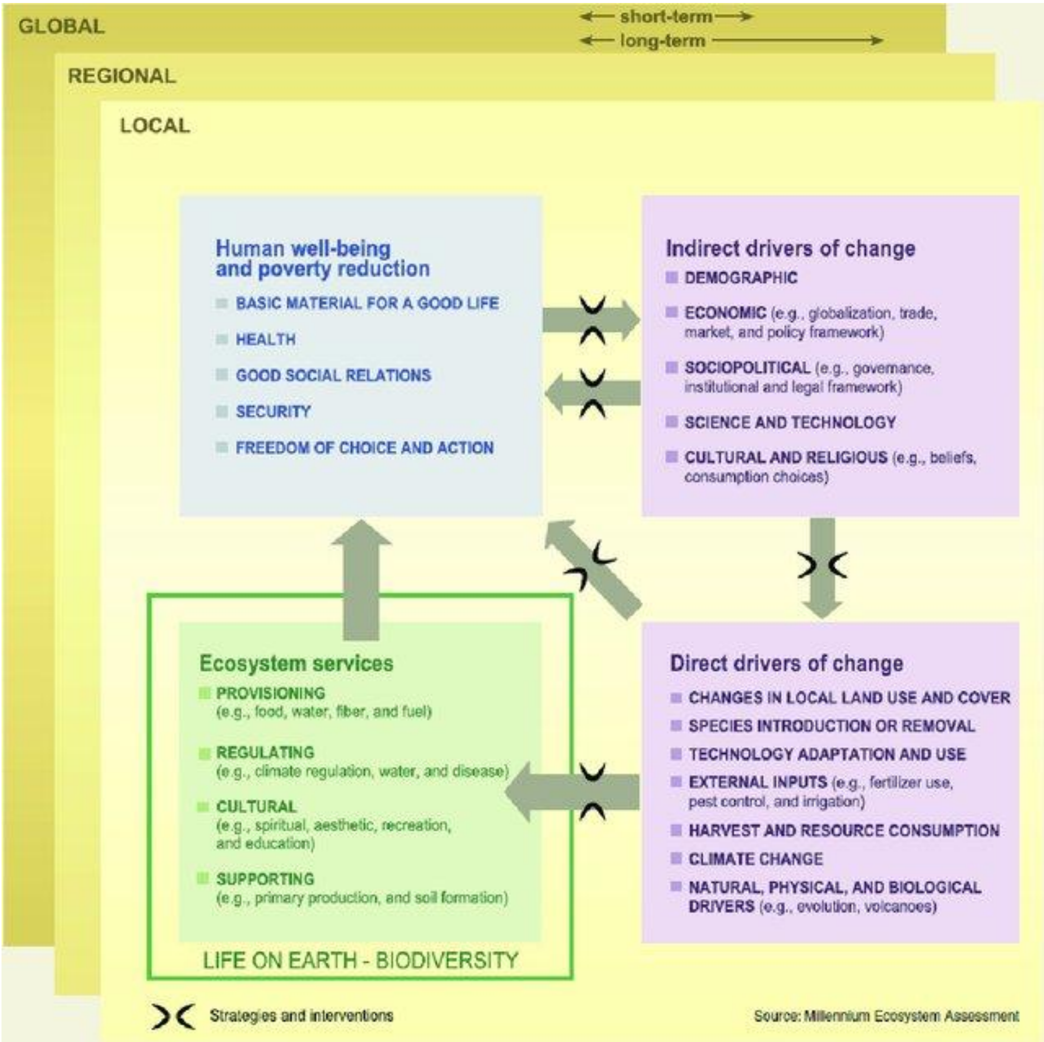

Figure 2.2: Millennium Ecosystem Assessment Conceptual Framework

Source: (MEA, 2005)

2.1.4 Common international classification of ecosystem services (CICES)

The Common International Classification of Ecosystem Services (CICES) is a hierarchical classification system developed to provide a standardised framework for categorising and assessing ecosystem services. It was initially developed in support of the System of Environmental-Economic Accounting (SEEA) and has since been widely adopted by the ecosystem services research community. The approach provides a classification scheme that facilitates the measurement, accounting for, and assessing ecosystem services. Ecosystem services are contributions that ecosystems make to human well-being mostly through the interactions between biotic and abiotic processes. CICES classification seeks to provide a formal systematic definition of different ecosystem services, proposing a new standard of classification to aid in essay identification, thus creating typologies for describing ecosystem services. Additionally, CICES also help support and analysis any changes in the value of different kinds of goods generated by these identified ecosystem services. It categorised the ecosystem services in their main categories (Table 2.1).

Table 2.1: Description of ESs categorised based on CICES classification

Categories of Ecosystem services	**Description**
Provisioning services	Benefits obtained from ecosystems, including food, freshwater, fibre, genetic resources, and other materials that humans utilise.
Regulating and Maintenance services	These services regulate natural processes and maintain ecosystem functions, such as climate regulation, water purification, pollination, erosion and flood control, carbon storage and urban cooling which are essential for sustaining life and human well-being.
Cultural services	These encompass nonmaterial benefits that people obtain from ecosystems, including recreational, aesthetic, spiritual, and educational values, highlighting the importance of nature for cultural identity and personal well-being.

Source: Haines-Young and Potschin (2018)

2.2 Theoretical framework

2.2.1 Concentric zone theory (Burgess, 1925)

In 1925, the Concentric Zone Theory was established by Ernest W. Burgess, who first theorised on the city of Chicago to gain insights into patterns of urban expansion of the city to inform zoning regulations and land use planning. According to this theory, metropolitan areas grow outwards in concentric ‘zones,’ each identified by the unique land uses. The increases in population density and commercial activity with the growth of a city increase pressure on urban core zones such as Central Business District (CBD) and Zone of Transition. Although cities rely on the natural ecosystems for services such as air and water purification, flood control, climate change mitigation or recreational opportunities, these services are weakened by the degradation of natural habitats at the expense of construction land. In the context of Grand Lomé and GAMA, this theory can be used to identify the effect of urban development on different ecosystem services. For example, as the commuter zone expands, the demand for land for housing, and infrastructure that drives conversion of agricultural land and natural habitats to building homes or businesses increases. The conversion of land affects the availability of services including flood control and carbon storage.

2.2.2 Urban ecological *footprints* (UEF)

The Urban Ecological Footprint (UEF) theory is an essential concept in sustainability science, offering a framework to measure the environmental impacts of cities, particularly in the context of urban sprawl and ecosystem services. The theory provides insights into how urban development patterns affect natural resources and ecosystem functions. Since its conception in the 1990s, the ecological footprint has emerged as a significant area of research focused on evaluating urban settlements and providing insights into urban sustainability (Ortega-Montoya and Johari, 2008). It serves as a valuable tool for assessing the sustainability of lifestyles and understanding how populations can sustain themselves in specific areas, a concern that has become increasingly critical in light of the ongoing challenges posed by climate change (Hameed, 2021). Environmental sustainability has become very important for urban development and can be achieved when a population can support a particular lifestyle indefinitely while still meeting the demands placed on an environment.

Furthermore, Sustainability may be accomplished by describing the components in a way which is transparent and ecologically stable (Yao *et al*., 2016). It can also encourage decision makers and the general public to incorporate environmental accounting into their day-to-day practice so that the community can maintain a viable competitive economy and sustainable environment for a long time to come (Solarin *et al*., 2019). The use of Urban Ecological Footprint's theory in the study of urban sprawl and its impact on ecosystem services provides a comprehensive framework for understanding and mitigating the environmental impacts of urban expansion. By quantifying the resource demands and environmental costs of sprawl, cities can develop strategies to promote more sustainable urban growth patterns that preserve and enhance ecosystem services.

2.3 Review of Related Studies

2.3.1 Drivers of urban expansion

Urban expansion is a worldwide phenomenon shaped by a variety of complex and interconnected factors. One of the most powerful and common drivers is rapid demographic growth, which results both from natural population increases and the migration of people from rural areas to cities (Rijal *et al*, 2020; Guo and Zhang, 2021; Li *et al.,* 2025). As cities develop into economic centres, they attract people looking for jobs and better services, while rising economic activity and investment further contribute to the physical growth of urban areas. Wang and Kintrea (2021) note that emerging economies, especially in Asia and Africa, are undergoing massive outward urban expansion at unprecedented rates. This surge in growth consumes large amounts of land in major cities, putting additional pressure on urban infrastructure and natural resources. Moreover, housing shortages and increasing land prices in city centres also drive cities to spread outward (Yussif *et al*., 2023).

When we focus on Africa and West Africa in particular, urban expansion is both rapid and significant. Africa's urban population is expected to double from 717 million in 2020 to 1.4 billion by 2050, surpassing urban populations of China, India, Europe, and the United States, and becoming the world's second-largest urban region after Asia (OECD, 2025). This growth is driven by high birth rates, rural-to-urban migration motivated by economic opportunities, and in some cases, shifts in land use policies. Cities in West Africa face unique challenges such as informal settlements, inadequate infrastructure, and governance issues, all of which shape the way their urban areas expand. Typically, urban growth in the region takes the form of rapid peripheral expansion characterised by low-density, often unplanned development, fuelled by poverty, population pressures, and limited urban planning capacity.

Looking specifically at the District Autonome du Grand Lomé (DAGL) in Togo and the Greater Accra Metropolitan Area (GAMA) in Ghana, these areas provide clear examples of common drivers behind urban expansion in West Africa. Both cities have grown quickly due to natural population increase, rural-to-urban migration, and economic transformation. The influx of migrants from surrounding rural communities seeking better livelihoods has led to the expansion of peri-urban areas. In addition, socio-economic factors like the growth of informal economies, a scarcity of affordable housing, and greater demand for infrastructure have pushed spatial growth further. Policy and governance challenges such as weak land-use planning and informal land tenure systems also play a significant role in shaping this expansion (ECA/AfDB, 2022). Environmental conditions, including the local terrain and closeness to the coast, additionally influence the direction and form of urban growth in these metropolitan regions.

2.3.2 Urban development dynamics and ecosystem services

Urbanisation in Africa has transformed Land Use and Land Cover, leading to the loss of natural habitats and a decline in ecosystem services. The rapid expansion of urban areas often results in the conversion of agricultural land and natural landscapes into built environments, negatively impacting biodiversity and ecosystem functionality (Agyapong *et al.*, 2018). For instance, in the GAMA, rapid urban growth has resulted in the degradation of green spaces and increased pressure on remaining natural resources (Puplampu and Boafo, 2021). This transformation reduces the availability of provisioning services such as wild fruits, fuelwood, and game that local farmer households traditionally relied upon, thus threatening their livelihoods (Abdulai and Osumanu, 2023).

The relationship between urban development dynamics and ecosystem services is complex and multifaceted. Urbanisation often leads to habitat fragmentation, which disrupts ecological processes. Urban expansion dynamic exerts significant pressure on ecologically sensitive areas such as wetlands, riparian zones, and coastal lagoons. These areas are frequently transformed into housing developments through drainage, landfilling, stream channelling, and construction of barriers. Such encroachments exacerbate flood hazards, as seen in many African cities (Andreasen *et al.*, 2022). For example, studies have demonstrated that urban sprawl reduces carbon sequestration capabilities and increases urban heat island effects due to the loss of vegetation cover (Rahaman *et al.*, 2022; Kafy *et al.*, 2022).

Geospatial analyses have been instrumental in understanding urban expansion dynamics. Eneogwe and Umunake, (2021) used Geographic Information Systems (GIS) and remote sensing methods to reveal how urban expansion in Abuja, Nigeria, has converted cultivated and uncultivated agricultural lands into urban areas. Similarly, Koko *et al*. (2021) quantified land use changes in Kano Metropolis, Nigeria, demonstrating rapid urbanisation's impact on agricultural landscapes. Awotwi *et al*. (2017) highlighted how urbanisation in Ghana has led to significant losses in agricultural land, vegetation cover, and water bodies while increasing built-up areas. In Addis Ababa, Ethiopia, Moisa and Gemeda, (2021) used geospatial techniques to show a substantial increase in built-up areas at the expense of agricultural land and grasslands. Salam *et al*. (2023) assessed land use changes in Oyo State, Southwestern Nigeria, revealing similar trends of expanding built-up areas accompanied by losses in vegetated zones. The implications of these changes extend beyond environmental degradation to socio-economic impacts. Iddrisu *et al*. (2023) examined land use changes in Tamale, Ghana, showing how horizontal urban expansion has shifted peri-urban livelihoods from agriculture-based activities to a more monetised urban economy. While this transition offers new economic opportunities for some households, it also presents challenges such as reduced access to natural resources like farmland and water. These findings underscore the need for integrated approaches that balance urban growth with ecosystem conservation.

2.3.2.1 Google earth engine (GEE) in environmental monitoring

Google earth engine is a powerful cloud-based geospatial processing platform that provides access to a wide range of unique datasets for environmental monitoring and analysis (Tamiminia *et al*., 2020). It's designed to store and process huge datasets for analysis and ultimate decision-making and has been recently in the remote sensing big data processing spotlight (Kumar and Mutanga, 2018). The easily accessible and userfriendly front and provides a convenient environment for interactive data and algorithm development. Users are also able to add and curate their own data and collections.

This platform hosts petabyte scales of over 50 years of remotely sensed data, such as Landsat, MODIS, National Oceanographic and Atmospheric Administration Advanced Very High-Resolution Radiometer (NOAA AVHRR), Sentinel 1, 2, 3 and 5-P; and Advanced Land Observing Satellite (ALOS) data (Gorelick *et al*., 2017). It also includes climate-weather and geophysical datasets. Additional ready-to-use products, such as the Enhanced Vegetation Index (EVI) and the Normalised Difference Vegetation Index (NDVI), are also available (Kumar and Mutanga, 2018). In addition to the availability of a large repository of raw remotely sensed imagery, users have access to pre-processed, cloud-removed and mosaicked images in the GEE data catalogue.

In addition, GEE supports secure data storage and easy retrieval of previous projects, which is particularly beneficial for analysing Land Use and Land Cover dynamics. As for statistical methods, GEE supports advanced analytical techniques such as time-series analysis, accuracy assessment, change detection, and machine learning classification algorithms (Rudiastuti *et al*., 2021). This capability allows researchers to conduct complex analyses efficiently while leveraging the extensive datasets within GEE. The combination of these extensive datasets and advanced analytical capabilities positions GEE as a leading platform for environmental monitoring and research on Land Use and Land Cover, forest mapping, deforestation, disaster risk mapping and prediction, crop yield, drought monitoring (Carrasco-Escobar *et al*., 2019; DeVries *et al*., 2020; Han *et al*., 2020; Saengprachatanarug *et al*., 2022*)*. Several packages are available, for instance machine learning, image processing, image collection, geometry features, reducers, charts and specialised algorithms. Archives of geospatial datasets within GEE along with its coding, sharing, parallel processing, and visualisation abilities have made it an unprecedented competitor among all existing cloud platforms.

2.3.2.2 The random forest (RF) classifier

The Random Forest (RF) classifier, introduced by Breiman in 2001, is a supervised ensemble learning algorithm that has become a cornerstone in machine learning. Its ability to combine multiple decision trees into a robust predictive model has made it widely applicable across various domains. To date, RF is considered one of the most widely used algorithms for Land Use and Land Cover classification using remote sensing data (Millard and Richardson, 2015; Jin *et al*., 2018; Maxwell *et al*., 2019). One significant advantage of the RF classifier is its capacity to manage high-dimensional data with complex interactions between variables, although it is somewhat sensitive to input data errors (Hengl *et al*., 2015). Additionally, this classifier has demonstrated exceptional performance compared to other classifiers, such as SVM, KNN or MLC, achieving higher accuracy in land cover mapping and projections across Africa and various regions worldwide (Breiman, 2001; Manzanas *et al*., 2014; Duan *et al*., 2019; Rudiastuti *et al*., 2021). RF combines multiple Classification and Regression Trees (CART) to create an ensemble classifier. It generates several decision trees through random selection of variables and training datasets, and evaluates its performance using non-training examples to provide an objective assessment of generalisation error (Breiman, 2001). The two key user-defined input factors are the number of parameters and the number of trees, with literature suggesting that the ideal number of variables is the square root of the total variables, and the ideal number of trees ranges from 100 and 500 (Belgiu and Dragut, 2016). Additionally, one-third of the training data are used to determine the prediction error, while two-thirds is used to construct the random forest model. This facilitates the assessment of the accuracy of the analysis.

2.3.3 Ecosystem services distribution and analysis for sustainable city planning and development

Ecosystem Services (ESs) are critical for urban sustainability, providing benefits such as air and water purification, climate regulation, biodiversity support, and cultural amenities (Kettunen and D'Amato, 2013). Urban areas, despite their dense populations and built infrastructure, rely heavily on these services to enhance resilience and improve the quality of life for residents (Wang *et al*., 2024). Regulatory services provided by urban trees, such as temperature control, stormwater management, and air purification, are particularly vital in mitigating urban challenges like heatwaves, flooding, and air pollution (Fryd *et al*., 2012; Selmi *et al*., 2021). For instance, green infrastructure interventions, such as urban parks, green roofs and community garden are increasingly recognized as effective strategies for improving urban resilience while addressing climate change impacts by enhancing the regulation of temperature, improving air quality, and reducing stormwater runoff (Pandey and Ghosh, 2023). However, the irregular distribution of these services across urban landscapes presents significant challenges to equitable development.

The distribution of ecosystem services in urban areas is often uneven, influenced by socio-economic disparities, land use patterns, and governance structures (Selmi *et al*., 2021). Burkhard *et al.* (2012) emphasises the need to differentiate between the supply of ecosystem services defined as the capacity of a given area to provide specific services and the demand for these services by local populations. This distinction is crucial for effective urban planning and resource allocation, as it allows policymakers to identify areas where ecosystem service delivery is insufficient and prioritise interventions accordingly. Moreover, various methodologies have been developed to assess and map ecosystem services at multiple spatial scales. Studies have utilised Geographic

Information Systems (GIS) and remote sensing techniques to quantify the availability of ecosystem services in urban areas (Avtar *et al*., 2017; García-Pardo *et al*., 2022). Remote sensing, in particular, has proven to be a valuable tool for quantifying urban ecosystem services. High-resolution satellite imagery allows for the assessment of Land Use and Land Cover (LULC) change over time, which directly impacts ecosystem service values. For instance, a study in Chandigarh, India, employed remote sensing and GIS to evaluate LULC dynamics and it impact on ESs, revealing significant changes in ESVs linked to urbanisation (Sharma *et al*., 2023). This approach not only highlights the relationship between land cover types such Water bodies, forest and vegetation, built-up, agriculture and shrubland and open spaces but also provides insights into how these changes affect the delivery of ecosystem services. Furthermore, innovative methodologies like the InVEST (Integrated Valuation of Ecosystem Services and Trade-offs) model allow for the assessment of multiple ecosystem services simultaneously, facilitating a comprehensive understanding of their spatial distribution and potential trade-offs (Sharp *et al*., 2018). In conclusion, understanding the distribution of ecosystem services through GIS and remote sensing technologies is vital for promoting sustainable urban development. As cities face increasing pressures from population growth and climate change, effective assessment methods will be essential for ensuring equitable access to ecosystem services.

2.3.3.1 Different models for ecosystem services analyses

The analysis and assessment of ecosystem services have become increasingly important in environmental management and urban planning, as they provide critical insights into the benefits that ecosystems offer to human societies. Various models have been developed to quantify and evaluate these services, utilising tools such as Geographic Information Systems (GIS) and remote sensing techniques. These models enable researchers and policymakers to identify service distribution, assess trade-offs, and inform decision-making processes regarding land use and resource management (Wang *et al*., 2024). One of the most widely utilised models for ecosystem services analysis is the Integrated Valuation of Ecosystem Services and Trade-offs (InVEST) model, developed by scientists from Stanford University, University of Minnesota, the Chinese Academy of Sciences, The Nature Conservancy, the World Wildlife Fund, the Stockholm Resilience Centre and the Royal Swedish Academy of Sciences (Natural Capital Project, 2023).

The InVEST model is a continually developed software package that models, quantifies and maps the values of ESs. It is widely used, including in a recent global application (Chaplin-Kramer *et al*., 2019). It relies on geographic data to produce maps that illustrate the spatial distribution of ecosystem services, helping stakeholders visualise potential impacts of land use changes. In addition to InVEST being open source, another significant benefit is its ease of deployment. InVEST runs on an open-source platform, and the updated interface does not need ArcGIS, but the results can be viewed in any GIS interface (Mukhopadhyay *et al*., 2024). The tool is modular in the sense that you do not have to model all the ecosystem services listed, but rather can select only those of interest. The model's applications in various cities worldwide demonstrate its flexibility and effectiveness in supporting local stakeholders in making informed decisions that promote both environmental health and community well-being. Additionally, the choice of this model is also due to its requirement of easily available data and its consideration of the landscape context.

InVEST requires predominantly GIS or map data as inputs, along with information tables typically formatted as CSV files. Users can prepare these inputs using mapping software such as QGIS or ArcGIS. Once the data is inputted, the model processes it to generate outputs that include maps, quantitative data on ecosystem services, and various statistics and reports. The interface allows users to easily navigate through different models. The output from InVEST is presented in an intuitive manner, often through visual maps that illustrate the spatial distribution of ecosystem services. This visualisation aids stakeholders in understanding how changes in land use or management practices can affect service delivery.

Building on the insights provided by the InVEST model, it is essential to recognize that various other models are also employed in the analysis of Ecosystem Services (ESs). These models offer diverse methodologies and frameworks for different aspects of ecosystem service evaluation. A summary of these models can be found in Appendix Section (see Appendix A and B).

2.3.3.2 Environmental challenges in DAGL

DAGL faces range of environmental challenges that threaten the sustainability of urban development and the provision of ecosystem services. These challenges are largely driven by rapid urbanisation, population growth, and inadequate infrastructure, which exacerbate issues such as urban sprawl, pollution, and the loss of green spaces. One of the most pressing environmental issues in DAGL is flooding (Polorigni *et al*., 2018). Flooding in this region is primarily caused by intense or prolonged rainfall, overflow of watercourses, and rising water tables. These natural factors are compounded by anthropogenic influences, including inadequate drainage systems and urbanisation-induced soil impermeability (Blakime *et al.*, 2024). The widespread use of impervious materials such as concrete reduces rainwater infiltration into the ground, leading to increased surface runoff and heightened flood risks. According to the IPCC’s Sixth (6) Assessment Report, West Africa is likely to experience more frequent and severe droughts and floods by the end of the 21st century, with DAGL being no exception (IPCC, 2022). Additionally, climate change is expected to intensify these challenges (Klassou, 2014).

Another significant environmental challenge in DAGL is the urban heat island (UHI) effect. The reduction of green spaces due to urban sprawl and the proliferation of impervious surfaces such as asphalt roads and buildings have led to elevated air temperatures in urban areas. Waste heat from industries, transportation, and residential activities further exacerbate this phenomenon (Edokossi and Bakis, 2019). In recent years, DAGL has experienced sporadic waves of extreme heat, which negatively impact human comfort, air quality, and energy management (Polorigni *et al*., 2018). Monitoring surface temperatures in urban environments is therefore essential for mitigating these localised heat effects.

Deforestation and biodiversity loss are other key challenges in DAGL. The expansion of agricultural land and overexploitation of natural resources have led to substantial reductions in forest cover. This not only threatens biodiversity but also undermines critical ecosystem services such as carbon sequestration. Urban expansion has converted natural habitats into built environments, diminishing their capacity to store carbon exacerbating climate change impacts. The degradation of these ecosystems highlights the urgent need for sustainable land-use planning.

2.3.3.3 Environmental challenges in GAMA

Since the Rio Summit, environmental issues in the Greater Accra Metropolitan Area (GAMA) have intensified, particularly in key areas such as pollution, urban congestion, biodiversity loss, and climate change. While the Ghanaian government has made efforts to address these public goods challenges, the relentless exploitation of natural resources to meet socio-economic demands has often led to neglect in implementing necessary precautions against resource depletion and mismanagement. Unsustainable development practises have resulted in severe consequences, including deforestation, land degradation, air and water pollution, soil erosion, overgrazing, and significant biodiversity loss. These environmental degradations threaten the very foundation of livelihoods for many Ghanaians. Flooding has emerged as one of the most pressing environmental challenges in GAMA, ranking among the top natural disasters affecting the region. It is estimated that flooding impacts over three million people annually and causes substantial economic losses (Okyere *et al*., 2012). The frequency and severity of flood events have increased in recent years, particularly in major urban areas. The consequences of flooding include loss of life and property, which exacerbate urban poverty and hinder development efforts. GAMA has a long history of flooding events attributed to human negligence, such as construction in waterways and inadequate sanitation practises that heighten the vulnerability of informal settlements (Obeng-Odoom, 2011; Cobbinah and Darkwah, 2016; Owusu and Obour, 2021). A notable incident occurred on June 3rd, 2015, when severe flooding in GAMA resulted in the tragic loss of approximately 205 lives and extensive damage to businesses and residential properties (Adjei-Darko, 2017).

In addition to flooding, GAMA faces rising temperatures due to urbanisation. The replacement of vegetation with impervious surfaces such as asphalt and concrete has led to the formation of urban heat islands that contribute to elevated land surface temperatures (Wemegah *et al*., 2020). Local authorities have issued health warnings regarding heat-related risks such as heat exhaustion and increased energy demands for cooling. Vulnerable populations, particularly low-income households living in densely populated areas, face heightened health risks and economic burdens as a result of these temperature increases.

The decline in vegetation cover within GAMA has serious ecological implications, notably a reduction in carbon storage capacity. Vegetation plays a critical role in carbon sequestration by absorbing CO_2 during photosynthesis; however, extensive urban development over the past three decades has led to significant habitat loss (Addae and Oppelt, 2019). This degradation diminishes ecosystem functionality and exacerbates climate change impacts. In summary, GAMA is grappling with multifaceted environmental challenges that include flooding, rising temperatures, pollution, declining vegetation cover, and inadequate waste management. These issues not only threaten ecosystem services but also undermine urban resilience and sustainable development efforts, hence the need for an urgent ecosystem management reawakening globally, and in Sub-Saharan Africa.

2.3.4 Relationship between urban sprawl, metropolitan city development, and ecosystem Services

The relationship between urban sprawl and ESs is complex, as urbanisation often leads to habitat fragmentation, loss of biodiversity, and alterations in the provision of essential services such as water purification, carbon sequestration, and recreational opportunities. For instance, a study Li *et al*. (2021) used correlation analysis to demonstrate a negative relationship between urbanisation indices and natural habitats, highlighting that increased urban sprawl correlates with diminished ecosystem service provision in the Changchun region in China. Bivariate spatial correlation analysis, particularly Moran's I, has been instrumental in understanding the spatial dependencies of ecosystem services in relation to urban sprawl. This method assesses whether high or low values of ecosystem services are clustered in space and has revealed significant spatial correlation in many metropolitan areas (Luo and Yang, 2024). For example, research conducted in China indicated that urban sprawl not only reduces local ecosystem service values but also influences neighbouring regions through spatial spillover effects (Yi *et al*., 2023). The findings suggest that while urban expansion may degrade local ecosystems, it can inadvertently enhance service provision in adjacent areas due to changes in land use patterns. This nuanced understanding underscores the importance of considering spatial relationships when evaluating the impacts of urbanisation on ecosystem services.

The Geographically Weighted Regression (GWR) and Ordinary Least Squares (OLS) regression has further helped in elucidating the relationship between urban sprawl and ecosystem services. For instance, a study by Dupras and Alam (2015) found that economic growth and population density significantly predicted declines in ecosystem service values across the Montreal Area in Quebec. Their results emphasised that effective urban planning must integrate considerations of both socioeconomic development and ecosystem service preservation to mitigate the adverse effects of sprawl. Overall, these analytical approaches highlight the critical need for sustainable urban development strategies that balance growth with the conservation of ecosystem services. Shao *et al*. (2020) employed both GWR and OLS regression models to investigate the spatial relationship between changes in Land Use and Land Cover (LULC) and ecosystem service value (ESV) in Xi'an, a city located in Shaanxi Province, China. Their findings demonstrated that the GWR model provided a more accurate explanation of the correlation between land use dynamics and ESV at the local level compared to the OLS model. Specifically, the GWR analysis revealed a significant negative association between LULC changes and ESV, highlighting spatial heterogeneity in this relationship. Also, Zhu *et al*. (2020) conducted an analysis using both ordinary least squares (OLS) and Geographically Weighted Regression (GWR) models to examine how urbanisation and changes in landscape patterns influence habitat quality. Their findings revealed that rapid urbanisation has a significant negative impact on habitat quality across different regions. However, the effects of landscape pattern changes on habitat quality were more complex, varying both temporally and spatially. Furthermore, Song *et al*. (2022) have employed OLS regression to analyse how urban sprawl affects vital ecosystem functions, with the most significant correlation with food production, indicating that urban land expansion had the strongest impact on food production.

2.3.5 Examples from other regions / countries

A comprehensive case study from China illustrates how urban sprawl affects ecosystem services. Using a dynamic spatial Durbin model, Yi *et al*. (2023) demonstrated that urban sprawl negatively impacts local ecosystem services, while occasionally benefiting neighbouring regions through spatial spillover effects. Resource-based cities experience intensified degradation due to land-use changes, and policies like low-carbon city initiatives improved sprawl control but had limited success in improving overall ecosystem service values. The study highlights complex trade-offs among ecosystem services. For instance, in Changchun, urban sprawl led to increased carbon storage and soil retention due to improved land management practices, but habitat suitability declined significantly due to extensive land conversion (Li *et al*., 2021). These findings underscore the need for integrated urban planning that balances development with ecological sustainability. They also show that while some ecosystem services may improve, others may deteriorate due to sprawl.

In North America, particularly in Atlanta metropolitan areas, urban sprawl has been linked to significant losses in ecosystem services. The work of Sun *et al*. (2018) shows that the expansion of impervious surfaces reduces natural habitats, diminishing biodiversity, and disrupts carbon sequestration processes, increasing flood risks. These findings emphasise the importance of compact city designs and green infrastructure to mitigate the adverse effects of sprawl.

In Sub-Saharan Africa, cities like Kampala and Mbarara in Uganda serve as illustrative examples of how urban sprawl leads to significant agricultural land conversion. These cities highlight the complex interactions between urban expansion and ecosystem services. Urban growth has encroached upon agricultural lands, reducing local food security and rural livelihoods. Kampala, being a larger urban centre, faced more pronounced land loss due to high demand for residential and commercial development (Muchelo *et al*., 2024). In Addis Ababa, Ethiopia, Hailu *et al*. (2024) found that urban sprawl resulted in substantial reductions in green spaces and croplands, leading to declines in ecosystem service values, particularly in food production and climate regulation. The rapid urbanisation in Kampala outpaced land conservation efforts, while Addis Ababa's urban expansion was driven by rapid population growth and rural-urban migration. The use of remote sensing and GIS in these studies provided detailed insights into land-use changes and their impacts on ecosystem services. Both Kampala and Addis Ababa emphasise the need for integrated urban planning to mitigate environmental costs. However, current policies often fail to balance development with ecological sustainability, and unregulated urban growth exacerbates environmental degradation. Efforts to integrate urban agriculture into land-use planning in Kampala aim to preserve green spaces and enhance food security. These examples from other regions demonstrate how urban sprawl profoundly impacts ecosystem services, which is directly relevant to the metropolitan areas of DAGL and GAMA as they navigate rapid urbanisation.

Key lessons from these case studies emphasise the importance of integrated planning, which involves coordinating urban development with environmental considerations to prevent habitat fragmentation. Policy support is crucial, achieved through strengthened land-use regulations that ensure sustainable development practises. The strategic use of technological tools such as remote sensing and GIS is vital for monitoring land-use changes effectively. Additionally, prioritising green infrastructure and implementing mixed-use zoning can help mitigate habitat fragmentation by preserving natural spaces and promoting more compact urban forms. These strategies are essential for balancing urban growth with ecological sustainability, particularly in rapidly urbanising regions like Sub-Saharan Africa.

2.3.6 The overview and key issues of the study

2.3.6.1 Overview

Urban sprawl dynamics in metropolitan areas such as DAGL in Togo and GAMA in Ghana reflect a complex interplay of historical, demographic, and ecological factors that have shaped their current urban landscapes. Lomé's expansion began in the late 19th century, driven by trade activities and colonial infrastructure development, which established it as a major economic hub. By the mid-20th century, rapid population growth and urbanisation fuelled its transformation into a sprawling metropolis, with significant environmental consequences (Biakouye, 2014; Bawa *et al.,* 2021). Similarly, GAMA has experienced accelerated urban growth over the past few decades due to high population influx and economic development. This expansion has led to extensive land-use changes, including the conversion of vegetative cover and farmlands into residential areas, resulting in ecological degradation and challenges to sustainable development (Osei *et al*., 2013; Agyeman, 2018). Both cities are now grappling with critical issues stemming from urban sprawl, including the degradation of ecosystem services. These dynamics underscore the need for integrated urban planning approaches that balance development with ecological preservation. Sustainable strategies such as eco-city models, affordable housing policies, and green infrastructure could mitigate the adverse impacts of urban sprawl while supporting resilient metropolitan growth.

2.3.6.2 Discussion of key issues

In both Togo and Ghana, the regulatory frameworks for preserving nature and ecosystems in urban areas are supported by constitutional provisions, laws, policies, and regulations. In Togo, the Constitution of 1992 guarantees the right to a healthy environment, serving as a foundation for environmental policies. Key legislation includes the Environment Framework Act No. 2008-005, which addresses waste management, pollution, and ecosystem conservation. In Ghana, the Constitution vests public lands in the President on behalf of the people, ensuring natural resources are managed in the public interest. Key legislation includes the Environmental Protection Agency (EPA) Act 490 (1994), which regulates activities impacting the environment, such as pollution and deforestation, critical in urban areas. Both countries face institutional challenges that impede the effective implementation of constitutional, legal, and policy goals. In Togo, inadequate resources and governance hinder the effectiveness of environmental policies. In Ghana, decentralised urban planning is compromised by unfavourable political environments and inadequate institutional capacity (Abubakari *et al.*, 2023). Limited human and financial resources restrict participatory planning processes and sustainable urban development projects. Strengthening institutional capacities and enhancing community participation are crucial for improving the sustainability of urban ecosystems.

Several initiatives are underway to address urban ecosystem challenges. In Togo, new funding rules for local authorities offer potential support for environmental initiatives, while in Ghana, decentralised urban planning and Community Resource Management Areas (CREMAs) are being explored to sustain urban commons and promote community participation in natural resource management. Ghana's National Urban Policy and Action Plan promote sustainability in urban development, but implementation is challenged by inadequate resources and governance (Anarfi *et al*., 2020). These initiatives demonstrate a commitment to addressing urban ecosystem challenges, but their success depends on effective implementation, strengthened capacities, and enhanced community participation.

In assessing the impact of urban sprawl dynamics on ecosystem services in metropolitan areas like Grand Lomé in Togo and GAMA in Ghana, it is crucial to consider regulatory, institutional, and programmatic factors. Despite existing literature highlighting the significant impacts of urban sprawl on ecosystem services, critical gaps persist in addressing its socio-environmental consequences. Urban sprawl involves a complex interplay between urban development and ecological health, with studies documenting changes in land use and their ecological consequences. However, there remains a notable gap in localised assessments within specific metropolitan areas like Grand Lomé and GAMA. While some research has addressed Land Use and Land Cover (LULC) changes in these regions, there is insufficient exploration of how these changes affect ecosystem services. Addressing these gaps is essential to enhance urban planning efforts that balance development with ecological sustainability. This research aims to fill these gaps by evaluating spatial and temporal changes in urban expansion, analysing variations in ecosystem service provision, and exploring the intricate relationship between urban development dynamics and ecosystem provision.

A key aspect of this study is its methodological approach, which incorporates buffer and directional analysis techniques that have not been adequately addressed in previous research on urban expansion. Furthermore, this research focuses on critical ecosystem services such as flood risk control, urban cooling, and carbon storage services that have not been thoroughly evaluated in prior studies despite their importance in mitigating climate change impacts in rapidly growing cities. The decline of these services can exacerbate vulnerabilities to climate-related hazards, making it imperative to assess their status within the context of ongoing urban development in Grand Lomé and GAMA. By addressing these critical gaps, this study will contribute valuable insights to inform sustainable urban planning strategies that prioritise ecological resilience and position ecosystem services as foundational to sustainable urban development. This approach is particularly relevant in regions like Ghana and Togo, where urbanisation is rapidly encroaching on natural habitats, leading to biodiversity loss and ecosystem degradation.

CHAPTER THREE

3.0 MATERIALS AND METHODS

3.1 Description of the Study Area

3.1.1 Study location and it's environment

The areas of interest in this study are the District Autonome du Grand Lomé (DAGL) in Togo and the Greater Accra Metropolitan Area (GAMA) in Ghana, which cover 382 km^2 and 1585 km^2, respectively. Both capital cities are located on the Atlantic coast of the Gulf of Guinea (Figure 3.1). DAGL lies on a geographic coordinate from latitudes 6º08'14'' N to 6º15'00'' N and between longitudes 1º12'45'' E to 1º12'25'' E. In contrast, GAMA extends geographically from latitudes 5°5′27″ N to 5°28′2″ N and stretches between longitude 0°4′58″ E to 0°37′2″ W.

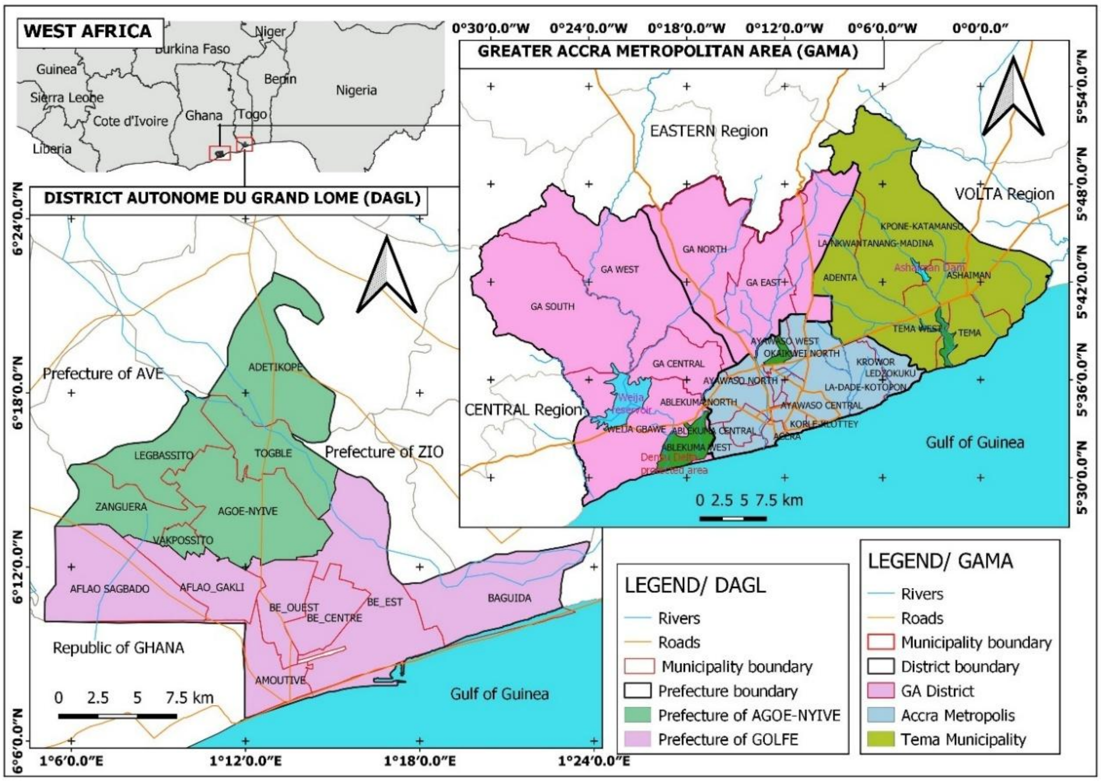

Figure 3.1: The Study Area

Source: Author, 2023

3.1.2 Climate

DAGL experiences subequatorial climate characterised by a bimodal pattern of two wet seasons (March to July and September to October) and two dry seasons (November to February and August) (Figure 3.2). As depicted on the Umbrothermal diagram, the average monthly temperature in DAGL ranges from 28 to 30 degrees Celsius throughout the year. The warmest periods are concentrated around March and April, while July and August appear to be slightly cooler. On average, DAGL experiences approximately 880 mm of annual rainfall, with peak precipitation occurring in June.

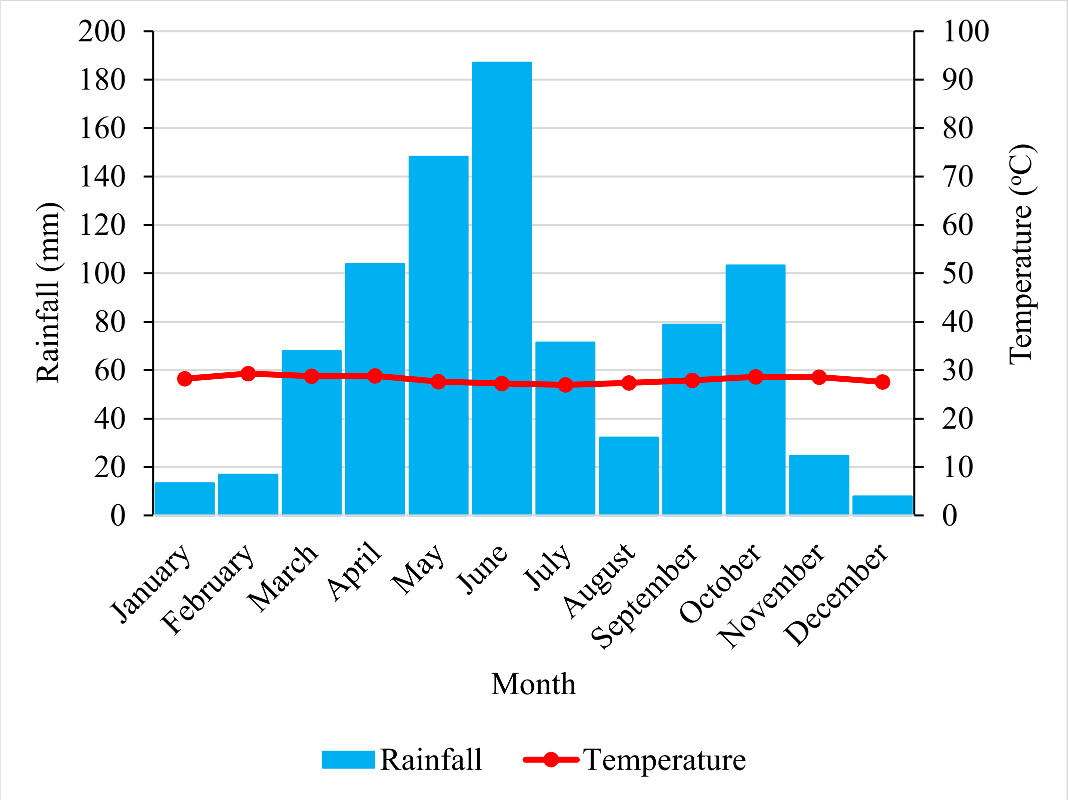

Figure 3.2: Umbrothermal diagram of DAGL from 1992 to 2022

Data source: Togolese meteorological office, 2023

In contrast, GAMA exhibits a tropical climate characterised by a bimodal rainfall pattern, with the primary wet season occurring from approximately April to June, peaking in June, and a minor wet season in October. The driest months are from July to September, with a notable decrease in rainfall during August, and again from December to February (Figure 3.3). Based on the Umbrothermal diagram, the annual rainfall is approximated to around 825 mm. The average temperature ranges between 27 ºC and 31ºC.

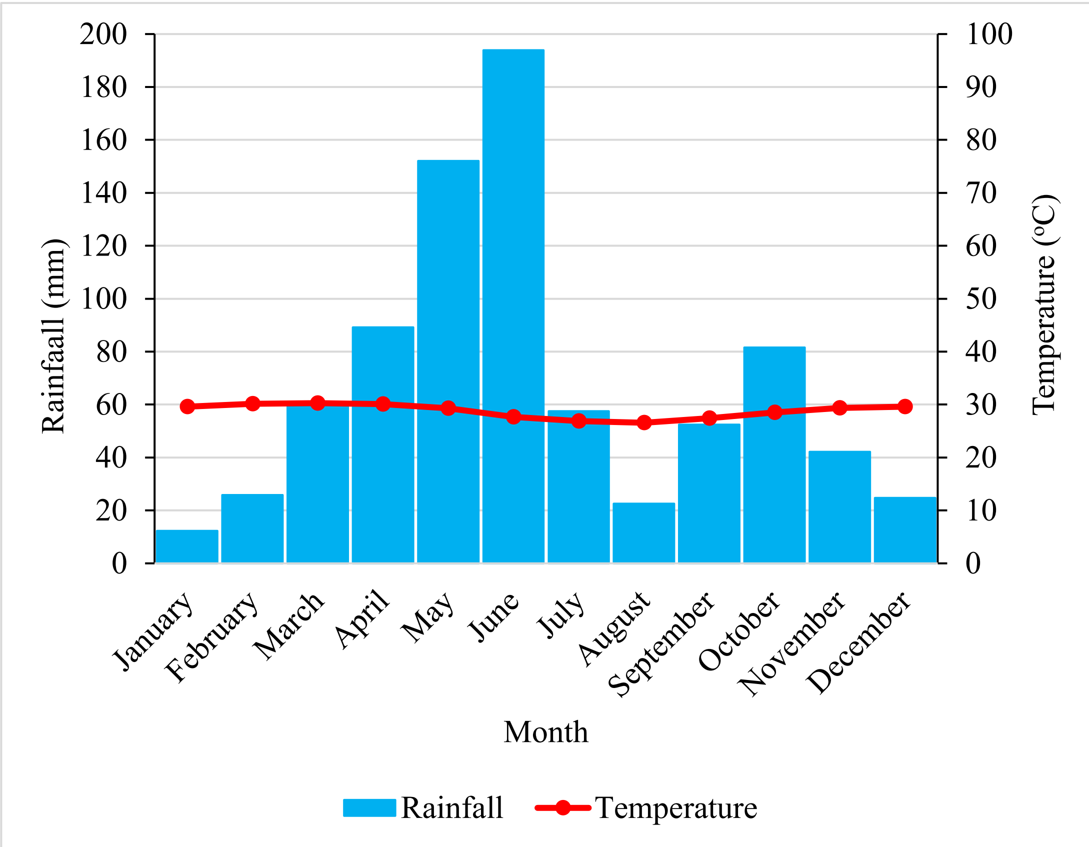

Figure 3.3: Umbrothermal diagram of GAMA from 1992 to 2022

Data source: Ghana Meteorological Agency, 2023

3.1.3 Soil, vegetation and hydrology

The soils in the coastal area of Togo that comprises Lomé is made up of fluvial-lagoon and maritime deposits with a texture ranging from sand to clay. The poorly developed soils of the floodplain depression are almost all hydromorphic, with Gley or pseudogley (characterised by poor drainage and waterlogging). They are sometimes salty and generally unsuitable for local crops, with the exception of bare land. On the other hand, GAMA is characterised by a diverse range of soil types, with a dominance of ferric acrisols accompanied by ferric luvisols (Schlüter, 2006). This variation in soil types contributes to the region's ecological diversity. Additionally, the soil texture in GAMA is marked by a mix of sandy, clayey, and loamy soils, which influences water retention, nutrient availability, and overall soil health (Owoade *et al*., 2020).

DAGL is characterised by a diversity of vegetation cover. The region features tree and shrub savannahs, herbaceous communities, and a few forest islands. Additionally, there are wetland areas such as mangroves and seagrass beds, which play a crucial role in the local ecosystem (Akpagana and Bouehet, 1994; Kokou, 1998; Afidégnon, 1999; Foucault *et al*., 2000). However, demographic pressure and rapid urbanisation threaten the natural habitats of Grand Lomé. Conservation efforts are necessary to protect the forest islands and maintain local biodiversity for the sustainable development of the region.

In contrast, the vegetation of GAMA is made up of savannah and herbaceous communities composed by trees and shrub savannahs. Also, GAMA is characterised with some wetlands, such as mangroves which play essential roles in the local ecosystem by providing habitats for various species and protecting coastal areas (Gyimah *et al*., 2023). On the other hand, it's believed that a large portion of the region was formerly covered in dense forest but has since disappeared due to human activity, rapid urbanisation and climate change posing challenges for biodiversity conservation (Addae and Oppelt, 2019).

The southern Togo is drained by three main rivers (Mono, Zio and Haho), smaller rivers (Boko, Gbaga and Elia), three main lagoon water bodies (Lake Togo, Lake Boko and Aného Lagoon) as well as permanent and/or temporary ponds and pools. Ghana on his own, is drained by many rivers such as Volta River basin which it shares with Burkina

Faso, Togo, Cote d'Ivoire and Mali, the Bia and Tano River basins, Weija reservoir and dansu river (Water Resource Management, (WRM)).

3.1.4 Population trend

The urbanisation process in sub-Saharan Africa is a crucial element of its population dynamics. The population growth has accelerated rapidly since the end of World War II and especially after independence (Dubresson, 1996). This rapid urbanisation process has been characterised by a shift towards capital cities, particularly in the coastal regions and immediate hinterlands (Gayibor *et al*., 1998). The population of DAGL and GAMA has experienced significant evolution over the past few decades. As the capital and largest city in Togo and Ghana respectively, they have attracted people from rural areas and neighbouring countries, leading to rapid urbanisation and population growth transforming them into the largest and most dominant urban centre. From 1960 to 2022, there has been a significant increase in the population of DAGL and GAMA (Biakouye, 2014; GSS, 2021; INSEED, 2022) (Figure 3.4).

Especially in 1986, in DAGL, the urban population was relatively low, with many areas characterised by rural features and basic infrastructure. By the year 2001, urbanisation accelerated due to increasing migration from rural areas, driven by economic opportunities (Biakouye, 2014). The trend continues in 2015, as DAGL became more cosmopolitan, with the improvement of public transport and health facilities. In 2023, DAGL has transformed into a big urban centre with a high rate of urbanisation. As of the latest estimates from the General Census on Population and Habitat (INSEED, 2022), DAGL has a population of over 2 million people (2,188,376 inhabitants) with an annual growth rate of 2.6 %. This can be explained by the economic growth driven by trade and investment opportunities that also attract migrants across the neighbouring countries.

Current policies focus on inclusive urban development that addresses housing shortages and promotes economic opportunities for all residents.

In contrast, in 1991, GAMA was characterised by a relatively low population density and limited urban infrastructure, with much of the area still rural. By 2002, urbanisation began to accelerate due to increased economic opportunities and infrastructural developments, including housing and transportation projects. The period leading up to 2017 saw GAMA experiencing substantial urban sprawl, with the urban built-up area expanding significantly. Key developmental activities included the construction of new residential areas and improvements in public transport systems, which were crucial in attracting immigrants seeking better living conditions and job opportunities. In the years 2023, GAMA has a population exceeding 5 million residents (5,455,692 inhabitants), with an estimated growth rate of 2.9 % based on the Ghana Statistical Service (GSS, 2021)**.**

Table 3.1 reveals that both cities have experienced rapid urbanisation leading to higher population density. DAGL's density growth is particularly striking. In contrast, GAMA's lower density despite a larger population suggests a more extensive area of development. However, the growing population still poses significant challenges related to urban management and environmental sustainability. Economic opportunities, better infrastructure, and improved living conditions have been primary drivers of this influx. This growth has resulted in increased demand for housing, services, and infrastructure, presenting both opportunities and challenges for urban planning and sustainable development in the two cities.

Table 3.1: Populations and Population Density in DAGL and GAMA

City	**Pop 1960**	**PD 1960**	**Pop 1981**	**PD 1981**	**Pop 2000**	**PD 2000**	**Pop 2010**	**PD 2010**	**Pop 2022**	**PD 2022**
DAGL	85,000	223	390,000	1,021	600,000	1,571	1,570,000	4,110	2,188,376	5,728.73
GAMA	449,430	284	1,922,898	1,213	2,905,726	1,833	3,656,423	2,307	5,455,692	3,442.07

Pop = Population PD = Population density (persons per square kilometre)

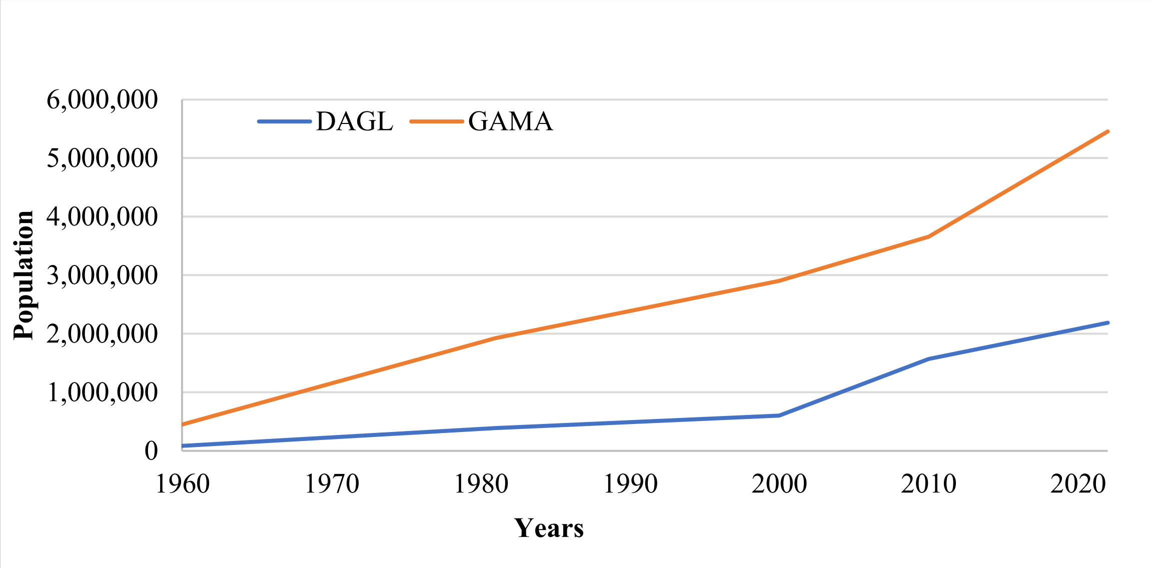

Figure 3.4: Population growth in DAGL and GAMA

Source*:* (Biakouye, 2014; GSS, 2021; INSEED, 2022)

3.1.5 Socio-economic activities

Togo's coastline has many sectors of activity that contribute to the life of the population. Among which fishing, maritime trade, financial, commerce of all kinds, agriculture, industry, tourism, mining, import and export infrastructure. It is a location that attracts human settlements and associated activities, primarily focusing on commerce and transportation. The services provided by the marine and coastal ecosystems play a very important role in the country's economy accounted for at least 70 % of Togo's GDP. Again, the informal sector is also developed especially in Lomé due to the high rate of unemployment with a dominance of women 54 % (Bawa *et al.*, 2021). However, the environmental dynamic implies impacts and opportunities facing these sectors or functions.

The city of GAMA also serves as an administrative centre, communication as well as an economic centre in Ghana and is home to over 70 % of the country's manufacturing industries. The leading occupational sector is sales, which employs majority of the region's economically active population with a larger proportion of the population in the city employed in the informal sector (Ghana Statistical Service). Agriculture is among the least employing sectors in GAMA.

3.2 Materials

3.2.1 Data type

3.2.1.1 Remote sensing data

The dataset used in the research includes multi-sensor remote sensing images provided by the United States Geological Survey (USGS) for the periods of 1986 to 2023 covering DAGL and from 1991 to 2023 for the Greater Accra Metropolitan Area (GAMA), all with less than 10 % cloud cover. The images were generated by several Landsat sensors, including Landsat 4 Thematic Mapper (TM) from 1986, Landsat 7 Enhanced Thematic Mapper Plus (ETM+) from 2001 and 2002, and Landsat 8 Operational Land Imager (OLI) and Thermal Infrared Sensor (TIRS) from 2015, 2017, and 2023 (Table 3.2).

In the selection of satellite imagery in this study, images with less than 10 % were used as criteria. Therefore, the image analysis for the Greater Accra Metropolitan Area (GAMA) actually began with 1991 imagery due to the lack of quality satellite imagery prior to that year. High-resolution Google Earth images from 2002, 2015, 2017, and 2023, along with global settlement characteristics data from 2018 and the World Settlement Footprint from 2015, were utilised for training and evaluating classification accuracy. Additionally, above-ground biomass data was obtained from the Earthmap.org platform, developed in collaboration with the FAO, while evapotranspiration data was sourced from the Google Earth Engine (GEE) platform. The hydrologic soil group (HSG) was obtained from global hydrologic soil groups [HYSOGs, Ross *et al*. (2018)].

Table 3.2: Summary of the Remote Sensing Dataset Used for Land Use and Land Cover Mapping in the Study

Area	Satellite	Sensor	Spatial resolution	Date
DAGL	Landsat 5	TM	30m	March, 1986
	Landsat 7	ETM+	30m	December, 2001
	Landsat 8	OLI/TIRS	30m	December, 2015
	Landsat 8	OLI/TIRS	30m	December, 2023
GAMA	Landsat 4	TM	30m	December, 1991
	Landsat 7	ETM+	30m	December, 2002
	Landsat 7	ETM+	30m	December, 2017
	Landsat 9	OLI/TIRS	30m	December, 2023

3.2.1.2 Ground data

The ground truth data used for image classification was collected through field surveys, employing a stratified sampling method to ensure comprehensive coverage of diverse land cover types. This method involved selecting locations to represent various land cover categories such as forest, grassland, built-up areas, water bodies, and agricultural land in both cities. A Garmin Etrex GPS device was utilised to record the precise geographical coordinates (latitude and longitude) of the visited locations (see Appendix C). For areas that were difficult to access during the field campaign, supplementary data was obtained from Google Earth Pro to support the validation process.

3.2.1.3 Climate data

The climatic data such as temperature, precipitation, and humidity data from 1986 to 2022 were obtained from the Togolese meteorological office (DGMN) and Ghana Meteorological Agency (GMet).

3.2.1.4 Data from literature

In the ecosystem services (Ess) assessment, data from literature were used as a proxy to create carbon pool for carbon storage and sequestration. The carbon stored in Aboveground Biomass value was obtained from the Intergovernmental Panel on Climate Change's IPCC (2006) methodology for determining greenhouse gas inventories in the Agriculture, Forestry and Other Land Use (AFOLU) taking into account the climate domain and ecological region. This value obtained from the IPCC (2006) was compared with the value obtained from the ESA CCI Global Forest Above Ground Biomass on Earth Map to get a mean value and ensure the reliability. The carbon in belowground biomass and the dead organic matter was obtained using the conversion factors provided in the IPCC (2006). The carbon stored in Soil value was obtained from the work of Owoade *et al*. (2020) on land use effects on Soil Carbon Accretion and Productivity in the Coastal Savanna Agro-ecological Zone of Ghana.

3.3 Methods

3.3.1 Spatial and temporal changes in the sprawl of urban areas and change in LULC in DAGL and GAMA

3.3.1.1 Land cover mapping

i. Image processing and classification

The Landsat images were imported into the Google Earth Engine (GEE) platform from the US Geological Survey (USGS) as the primary input. A median filter was used to integrate the Landsat data from each year into a composite image. For additional processing and analysis, the areas of interest were extracted from the feature collection for data normalisation. For the classification, the stratified random sampling technique was used to create training polygons for each land cover type identified in the study areas. The training samples were collected from various sources, including Google Earth Pro, World Settlement Footprint, Global Settlement characteristics, field visits and GEE base maps (Olofsson *et al*., 2014). Ground-truth samples were collected during the field visits in DAGL and GAMA for the year 2023.

The QGIS interface facilitated the collection of points from the reference data, specifically the World Settlement Footprint 2015 and Global Settlement characteristics 2018 obtained from GEE. The 'historical imagery' tool in Google Earth Pro allowed visualisation of Google Maps from previous years 2001, 2002, 2015, 2017. The training data was then entered as a feature collection table into the GEE. The training data were created by examining the LULC types through spectral indices and visual interpretation of the land features. To enhance the classification accuracy, specific indices were computed for each composite image and added to the band set, including the Normalised Difference Vegetation Index (NDVI) for identifying vegetation cover, the Normalised Difference Built-up Index (NDBI) for distinguishing urban areas and the Normalised Difference Water Index (NDWI) for detecting water bodies (Loukika *et al*., 2021) (equations 3.1; 3.2; 3.3). The geometry tool was used to design training sites for the defined classes.

Thirty percent (30 %) of the training datasets were utilised as validation sets, while seventy percent (70 %) were used for training. Based on spectral characteristics of the image and literature knowledge, five LULC classes were defined for the purpose of the study (Table 3.3). The Random Forest (RF) algorithm, a classifier under the supervised classification in the GEE was used to classify the images into five classes for each city using the "ee. Classifier.smileRandomForest" function. The supervised classification is preferred in this study for its capability to identify a certain type of land cover based on provided training data as illustrated in Figure 3.5. One significant advantage of the RF classifier is its capacity to manage high-dimensional data with complex interactions between variables, although it is somewhat sensitive to input data errors (Hengl *et al.*, 2015).

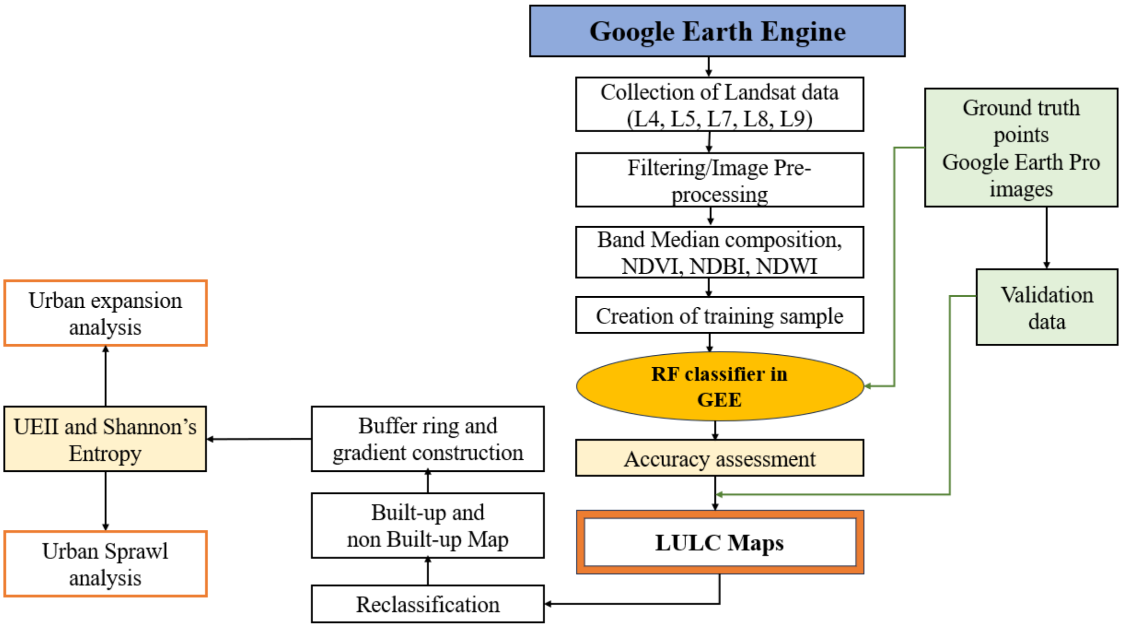

Figure 3. 5: Flow chart of the research methodology

Additionally, this classifier has demonstrated exceptional performance compared to other classifiers, achieving higher accuracy in land cover mapping and projections across Africa and various regions worldwide (Yang *et al.*, 2017; Loukika *et al.*, 2021). Moreover, DAGL and GAMA present a complex landscape, making GEE an efficient tool for mapping LULC due to its faster visualisation and its analytical capabilities. RF combines multiple Classification and Regression Trees (CART) to create an ensemble classifier. It generates several decision trees through random selection of variables and training datasets, and evaluates its performance using non-training examples to provide an objective assessment of generalisation error (Breiman, 2001). The two key user-defined input factors are the number of parameters and the number of trees, with literature suggesting that the ideal number of variables is the square root of the total variables, and the ideal number of trees ranges from 100 and 500 (Belgiu and Dragut, 2016). Additionally, one-third of the training data are used to determine the prediction

error, while two-thirds is used to construct the random forest model that facilitates the assessment of the accuracy of each analysis.

$$NDVI = \frac{(NIR-Red)}{(NIR+Red)} \tag{3.1}$$

$$NDBI = \frac{(SWIR-NIR)}{(SWIR+NIR)} \tag{3.2}$$

$$MNDWI = \frac{(Green-SWIR)}{(SWIR+SWIR)} \tag{3.3}$$

Table 3. 3: Description of Land Use and Land Cover Classes

LULC types	**Description**
Forest	Forest reserves, Land dominated by trees
Grassland	Mixed grassland with scatter trees, Herbaceous vegetation, shrub, garden, parks
Agricultural land	Irrigated and rainfed croplands, plantations, pastures
Built-up/ Bare-land	Residential, industrials and Commercials units, Highways and transportation, power and communications facilities, lands with exposed soil surface, exposed rock, quarries and gravel pits
Water-bodies	Lakes, rivers, streams, canals, reservoirs, lagoons

ii. Accuracy assessment

After the completion of the classification process using a machine learning algorithm (RF), an accuracy assessment was carried out using an error matrix to ascertain the accuracy of the classified images. Since the accuracy measures the degree of agreement between the classified image and baseline data, the quality of the result after classification, is critical for change detection analysis (Mosammam *et al*., 2016). The accuracy of the different classified images was assessed in this study in order to measure the quality of the classification results. An algorithm included in GEE, called a confusion matrix, verifies and then assesses the image's classification accuracy. The accuracy evaluation of LULC maps was conducted using the validation error matrix that was generated in GEE. The correlation between known ground or reference data and the corresponding results of automated classification is compared in the error matrix. The overall accuracy (OA), user's accuracy (UA), and the producer's accuracy (PA), Omission error (OE) and Commission error were calculated. The Overall accuracy is the whole accuracy of the classified images and it is expressed as a percent, with 100% accuracy being where all reference site were classified correctly. User's accuracy is the probability that a pixel classified in a given class of the map represents that class on the ground or how often the class on the map will truly be present on the ground. The Producer accuracy is the probability that a pixel was correctly classified in a given class or the probability that a certain land cover of an area on the ground is classified as such (Jain *et al.*, 2016). Error of commission is the prospect of an explicit class which is incorrectly classified on the ground. Whereas Error of omission is the prospect of an explicit class to be incorrectly classified in the reference data (Frimpong *et al.*, 2022). The formulae for calculating these accuracies are stated below (equations 3.4 to 3.8) (Kotapati *et al.*, 2021; Nasiri *et al.*, 2022):

$$\text{Over all accuracy (OA)} = \frac{\text{Number of Correctly classified Samples}}{\text{Number of Total Samples}} \times 100 \tag{3.4}$$

$$\text{UA} = \frac{\text{Number of Correctly Classified Samples in each Class}}{\text{Number of Samples Classified to that Class}} \times 100 \tag{3.5}$$

$$\text{PA} = \frac{\text{Number of Correctly Classified Samples in each Class}}{\text{Number of Samples from Reference Data in each Class}} \times 100 \tag{3.6}$$

$$\text{OE} = \frac{\text{Number of Incorrectly classified Samples}}{\text{Number of Samples from Reference Data in each Class}} \times 100 \tag{3.7}$$

$$\text{CE} = \frac{\text{Number of Incorrectly classified Samples}}{\text{Number of Samples Classified to that Class}} \times 100 \tag{3.8}$$

iii. Change detection

To determine the differences between the identified time series images used in this study, a change detection analysis was carried out (Wiafe and Asamoah, 2018). The LULC post-classification within the Semi-Automatic Classification Plugin (SCP) in the QGIS interface was used to analyse temporal changes in DAGL (1986-2001, 2001-2015, 2015-2023 and 1986-2023) and for GAMA (1991-2002, 2002-2015, 2015-2023 and 1991-2023). A pixel-by-pixel cross-tabulation analysis was used to analyse cross-classes conversions. The magnitude of change between years (absolute change), and average annual rate of change (%) were then computed from the change matrix using the equations below (Long *et al*., 2007; García-Álvarez *et al*., 2022). The absolute change and the annual rate of change were then calculated. The absolute change was computed by subtracting the area of land cover of the initial year (AreaYear-x) from the area of land cover for the subsequent year of the following data (AreaYearx+1). The average annual rate of change was computed by subtracting the initial area from the final area. Next by dividing this difference by the initial area. Then, convert this result into a percentage by multiplying by 100 and dividing the result by the number of years between the initial year and final year (Long *et al*., 2007). The formula is stated in equation 3.9, and 3.10.

$$\text{Absolute change}, AC = A_{t2} - A_{t1} \ (\text{km}^2) \qquad (3.9)$$

Positive percentage values suggest an increase whereas negative values imply a decrease in area coverage.

$$\text{C} = \frac{\frac{(B_2 - B_1)}{B_1} \times 100}{T_2 - T_1} \qquad (3.10)$$

Where C is the average annual rate of change, B_1 is the area of land cover type in time 1 (T_1); and B_2 is the amount of land cover type in time 2 (T_2).

3.3.1.2 Urban expansion analysis

An urban built-up map was generated by extracting the built-up images from the classified images. Following the extraction, built-up maps were overlaid, and the resulting images were recorded. For each image in the two cities, the urban expansion intensity index (UEII), a crucial metric that shows the rate or speed of urban expansion at various times, was determined (equation 3.11). Around a selected centre point, fourteen concentric multiple-ring buffer zones were constructed with 2 km intervals for DAGL, while twenty were constructed for GAMA. The independence square representing the city centre was chosen for DAGL while the central business district, Makola market circle, was chosen as the centre point for GAMA for generating the buffer zones. These points were generated from the Google Earth pro-interface. The 2km interval is found to be an appropriate scale that captures the key spatial details of urban features and the number of rings generated depends on the size and spatial extent of each city. Additionally, to identify the trend of urban spatial patterns in various directions, the direction-wise method has been used (Cao *et al*., 2019; Kafy *et al*., 2020). An equal interval of 22.5 degrees for each direction was used which is well effective (Qian and Wu, 2019), and the study areas and the concentric ring were divided into sixteen directions. In order to quantify the expansion in different directions, a number of quadrants (Q) were generated and captured. There were some quadrants eliminated since they did not cover the study area boundaries. Finally, 7 and 8 quadrants were considered for DAGL and GAMA. The directional analysis reveals the area of the city that is expanding the fastest and identify key factors or divers. This is crucial to know where natural habitats are most at risk to develop conservative strategies and guide planning for future expansion.

$$UEII_i = \frac{ULA_i^{t2} - ULA_i^{t1}}{TLA_i \times \Delta t} \times 100 \tag{3.11}$$

where $UEII_i$ is the Urban Expansion Intensity Index of unit i; ULA_i^{t2} and ULA_i^{t1} are the areas of urban built-up land at times $t1$ and $t2$; TLA_i is the total land area within the study area i, and Δt is the study time period (i.e., $t2$ _ $t1$) (Akubia and Bruns, 2019). The *UEII* standard is scaled as follows: <0.28 is "very slow expansion"; 0.28 to 0.59 is "slow expansion"; 0.59 to 1.05 is "medium-speed expansion"; 1.05 to 1.92 indicate "high-speed expansion"; and >1.92 is "very high-speed expansion" (Akubia and Bruns, 2019; Norouzi, 2023).

Moreover, the density of urban expansion in each buffer zone for each city was computed using the formula adopted from (Stemn *et al*., 2014) to ascertain its relationship with the city centre.

$$Density\ \text{urban expansion} = \frac{\text{Amount of spatial urban expansion in each buffer zone}}{\text{Total amount of land in each buffer zone}} \tag{3.12}$$

3.3.1.3 Urban sprawl quantification

For Shannon's entropy calculation, the total number of pixels in each buffer, the amount of built-up in each zone, and the total number of built-up areas were computed using the zonal statistics tool in ArcGIS. The results of the zonal statistics for each image were saved and exported to the Microsoft Excel table where further calculations using the Shannon entropy formula were applied. Shannon Entropy measures the compactness and or dispersion of built-up area among n zones (Rahman, 2016). The Relative Shannon Entropy (RSE) value for each and overall ring buffers for each year has been calculated using the formula below (equation 3.13; 3.14; 3.15).

$$\text{Absolute entropy} = \sum_i^n Pi\ log(\frac{1}{Pi}) \tag{3.13}$$

Where, En=the relative entropy

Pi=probability or proportion of built-up in the zone n = number of zones

$$Pi = Xi / \sum_i^n Xi \qquad (3.14)$$

However, it's more suitable to rescale the entropy value into the range of 0 and 1. This can be done by computing the relative entropy (En) which is expressed bellow (equation 3.15)

$$En = \sum_i^n Pi \, log(\frac{1}{Pi}) / Log(n) \qquad (3.15)$$

Where

Xi= the density of developed land, which equals to the amount of built-up land divided by the total amount of land in the i^{th} zone in n total zones.

The value of Shannon entropy ranges from 0 to log n. Value of 0 indicates that the distribution is a very compact and high-density urban development nearer to 1 indicates low-density urban development and high degree of urban sprawl (Malligai and Jegankumar, 2018).

3.3.2 Distribution and variation in the provision of selected ecosystem services in DAGL and GAMA.

To assess the spatial and temporal distribution and variation of these ecosystem services, the InVEST model (Integrated Valuation of Ecosystem Services and Trade-off) was used.

3.3.2.1 Structure of the model

The InVEST model quantifies and maps the values of ESs. It relies on geographic data to produce maps that illustrate the spatial distribution of ecosystem services. InVEST requires predominantly GIS or map data as inputs, along with information tables typically formatted as CSV files. Once the data is inputted, the model processes it to generate outputs that include maps, quantitative data on ecosystem services, and various statistics and reports. The interface allows users to easily navigate through different models. The modules under the InVEST Model are focused on key ESs (Figure 3.6).

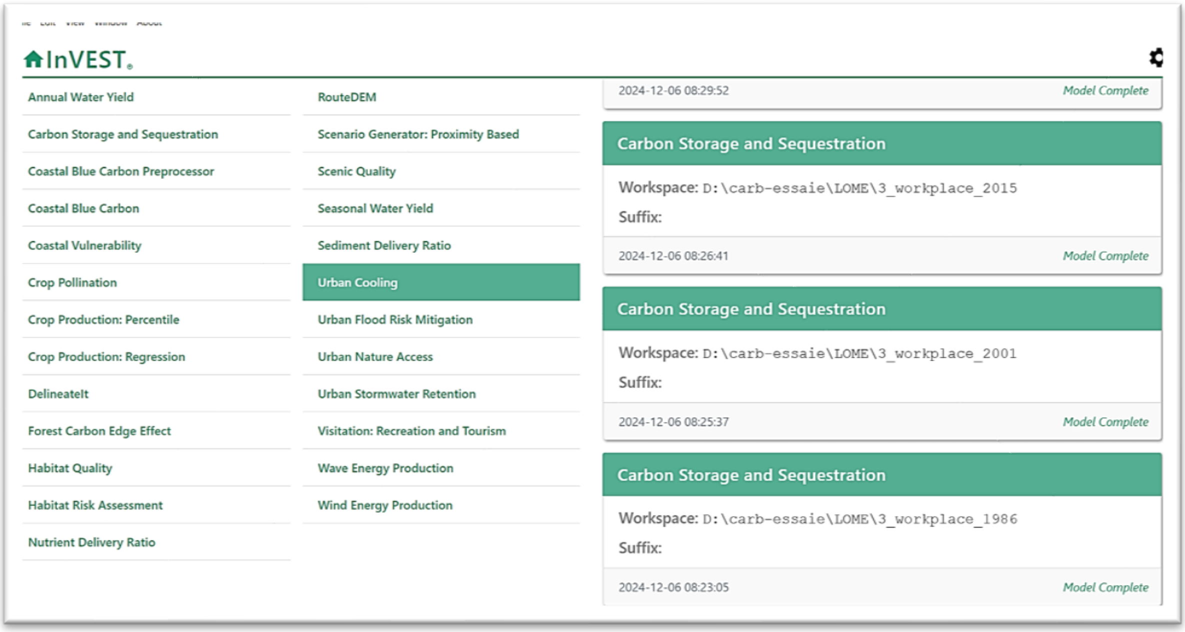

Figure 3. 6: InVEST model interface

3.3.2.2 Model description

i. Carbon storage and sequestration

The InVEST carbon storage and sequestration Model calculates the total carbon stored in the landscape by summing the carbon in all four pools for each pixel, based on the LULC type of that pixel (equation 3.16). The InVEST Carbon Sequestration Model operates on the premise that different Land Use and Land Cover (LULC) types store varying amounts of carbon in different pools. The model calculates both the total carbon stocks at a given time and the changes in carbon stock over time, which is referred to as carbon sequestration.

Carbon Storage :

$$Ci = Ci_{(above)} + Ci_{(below)} + Ci_{(soil)} + Ci_{(dead\ matter)} \tag{3.16}$$

where Ci represents the total carbon storage of grid cell i

$Ci_{(above)}$ = Carbon stock in aboveground biomass

$Ci_{(below)}$ = Carbon stock in belowground biomass

$Ci_{(soil)}$ = Soil carbon organic matter

$Ci_{(dead\ matter)}$ = Dead organic matter

Carbon variation over years (equation 3.17):

$$S = C^{T2} - C^{T1} \qquad (3.17)$$

C^{T2}: carbon storage in previous year

C^{T1}: carbon storage in the current year

To run InVEST carbon storage and sequestration model, requires several input data such as the LULC map (classified map) of the different years under study and the carbon pool table. This table includes data on carbon stored in different pools such as aboveground biomass, belowground biomass, soil and dead organic matter (in metric tons per hectare) for each class of land cover. This table provides essential data on how much carbon can be stored in various ecosystems. Aboveground biomass comprises all live plant components above the ground, whereas belowground biomass contains the living root systems associated with aboveground plants. The largest terrestrial carbon store, soil organic matter, represents the important organic component of the soil, whereas dead organic matter covers litter as well as dead trees, either on the ground or in an upright posture (Sharp *et al.*, 2014). If data for a specific pool is unavailable, the carbon stock can be estimated using information from other pools. Additionally, existing literature on carbon storage may be utilised to estimate carbon storage in the study area (Abera *et al.*, 2021). For this study, the carbon pool data was derived from EarthMap (ESA CCI Global Forest Above Ground Biomass), the Intergovernmental Panel on Climate Change's IPCC,

(2006) methodology for determining greenhouse gas inventories in the Agriculture, Forestry and Other Land Use (AFOLU) sector considering the tropical shrubland climate domain of which are part the two cities, the work of Owoade *et al*. (2020) on soil physical and chemical properties for the different District Locations and Land use systems in the Coastal Savanna domain. To get direct carbon stock from the biomass, equation (3.18) was used.

$$Total\ Carbon\ Stock\ (ton\ metrics/ha) = \quad Total\ AGB\ \ X \quad 0.47 \tag{3.18}$$

Where AGB is aboveground biomass and 0.47 is the conversion factor of dry biomass suggested by (IPCC, 2006; Zaki and Latif, 2016). The carbon stored in the Belowground biomass was obtained from the Aboveground biomass carbon value using the conversion factor of the Root to Shoot Ratio provided by IPCC, (2006) and by Macdicken, (1997). The carbon pool table is shown in Table 3.4 for DAGL and in Table 3.5 for GAMA. The model typically assigns zero carbon stock values for built-up and water, as they do not contribute to carbon storage in the same way that vegetative and soil carbon pools do (Tadese *et al*., 2023).

Table 3.4: Carbon Pool for DAGL

LULC	C_above	C_below	C_soil	C_dead matter
Water	0	0	0	0
Built-up	0	0	0	0
Forest	34.3	6.06	147.24	2.1
Grassland	15	35	30	4
Agricultural land	15	35	30	4

Table 3.5: Carbon Pool for GAMA

LULC	C_above	C_below	C_soil	C_dead matter
Water	0	0	0	0
Built-up	0	0	0	0
Forest	32	6.06	147.24	2.1
Grassland	15	35	30	4
Agriculture-land	5	0.45	85.71	0

ii. The urban temperature regulation (Urban cooling capacity and heat mitigation)

The InVEST Urban Cooling Model is designed to estimate urban temperature regulation by calculating an index of heat mitigation. This index is derived from several key biophysical parameters: shade, evapotranspiration, albedo, and the distance to cooling islands such as parks. These factors collectively determine how effectively vegetation can reduce air temperatures in urban environments. Shade provision refers to the extent to which vegetation provides cover to surfaces, playing a critical role in directly lowering surface temperatures and reducing heat absorption. Evapotranspiration, the process through which water evaporates from soil and plant surfaces, contributes significantly to cooling as water vapour absorbs heat from the environment. Albedo, which measures surface reflectivity, influences the amount of solar energy absorbed or reflected; vegetation typically has a higher albedo compared to built surfaces, enhancing cooling effects.

The model outputs a heat mitigation index that quantifies the cooling capacity of the LULC type for a given pixel based on these parameters (equation 3.19) (Zardo *et al.*, 2017; Hamel and Remme, 2021). This index is the main output of the InVEST Urban cooling model and ranges from 0 to 1, where 0 means no heat is mitigated in a cell and 1 means the UHI is fully mitigated.

$$cc\ (i) = W_s \cdot S(i) + W_A \cdot A(i) + W_E \cdot E(i\ ) \tag{3.19}$$

Where CC(i) is the cooling capacity index (the extent to which a specific green space contributes to temperature reduction compared to its surroundings). The average cooling capacity is quantified on a scale from 0 to 1, where a value of 0 indicates no cooling capacity (typical of areas devoid of vegetation or those with ineffective green spaces) while a value of 1 signifies maximum cooling capacity within the study area.

S(i) (Shade) is the capacity of trees to provide shading, ranging from 0 to 1, 0 for no tree and 1 for full tree cover of height > 2 m;

A(i) (Albedo) ranging from 0 to 1, with 1 indicating maximum reflectance of solar radiation, and 0 indicates maximum absorption; E(i) is the evapotranspiration index for the pixel i. They are each weighted by a coefficient W_S, W_A, and W_E (0.6, 0.2, 0.2, respectively) constant across the study area. These weights assigned to the model's recommendations are based on empirical data.

Inputs for the InVEST Urban cooling Model include LULC raster, a raster reference evapotranspiration obtained from GEE platform, a vector of the area of interest, and a biophysical table. The biophysical table contains data on shade, crop coefficient (Kc, indicating the rate of evapotranspiration for the different land cover types), and albedo for each land cover types according to the parameters recommended the InVEST model (Hu *et al*., 2023) (see Appendix D). The InVEST model's recommended values were selected because they encompass a variety of urban land cover types that are typical of cities around the globe, including DAGL and GAMA. Numerous studies have confirmed these parameters, and they have been applied in diverse urban settings (Hu *et al*., 2023; Wu *et al*., 2024). In addition, a number of parameters need to be defined, such as the maximum cooling distance, air blending distance, UHI effect magnitude, and reference air temperature. For the maximum cooling distance, the InVEST model recommends using 450m as an estimate due to a lack of local studies. For the air blending distance, the model recommends an initial range of values from 500m to 600m (Schatz and Kucharik, 2014; Lonsdorf *et al*., 2021).

Due to the absence of local research, this value was obtained from the global surface UHI explorer by Yale University (https://yceo.users.earthengine.app/view/uhimap). The reference air temperature was obtained based on the data from the Togolese Meteorological office and Ghana Meteorological Agency (see Appendix E and F).

iii. Flood risk mitigation

The Flood Risk Mitigation model estimates the run-off production and retention over the study area. The precipitation (P in mm) received over the research region and the land use parameters serve as the primary foundation for the quantification of runoff. The Soil Conservation Service-Curve number (SCS-CN) approach uses the potential maximum retention ($S_{max,i}$) and CNi values for each pixel (i) to estimate the run-off production ($Q_{p,i}$) due to precipitation (P) (Equation 3.20). Equation 3.21 gives the empirical relationship between $S_{max,i}$ and CNi. For the study areas, an initial abstraction (λ) factor of 0.2 times of $S_{max,i}$ was taken into consideration. The Curve Number (CN) values, which are derived from the Hydrological Soil Group (HSG) and LULC, represent the hydrological behaviour of the study region at the pixel level.

Additionally, the model computes the run-off retention index (Ri), which is a ratio of the total precipitation over a pixel and the amount of precipitation retained (P–Q) (Equation 3.22). The volume of run-off retained ($R_{vol,i}$ m^3) is calculated by multiplying the run-off retention index per pixel (mm) with the area of each pixel (m^2), as shown in Equation 3.23. Similarly, the run-off generated ($Q_{vol,i}$ m^3) is calculated using Equation 3.24. The equations are sourced from the InVEST model User Guide (Natural Capital Project, 2023, https://naturalcapitalproject.stanford.edu/software/invest).

$$Q_{p,i} = \left\{\frac{(P - \lambda S_{max,i})^2}{P+(1-\lambda)S_{max,i}} \;\; if\ P > \lambda S_{max,i}\,;\ otherwise\ Q_{p,i} = 0\right\} \tag{3.20}$$

$$S_{max,i} = \frac{25400}{CN_i} - 254 \tag{3.21}$$

$$R_i = 1 - \frac{Q_{p,i}}{P} \tag{3.22}$$

$$R_{vol,i} = R_i.P.PixelArea \tag{3.23}$$

$$Q_{vol,i} = Q_{p,i}\,.PixelArea \tag{3.24}$$

The model requires the raster layer of hydrologic soil group (HSG) covering the study area. Each soil group is represented by A, B, C or D category with varying degrees of responsiveness towards the generation of run-off, LULC and curve number (CN) over the study area. The run-off curve numbers (CN) are dimensionless values which are empirical estimations for quantification of run-off depth from the rainfall events. The CN values are dependent on the Hydrologic soil group (HSG-A, B, C and D) and the LULC. Typically, the CN values vary between 0 and 100 representing the extreme values of low and high run-off generation. The CN values developed for urban environments by Chow *et al*. (1988) were adapted in the present study (see Appendix G).

3.3.3 Evaluate the relationship between urban expansion and ecosystem service degradation in DAGL and GAMA.

To achieve this, Pearson's correlation analysis was used in RStudio software to explore the interrelationships between the urban area, population density and Ecosystem Services (ESs). Pearson's correlation analysis is particularly suitable for this purpose and can better explain continuous data variables compared to other correlation analysis methods.

This study also uses the spatial regression analysis, specifically the Geographically Weighted Regression (GWR) model, to explore the spatial correlation between urban expansion and ecosystem services (Li and Zhao, 2019). The GWR model is chosen for its ability to capture spatial, providing more accurate results compared to traditional Ordinary Least Square (OLS) models (Li and Zhao, 2019; Shao *et al*., 2020; Zhang *et al*., 2020). To analyse the spatial relationship between urban expansion and ecosystem services, NDVI (Normalised Difference Vegetation Index) and NDBI (Normalised Difference Built-up Index) were used as key indices. NDVI serves as a proxy for vegetation health, while NDBI quantifies urban expansion. The GWR is expressed by Equation 3.25. The mean NDVI and NDBI were used as independent variables and carbon storage, urban cooling, flood mitigation risk as the dependent variables.

$$y_i = \beta_0(u_i, v_i) + \sum_{j=1} \beta_{j(u_i, v_i)} x_{ij} + \varepsilon_i \quad (3.25)$$

Where yi is the dependent variables (carbon storage, urban cooling, flood risk mitigation), xij is the jth independent variable at the ith location, εi is the random error at the ith location, (u_i, v_i) the spatial coordinates of location i, $\beta_{j(u_i, v_i)}$ is the coefficient of the jth variable at location i. In this study, GIS software was used to run the GWR model.

CHAPTER FOUR

4.0 RESULTS AND DISCUSSION

4.1 Results

4.1.1 Spatial and temporal changes in the sprawl of urban areas and the change in Land Use and Land Cover in DAGL and GAMA

4.1.1.1 Land use and land cover (LULC) change in the metropolitan areas

The LULC change assessment provides critical insights into the environmental transformation in DAGL and GAMA. The results derived from the classified maps (Figure 4.1) reveal substantial shifts in land use over the studied period. In both regions, the built-up areas have increased dramatically, while the surface covered by forests, grasslands, agricultural lands, and water bodies have declined. This trend suggests urban development over the past three decades.

In DAGL, the land use has shifted from primarily vegetated land in 1986, where agricultural land occupied 35.36 %, forest covered 24.04 %, and grassland 22.09 % to a major built-up area of 76 % by 2023. The agricultural land has decreased to 27.12 %, while forest and grassland have seen significant reductions, now covering 3.43 % and 3.88 %, respectively. Figure 4.2 visually represents the land cover changes and confirms the dramatic shift from natural land cover to built-up areas over the entire study period (1986-2023). Most of the land use and land cover types (agricultural land, forest, and grassland) have been substantially converted into built-up areas over time. This trend accelerates from 2015 to 2023 and confirms the intensifying urbanisation and its impact on natural landscapes.

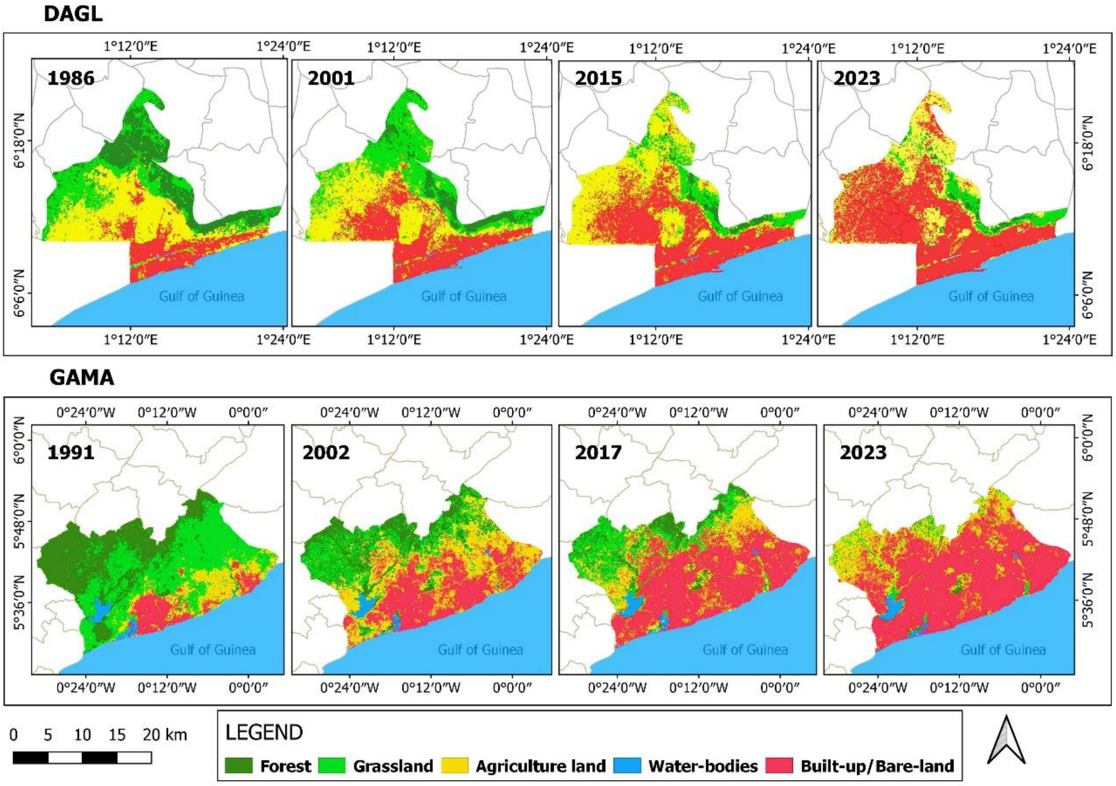

Figure 4.1 : Land use and land cover map of DAGL and GAMA

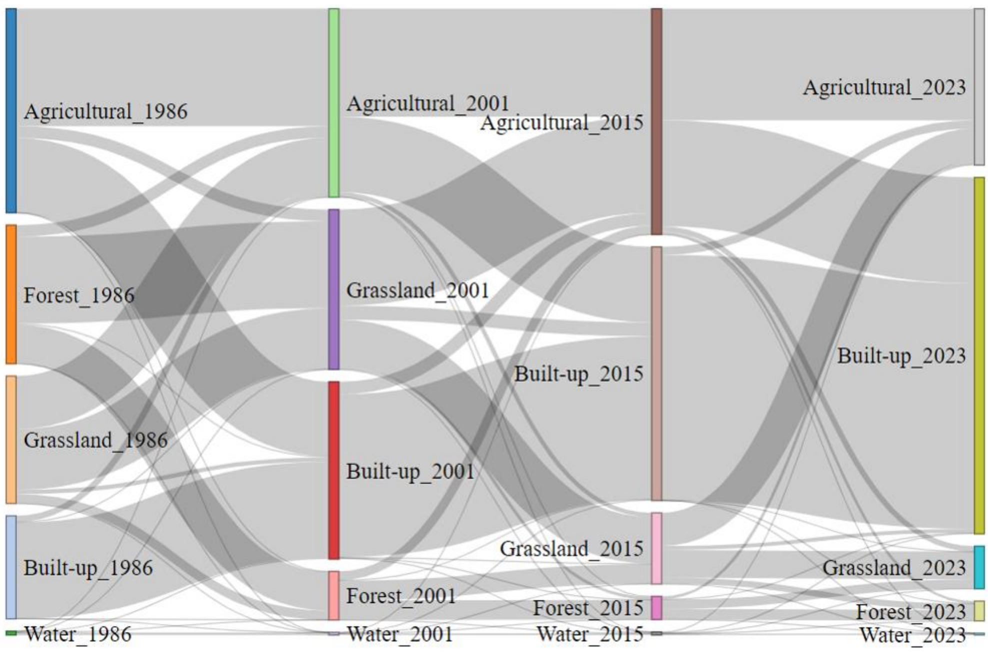

Figure 4.2: Land use and land cover change in DAGL in 1986, 2001, 2015, and 2023

The transition matrix table (Table 4.1) shows that between 1986 and 2001, built-up and bare land remained quite stable, with over 93% of these areas unchanged, but they also expanded noticeably into agricultural land (36.5%) and water bodies (31%), signalling early stages of urban growth encroaching on farmland and wetland. During this time, forest cover declined sharply, with only 28% remaining intact as most forest areas converted to grassland and some to agricultural use, reflecting deforestation and land degradation. Agricultural land held up moderately but was increasingly overtaken by urban development.

From 2001 to 2015 (Table 4.2), built-up areas continued to dominate, maintaining about 92% persistence while further converting agricultural land (40%) and water bodies (39%) for urban use. Although forest cover showed a slight rebound with 40% persistence, substantial portions still gave way to grassland and agriculture, pointing to continued pressure on natural ecosystems. In the most recent period, 2015–2023 (Table 4.3), urban areas grew even more intensively, built-up land persisted at nearly 97%, with nearly half of agricultural land converting to urban uses, alongside continued reduction of water bodies and surrounding lands. Forests remained fragmented and reduced, while grasslands shrank due to a mix of agricultural expansion and urban expansion.

The built-up area in DAGL was initially concentrated in the districts of Amoutive, Be Est, and Baguida, located along the coastal line, as of 1986. By 2001 and 2015, the built environment had expanded into the prefecture of Agoènyivé, encompassing the districts of Vakpossito and Agoènyivé. Additionally, development extended to Aflao Sagbado and Aflao Gakli, two districts within the prefecture of Golf. These areas were previously used for agricultural production by local residents. As of 2023, the built-up area has spread throughout the city, covering the remaining districts of the prefecture of Agoènyivé, including Zanguera, Legbassito, Togble, and Adetikope.

Table 4.1: Land Use and Land Cover Transition Matrix from 1986 to 2001 in DAGL in Percentage

	2001						
	LULC types	**Water Bodies**	**Built-up/Bare-land**	**Forest**	**Grassland**	**Agricultural Land**	**Total**
1986	Water Bodies	64.80	31.00	0	0.70	3.40	0.66
	Built-up/Bare-land	0.20	93.30	0.03	0.50	6.00	17.90
	Forest	0.02	0.80	28.10	62.80	8.30	24.00
	Grassland	0.01	3.30	7.30	47.70	41.70	22.10
	Agricultural Land	0.02	36.50	0.16	5.70	57.60	35.40
	Total	0.47	30.70	8.40	27.70	32.70	100

Table 4.2: Land Use and Land Cover Transition Matrix from 2001 to 2015 for DAGL in Percentage

	2015						
	LULC types	**Water Bodies**	**Built-up/Bare-land**	**Forest**	**Grassland**	**Agricultural Land**	**Total**
2001	Water Bodies	57.20	38.90	0.50	1.70	0.60	0.48
	Built-up/Bare-land	0.70	91.80	0.04	0.40	7.10	31.30
	Forest	0	0.80	40.30	40.50	18.30	8.60
	Grassland	0.07	8.70	1.90	29.20	60.10	28.30
	Agricultural Land	0.15	40.00	0.26	2.20	57.20	33.40
	Total	0.56	45.10	4.10	12.70	37.60	100

Table 4.3: Land Use and Land Cover Transition Matrix from 2015 to 2023 for DAGL in Percentage

		2023					
	LULC types	**Water Bodies**	**Built-up/Bare-land**	**Forest**	**Grassland**	**Agricultural Land**	**Total**
2015	Water Bodies	45.80	24.10	1.30	6.40	21.10	0.56
	Built-up/Bare-land	0.03	96.70	0.04	0.03	3.20	44.80
	Forest	0.13	1.73	46.10	39.50	12.60	4.10
	Grassland	0.29	5.40	8.90	38.90	46.60	12.60
	Agricultural Land	0.02	46.90	1.15	2.44	49.40	40.00
	Total	0.32	63.20	3.50	7.60	25.50	100

Between 1986 and 2001, grassland increased at the expense of the degraded forest areas, but from 2015 to 2023, DAGL experienced the highest rate of losses in grassland (-5.03 %). Specifically, from 2015 to 2023, DAGL experienced the highest rate of losses in all the classes compared to the periods 1986–2001 and 2001–2015. Between 1986 and 2001, forests, agricultural, and water bodies exhibited reduction in the average annual rate of -4.33 %, - 0.51 %, and -1.94 %, respectively, while there was an increase in grassland at a rate of 1.71 % (Table 4.4).

Similarly, GAMA's land cover has undergone considerable changes. Initially dominated by grassland (42.58 %) followed by forest (34.18 %) and agricultural land (11.81 %) in 1991, GAMA's built-up area has increased significantly to 70 % by 2023, while grassland has declined to 3.88 % and forest cover has dropped to 2.43 %. Agriculture has slightly increased to 21.48 % compared to the year 1991. Figure 4.3 visually represents the land cover changes and confirms the dramatic shift from natural land cover to built-up areas over the entire study period (1991-2023). Most of the land use and land cover types (agricultural land, forest, and grassland) have been substantially converted into built-up areas over time. This trend accelerates from 2017 to 2023 and confirms the intensifying urbanisation and its impact on natural landscapes.

The transition matrix (Table 4.5) shows that between 1991 and 2002, GAMA saw rapid urban growth, mostly at the expense of agricultural land, with nearly two-thirds (63.8%) of farmland converted into built-up areas. The existing urban land remained largely intact, with 94.5% of those areas staying built-up, showing strong consolidation and expansion of the city. During this time, forest cover took a significant hit, with less than half (46.7%) remaining, as large portions transformed into grassland and farmland, indicating deforestation and fragmentation of natural habitats. Water bodies were relatively stable, retaining 83.1%, though some areas were lost to urban development.

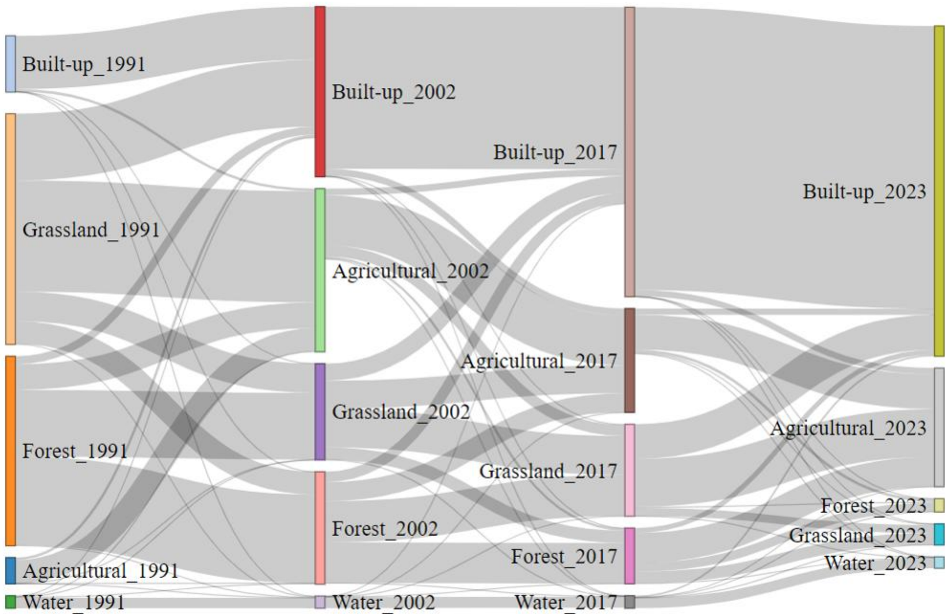

Figure 4.3: Land use and land cover change in GAMA in 1991, 2002, 2017, and 2023.

Table 4.4: Area Coverage, Absolute Change and Average Annual Rate of Change for DAGL

Land cover type	**Area (km^2)**				**Absolute change (km^2)**				**Average annual rate of change (%)**			
	1986	2001	2015	2023	1986-2001	2001-2015	2015-2023	1986-2023	1986-2001	2001-2015	2015-2023	1986-2023
Forest	92.31 (24.04%)	32.34 (8.42 %)	15.42 (4.01 %)	13.17 (3.43 %)	-59.96	-16.93	-2.25	-79.14	-4.33	-3.74	-1.82	-2.32
Grassland	84.81 (22.09 %)	106.52 (27.74 %)	47.40 (12.34 %)	28.32 (7.38 %)	21.70	-59.12	-19.07	-56.49	1.71	-3.96	-5.03	-1.80
Agricultural land	135.78 (35,36 %)	125.44 (32.66 %)	150.36 (39.15 %)	104.15 (27.12 %)	-10.33	24.92	46.22	-31.63	-0.51	1.42	-3.84	-0.63
Water-bodies	2.56 (0.67 %)	1.81 (0.47 %)	2.12 (0.55 %)	1.21 (0.32 %)	0.74	0.31	-0.91	-1.34	-1.94	1.21	-5.35	-1.42
Built-up/Bare-land	68.58 (17.86 %)	117.93 (30.71 %)	168.76 (43.94 %)	237.16 (61.67 %)	49.35	50.83	68.40	168.58	4.80	3.08	5.07	6.64

From 2002 to 2017 (Table 4.6), urban expansion accelerated. Built-up land remained stable at 95.2%, while it expanded further by converting over 60% of agricultural land and nearly 18% of grasslands. Forests continued to shrink, with just 36% of the original area untouched, much of the loss going to grasslands and urban areas. Grasslands also declined quite sharply, holding on to just 40.3% of their previous extent. Water bodies remained mostly unchanged but showed some continued shrinkage. In the most recent period, 2017 to 2023 (Table 4.7), urban areas became even more dominant. Built-up land saw a persistence of 97.6% and further expanded by taking over more than 62% of agricultural lands and almost 38% of grasslands. Agricultural lands suffered significant losses, with only about a third remaining unchanged. Forest and grassland areas faced severe fragmentation and reduction, with just 15.8% and 8.9% left intact, respectively. Water bodies also declined moderately, mostly due to ongoing urban encroachment.

Table 4.5: Land Use and Land Cover Transition Matrix from 1991 to 2002 for GAMA in Percentage

		2002					
	LULC types	**Water**	**Built-up**	**Forest**	**Grassland**	**Agricultural**	**Total**
1991	Agricultural	0.18	63.80	0.19	0.37	35.50	4.70
	Built-up/Bare-land	0.87	94.50	0.06	0.01	4.50	4.00
	Forest	0.30	4.20	46.70	35.10	13.50	13.60
	Grassland	0.25	28.90	9.90	12.70	48.10	16.60
	Water	83.10	5.50	7.40	0.01	3.80	0.90
	Total	8.70	12.20	8.10	6.90	64.10	100

Table 4.6: Land Use and Land Cover Transition Matrix from 2002 to 2017 for GAMA in Percentage

		2017					
	LULC types	**Water Bodies**	**Built-up/Bare-land**	**Forest**	**Grassland**	**Agricultural Land**	**Total**
2002	Water Bodies	90.90	3.20	1.90	1.00	2.00	8.70
	Built-up/Bare-land	0.40	95.20	0.10	0.40	3.90	12.20
	Forest	0.50	9.30	36.00	36.60	16.90	8.10
	Grassland	0.00	17.70	12.90	40.30	28.90	6.90
	Agricultural Land	0.15	60.70	1.40	6.80	30.60	11.70
	Total	8.90	20.70	4.00	6.60	59.80	100

Table 4.7: Land Use and Land Cover Transition Matrix from 2017 to 2023 for GAMA in percentage

		2023					
	LULC types	**Water Bodies**	**Built-up/Bare-land**	**Forest**	**Grassland**	**Agricultural Land**	**Total**
2017	Water Bodies	81.30	13.40	3.00	2.00	0.30	8.90
	Built-up/Bare-land	0.05	97.60	0.10	0.04	2.10	20.70
	Forest	0.80	8.80	15.80	20.80	53.60	4.00
	Grassland	0.08	37.70	1.20	8.90	52.00	6.60
	Agricultural Land	0.56	62.40	2.70	0.88	33.50	7.40
	Total	8.30	28.10	1.00	1.50	61.10	100

The built environment was historically concentrated in the Accra Metropolis and the district of Tema. However, between 2002 and 2023, urban development began encroaching on forested areas, grasslands, and agricultural lands, particularly within the Ga District and Tema Municipality. This expansion reflects a shift from concentrated urban centres to broader suburban and peri-urban development, resulting in significant changes in land use.

Between 2000 and 2017, GAMA experienced a gradual rise in the built environments, alongside declines in grassland and forest cover. The period from 2017 to 2023 marked the most significant reductions in forest and grassland at an average rate of -12.63 % and -12.76 %, respectively, while there was an increase at the rate of 2.09 % for agricultural land and 5.79 % for built-up area (Table 4.8).

In both regions, DAGL and GAMA, there has been a dramatic increase in built-up areas at the expense of natural habitats like forests, grasslands, agricultural lands, and water bodies over the past three decades. The development pattern differs between DAGL and GAMA. GAMA displays a higher coverage of built area more than DAGL due to its larger size, high population density and more economic activities compared to DAGL even though the two regions are the economic centre in their respective countries. In the two metropolitan areas, the agricultural lands are not stable. In DAGL, agricultural lands increased at an average rate of 1.42% between 2001 and 2015, but decreased at rates of -0.51% during the period 1986–2001 and -3.84% between 2015–2023. In contrast, GAMA's agricultural lands faced a decrease between 2002 and 2017 at an average rate of -2.33%, but increased during the periods of 1991–2002 and 2017–2023.

Table 4.8: Area Coverage, Absolute Change and Annual Rate of Change for GAMA

Land cover type	Area (km²)				Absolute change (km²)				Annual rate of change (%)			
	1991	2002	2017	2023	1991-2002	2002-2017	2017-2023	1991-2023	1991-2002	2002-2017	2017-2023	1991-2023
Forest	511.78 (34 %)	304.15 (20 %)	150.50 (10 %)	36.45 (2 %)	-207.62	-153.65	-114.05	-475.33	-3.69	-3.37	-12.63	-2.90
Grassland	622.57 (42 %)	259.54 (17 %)	247.80 (16 %)	58.13 (4 %)	-363.03	-11.74	-189.66	-564.44	-5.30	-0.30	-12.76	-2.83
Agricultural land	176.84 (12 %)	439.38 (29 %)	285.91 (19 %)	321.69 (21 %)	262.54	-153.48	35.78	144.85	13.50	-2.33	2.09	2.56
Water-bodies	33.86 (2 %)	32.92 (2 %)	33.73 (2 %)	30.92 (2 %)	-0.93	0.81	-2.81	-2.94	-0.25	0.16	-1.39	-0.27
Built-up/Bare-land	152.23 (10 %)	461.28 (31 %)	779.34 (52 %)	1050 (70 %)	309.05	318.06	270.75	897.86	18.46	4.60	5.79	18.43

4.1.1.2 Accuracy assessment

The percentage of pixels that are correctly classified is shown by the overall accuracy. The User Accuracy refers to the probability that a pixel labelled as a specific land cover class on the map is indeed that class in reality. This metric is crucial because it informs users about how reliable the classification is when they encounter specific land cover types on the map. Producer Accuracy, on the other hand, measures how well real-world land cover types are classified on the map from the perspective of the map creator. This measure helps assess how effectively different land cover classes are captured by the classification process. In summary, both user and producer accuracy provide essential insights into the performance of land cover classifications. The combination of these metrics allows for a comprehensive evaluation of classification quality and reliability across different land cover types and years.

The accuracy assessments for the DAGL and GAMA regions, as presented in Tables 4.9 and 4.10, provide a comprehensive overview of the reliability of land cover classifications over different years. Both regions demonstrate high overall accuracy, with DAGL improving from 90.12 % (1986) to 95.59 % (2023) and GAMA increasing from 91.36% (1991) to 97.34% (2023), reflecting consistent advancements in classification precision over time.

User accuracy for water bodies remained consistently high for both regions, reaching 100 % for DAGL and 99 % for GAMA in recent assessments, indicating excellent classification reliability for this category. The built-up/bare-land (Blt/Brl) category also showed notable improvements, with user accuracy rising from 90 % (1986) to 97 % (2023) in DAGL and producer accuracy reaching 100 % (2023) in GAMA, signifying reliable classification of built-up areas.

However, notable differences emerge in other categories. For instance, GAMA exhibits higher accuracy improvements in forest classification, with producer accuracy reaching 100 % (2023) compared to DAGL's 93 % (2023). Conversely, DAGL shows greater stability in agricultural land classification, with user accuracy improving to 95% (2023) versus GAMA's 96 %, but with slightly more consistent producer accuracy over time.

Overall, while both regions exhibit similar trends in improving Land Use and Land Cover classification accuracy over time, GAMA achieves slightly higher overall accuracy and excels in forest classification, whereas DAGL demonstrates more consistent performance in agricultural land categorisation. These differences may reflect variations in landscape complexity between the two regions. Anderson (1976) established that a minimum accuracy assessment of 85 % is considered acceptable; therefore, the evaluation results are reliable for further analysis in both regions (see Appendix H and I for the detailed accuracy assessment for the different years respectively in DAGL and GAMA)

Table 4.9: Accuracy Assessment of Different Years for DAGL

Years	User accuracy (%)					Producer accuracy (%)					Overall accuracy (%)
	Water	Blt/Brl	Frs	Gras	Agric	Water	Blt/Brl	Frs	Gras	Agric	
1986	100	90	89	89	91	100	85	94	87	88	90.12
2001	96	96	88	92	89	100	97	86	88	92	91.36
2015	97	98	91	91	90	100	99	86	86	96	93.94
2023	98	97	92	92	95	100	100	93	86	93	95.59

Blt/Brl Built-up/Bare-land, **Frs** Forest, **Gras** Grassland, **Agric** Agriculture land

Table 4.10: Accuracy Assessment of Different Years for GAMA

Years	User accuracy (%)					Producer accuracy (%)					Overall accuracy (%)
	Water	Blt/ Brl	Frs	Gras	Agric	Water	Blt/ Brl	Frs	Gras	Agric	
1991	99	94	91	90	91	100	95	91	90	90	91.36
2002	98	97	93	96	94	100	99	93	91	96	95.13
2017	100	99	96	95	94	100	100	91	88	99	96.47
2023	99	99	94	94	96	100	99	100	95	92	97.34

Blt/Brl Built-up/Bare-land, **Frs** Forest, **Gras** Grassland, **Agric** Agriculture land

4.1.1.3 Urban expansion dynamics and sprawl

It has been proven that there is an intimate relationship between urbanisation and land use dynamism, with increased urbanisation leading to significant changes in land use types and a more diversified land use distribution over time. Over the past three decades, built-up development in terms of residential as well as commercial purposes has significantly impacted urbanisation in DAGL and GAMA. The density of built-up areas varies from the city centre to the periphery, as depicted in Figure 4.4. The periphery has gradually transformed into sporadic residential buildings, demonstrating how cities typically develop around a central core characterised by dense concentrations of residential areas, historical and cultural sites, administrative buildings, hospitals, and commercial establishments. New developments generally expand outward from the city centre, resulting in declining urban density; high density concentrated at the core, while lower densities are found at the periphery. Contributing factors to this trend include high land prices, and scarcity in the city core.

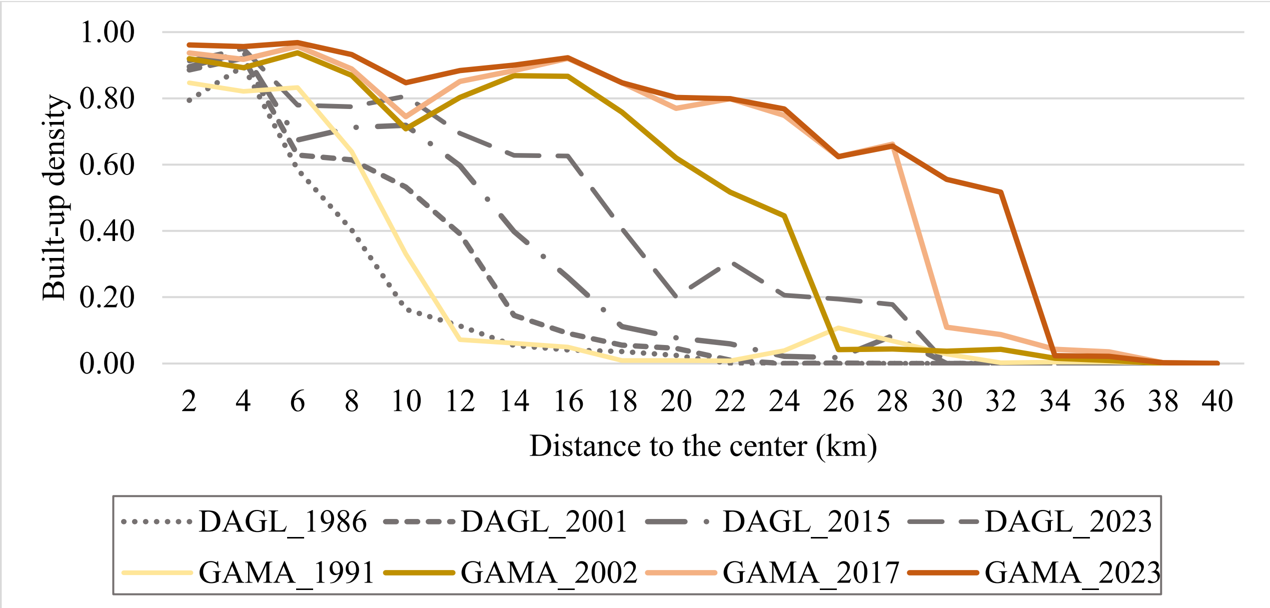

Figure 4.4: Density of built-up area over DAGL and GAMA

Over the years, as shown in Table 4.11 and Table 4.12, the built-up area has expanded gradually across all quadrants: 7 quadrants (Q1, Q2, Q3, Q4, Q14, Q15, and Q16) in DAGL and 8 quadrants (Q1, Q2, Q3, Q12, Q13, Q14, Q15, and Q16) in GAMA. The overall Urban Expansion Intensities index (UEII) ranges from 1.05 % to 1.92 % indicating rapid urban expansion for both DAGL and GAMA. Moreover, the Shannon's entropy value in the two metropolitan areas almost equal to 1, revealing a dispersed urban area. Quadrant Q16 and Q14 in DAGL, both exhibited rapid growth between 1986 and 2001 and from 2015 to 2023 respectively. As illustrated in Figure 4.5, urban expansion is particularly evident in the northwest part of the city, where the Agoe-Nyive municipality and its districts Aflao Gakli, Aflao Sagbado, Vakpossito, Zanguera, and Agoe-Nyive located in the peri-urban areas, are experiencing significant growth. Table 4.5 presents the UEII for DAGL across various years. The UEII values for quadrants Q14 and Q15 from 1986 to 2001 ranged from 1.05 and 1.92 indicating high-speed expansion in these areas, whereas medium-speed expansion was observed in quadrants Q1, Q2, and Q3. From 2001 to 2015, similar high-speed expansions were noted in quadrants Q14 and Q15 while low expansion rates were recorded in Q16. Between 2015 and 2023, very high-speed expansion occurred in quadrants Q1, Q14, Q15, and 16 with moderate expansion noted in Q2, Q3, and Q4. The Relative Shannon's entropy for DAGL over the period from 1986 to 2023 is recorded at values of 0.76, 0.88, 0.92, and 0.95.

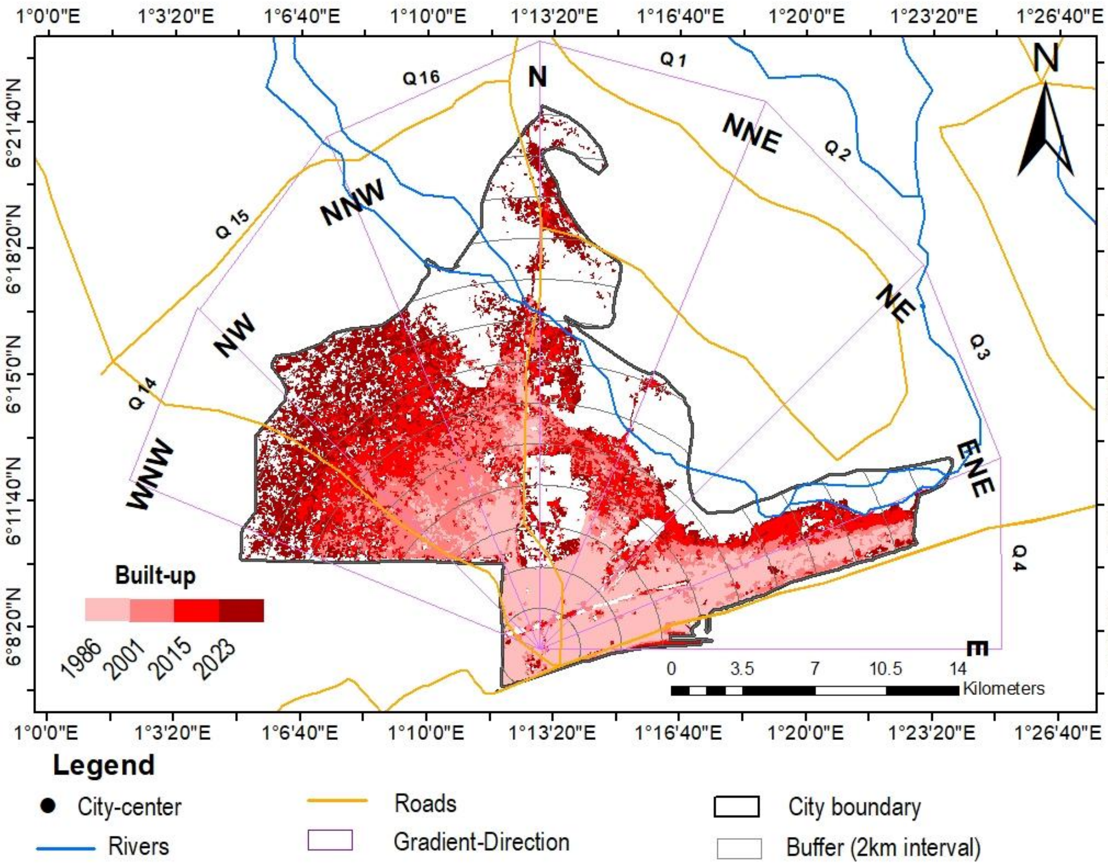

Figure 4.5: Spatial orientation of urban expansion with gradient-direction in DAGL

Table 4.11: The Built-up Area in Different Quadrants-wise Direction and UEII Value from 1986 to 2023 in DAGL

Quadrants	Built-up area (km^2)				Difference in Area (km^2)			UEII (%)		
	1986	2001	2015	2023	1986-2001	2001-2015	2015-2023	1986-2001	2001-2015	2015-2023
Q1	4.78	8.30	15.41	26.29	3.52	7.10	10.89	0.34	0.72	1.94
Q2	7.97	10.65	15.94	17.82	2.68	5.28	1.88	0.54	1.14	0.71
Q3	10.93	14.89	22.46	25.11	3.96	7.57	2.65	0.57	1.18	0.72
Q4	21.34	26.51	29.81	31.54	5.16	3.30	1.73	1.04	0.71	0.66
Q14	1.06	8.89	16.87	32.52	7.83	7.98	15.65	1.24	1.36	4.66
Q15	6.51	19.87	33.48	52.82	13.36	13.61	19.34	1.44	1.57	3.90
Q16	10.90	22.77	28.66	42.87	11.87	5.90	14.20	0.92	0.49	2.06

In contrast to DAGL's trends, GAMA shows a high rate of built-up area expansion in the peri-urban areas and particularly towards the Nord-Est region where Kpone Katamanso, Adenta Municipal, and Tema Metropolis are located. This expansion is more pronounced in quadrant Q3 between 1991 and 2002 and in quadrant Q2 between 2002 and 2017 (Figure 4.6). Quadrants Q1 and Q14 recorded the highest growth rates between 2017 and 2023. The rapid urban expansion observed in quadrants Q15 and Q16 between 1986 and 2015 indicates significant peri-urbanisation activity.

According to Table 4.6 detailing the UEII for GAMA, values exceeding 1.92 were recorded in quadrants Q2, Q3, Q12, and Q13 from 1991 to 2002, indicating a very high-speed urban expansion during this period. High-speed expansions were also observed in quadrants Q15 and Q16, while medium-speed expansion occurred in quadrants Q1 and Q14.

From 2002 to 2017, very high-speed expansion was noted in quadrants Q2 and Q12; high-speed expansion occurred in quadrants Q1, Q3, Q15, and Q16; medium-speed expansion was recorded in quadrant Q14; and slow expansion was observed in quadrant Q13. From 2017 to 2023, all quadrants experienced very high-speed expansion, only quadrant Q3 demonstrated high speeds of expansion. The relative Shannon's entropy for GAMA ranges from values of 0.82, to 0.96 between 1991 and 2023, revealing a scattered urban region.

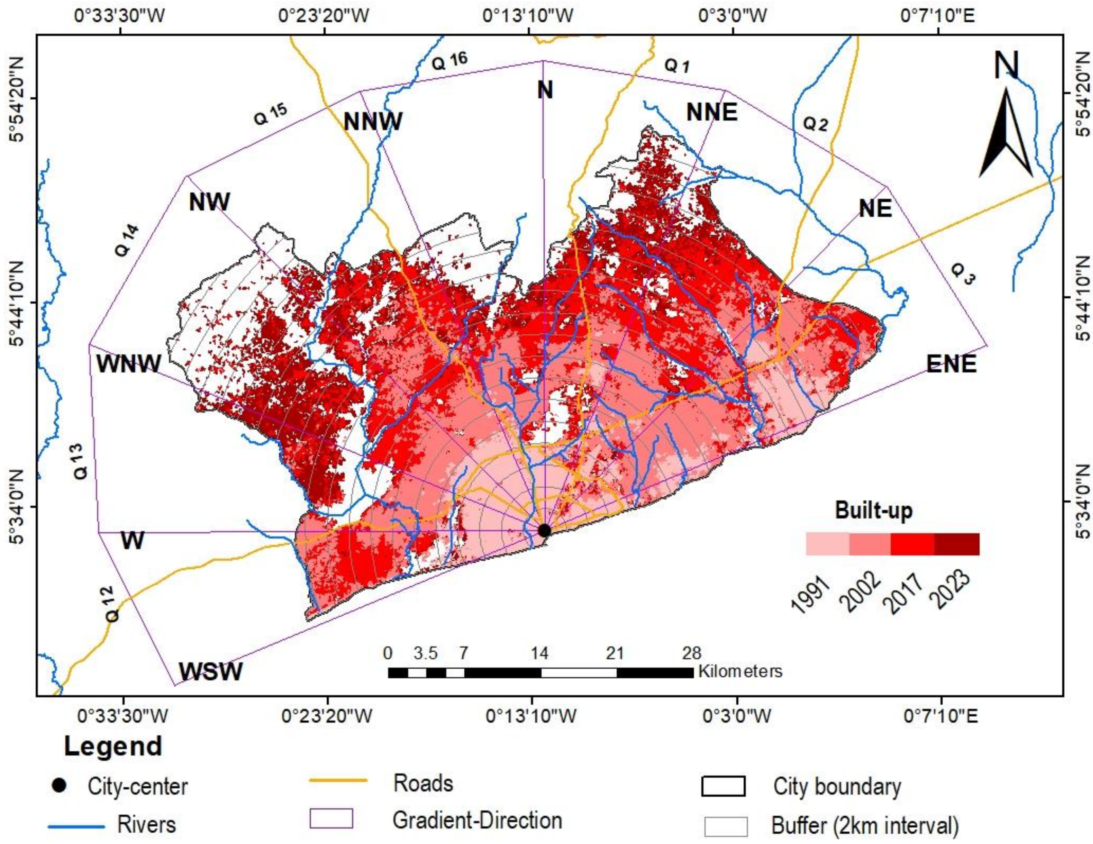

Figure 4.6: Spatial orientation of urban expansion with gradient-direction in GAMA

Tables 4.13 to 4.20 present the built-up area coverage in DAGL and GAMA across various distances and quadrants from 1986 to 2023 and from 1991 to 2023 respectively. Over the years, in DAGL, there is a clear trend of increasing built-up areas, particularly in closer buffers (2 km to 10 km), indicating significant urban expansion. Quadrant 4 (Q4) consistently shows the highest built-up coverage, suggesting it is a focal point for development. In contrast, some quadrants like Q14 exhibit minimal growth, especially at greater distances, reflecting uneven urbanisation patterns.

Table 4. 12: The Built-up Area in Different Quadrants-wise Direction and UEII Value from 1991 to 2023 in GAMA

Quadrants	Built-up area (km^2)				Difference in Area (km^2)			UEII (%)		
	1991	2002	2017	2023	1991-2002	2002-2017	2017-2023	1991-2002	2002-2017	2017-2023
Q1	11.16	35.30	80.57	136.84	24.15	45.26	56.28	1.04	1.43	4.45
Q2	7.48	59.49	131.40	168.29	52.01	71.91	36.89	2.21	2.24	2.88
Q3	39.32	134.69	188.20	202.29	95.37	53.51	14.09	4.00	1.64	1.08
Q12	12.75	32.23	62.95	73.81	19.47	30.73	10.86	2.04	2.36	2.09
Q13	12.87	39.85	50.03	83.34	26.99	10.18	33.31	2.01	0.56	4.55
Q14	17.96	41.48	75.67	132.55	23.51	34.19	56.88	0.75	0.80	3.34
Q15	18.33	53.97	101.31	141.35	35.64	47.33	40.04	1.69	1.64	3.48
Q16	13.14	38.17	64.45	84.96	25.03	26.28	20.51	1.61	1.24	2.41

In GAMA, there is a clear trend of increasing built-up areas, particularly in the closer buffers (2 km to 10 km), indicating significant urban expansion. Quadrant 3 (Q3) shows substantial growth, especially in the years 2002 and 2017, reflecting its role as a key development area. In contrast, some quadrants like Q12 exhibit more modest increases, suggesting uneven urbanisation patterns.

Table 4. 13: Built-up Area Coverage per Buffer per Direction in DAGL in 1986

Distance (Km)	Area_built-up													
	2	**4**	**6**	**8**	**10**	**12**	**14**	**16**	**18**	**20**	**22**	**24**	**26**	**28**
Q1	0.59	2.34	0.79	0.46	0.19	0.39	0.005	0	0	0	0	0	0	0
Q2	0.53	2.13	3.14	1.66	0.27	0.2	0	0						
Q3	0.77	1.71	2.85	2.97	1.85	0.76	0.02	0	0	0	0			
Q4	0.76	2.32	3.32	3.62	2.7	2.57	2	2.11	1.63	0.65				
Q14	0.42	0.18	0	0.25	0.18	0.02	0	0	0					
Q15	0.61	1.36	0.99	2.26	1.24	0.04	0	0	0	0				
Q16	0.62	2.27	1.52	2.74	0.77	1.85	1.01	0.07	0.04	0	0	0		

Table 4. 14: Built-up Area Coverage per Buffer per Direction in DAGL in 2001

Distance (km)	Area_built-up													
	2	**4**	**6**	**8**	**10**	**12**	**14**	**16**	**18**	**20**	**22**	**24**	**26**	**28**
Q1	0.59	2.19	0.88	0.62	1.68	2.02	0.1	0.06	0	0.005	0.11	0	0	0
Q2	0.65	2.18	3.23	2.46	1.71	0.39	0	0						
Q3	0.72	1.93	2.74	3.66	3.46	1.66	0.61	0.07	0	0	0			
Q4	0.77	2.31	3.51	3.76	3.1	3.15	3.15	3.16	2.38	1.19	0			
Q14	0.55	0.17	0	1.39	3.1	3.32	0.33	0	0					
Q15	0.68	1.43	1.42	5.31	6.49	3.47	0.8	0.22	0.001	0				
Q16	0.69	2.24	1.73	3.54	3.82	6.08	3.17	1.29	0.16	0	0	0	0.006	

Table 4. 15: Built-up Area Coverage per Buffer per Direction in DAGL in 2015

	Area_built-up													
Distance (km)	**2**	**4**	**6**	**8**	**10**	**12**	**14**	**16**	**18**	**20**	**22**	**24**	**26**	**28**
Q1	0.69	2.29	0.78	0.94	3.38	3.96	1.13	1.36	0.0045	0.031	0.63	0.12	0.009	0.025
Q2	0.61	2.31	3.52	3.69	4.85	0.77	0.059	0.099						
Q3	0.78	1.86	2.99	4.76	5.08	2.42	2.8	1.38	0.33	0	0			
Q4	0.78	2.34	3.72	4.16	3.02	3.08	3.19	3.83	3.74	1.89	0			
Q14	0.55	0.19	0	1.35	4.16	5.45	4.36	0.71	0.088					
Q15	0.67	1.51	1.55	5.39	6.91	7.83	5.92	3.1	0.55	0.004				
Q16	0.67	2.14	1.91	3.73	4.19	7.1	4.93	3.3	0.39	0.086	0.046	0.017	0.1	

Table 4. 16: Built-up Area Coverage per Buffer per Direction in DAGL in 2023

	Area_built-up													
Distance (km)	**2**	**4**	**6**	**8**	**10**	**12**	**14**	**16**	**18**	**20**	**22**	**24**	**26**	**28**
Q1	0.69	2.3	1.96	1.54	4.15	4.79	3.03	2.63	0.24	1.12	2.31	0.81	0.61	0.05
Q2	0.62	2.33	3.54	4.02	5.81	1.1	1.18	0.17						
Q3	0.78	1.9	3.12	4.98	5.73	2.78	3.06	2.08	0.61	0.0045	0.011			
Q4	0.78	2.35	3.79	4.35	3.08	3.28	3.41	3.85	3.99	2.52	0.1			
Q14	0.54	0.19	0	1.55	4.72	7.32	8.36	7.77	2.02					
Q15	0.64	1.51	1.76	5.45	7.01	8.32	9.06	9.35	8.54	1.14				
Q16	0.67	2.19	2.58	4.24	4.93	8.01	7.54	6.7	3.27	0.44	1.11	0.52	0.6	

Table 4. 17: Built-up Area Coverage per Buffer per Direction in GAMA in 1991

Distance (km)	Area_built-up																			
	2	**4**	**6**	**8**	**10**	**12**	**14**	**16**	**18**	**20**	**22**	**24**	**26**	**28**	**30**	**32**	**34**	**36**	**38**	**40**
Q1	0.52	2.25	3.84	1.59	0.54	0.21	0	1.93	0.13	0.15	0	0	0	0	0	0	0	0	0	
Q2	0.49	0.45	1.34	1.80	1.28	1.35	0.55	0.05	0	0.04	0	0	0.12	0	0	0	0	0	0	
Q3	0.70	1.53	1.56	1.73	0.85	0.40	2.63	1.54	0.47	0.63	0.78	3.68	11.2	7.68	3.10	0.21	0.30	0.24	0.05	
Q12	0.59	1.59	3.72	3.55	2.01	0.44	0.20	0.25	0.11	0.04	0.13	0.09								
Q13	0.64	2.23	3.90	3.99	1.91	0.14	0.01	0.04	0	0	0	0	0	0	0	0	0	0		
Q14	0.77	2.35	3.82	5.26	5.42	0.34	0.00	0	0	0	0	0	0	0	0	0	0	0	0	0
Q15	0.79	2.26	3.83	5.47	5.58	0.34	0.01	0	0.03	0.02	0	0	0	0	0	0	0	0	0	
Q16	0.79	2.33	3.73	4.05	1.43	0.52	0.29	0	0	0	0	0	0	0	0					

Table 4. 18: Built-up Area Coverage per Buffer per Direction in GAMA in 2002

Distance (km)	Area_built-up																			
	2	**4**	**6**	**8**	**10**	**12**	**14**	**16**	**18**	**20**	**22**	**24**	**26**	**28**	**30**	**32**	**34**	**36**	**38**	**40**
Q1	0.6	2.2	3.8	3.3	1.2	1.2	2.1	7.7	5.9	5.2	0.9	1.0	0.1	0	0	0	0	0	0	
Q2	0.6	0.9	1.7	2.7	4	6.6	8.3	9.5	8.5	3.8	1.6	2.4	3.8	3.1	1.2	0.7	0.01	0	0	
Q3	0.8	1.9	2.9	3.3	5.3	8.3	10	11.6	10	9.6	5.9	8.5	16.	16	13	6	2.9	1.7	0.1	
Q12	0.7	1.8	3.9	4.2	2.3	1.1	2.7	2.7	1.6	2.1	6.1	2.8								
Q13	0.7	2.2	3.9	4.5	3.8	7.1	8.2	5.06	0.9	0.3	1.9	0.9	0.3	0	0	0	0	0		
Q14	0.76	2.34	3.80	5.34	6.95	8.40	7.54	2.06	1.22	1.92	0.25	0.34	0.47	0.01	0	0	0	0	0	0
Q15	0.76	2.09	3.77	5.45	7.06	7.66	8.33	4.05	1.41	5.02	4.27	2.91	0.91	0.30	0	0	0	0	0	
Q16	0.8	2.3	3.7	4.1	2.9	6.9	6.4	5.28	4.3	1.1	0.1		0	0	0					

Table 4. 19: Built-up Area Coverage per Buffer per Direction in GAMA in 2017

Distance (km)	Area_built-up																			
	2	**4**	**6**	**8**	**10**	**12**	**14**	**16**	**18**	**20**	**22**	**24**	**26**	**28**	**30**	**32**	**34**	**36**	**38**	**40**
Q1	0.6	2.23	3.89	3.94	2.51	2.55	4.30	10.95	10.92	11.74	9.67	9.73	3.73	2.17	0.69	0.45	0.34	0.16	0.07	
Q2	0.65	1.04	2.43	3.57	5.14	7.96	9.64	11.27	11.41	10.77	14.07	10.61	12.11	13.01	11.44	5.96	0.17	0.13	0.06	
Q3	0.71	1.92	3.07	3.82	5.77	8.42	10.11	11.63	12.89	13.11	11.58	12.76	18.64	19.57	18.34	17.57	11.67	6.34	0.18	
Q12	0.57	1.51	3.91	4.05	1.78	2.55	4.76	8.52	9.35	9.98	12.53	3.38								
Q13	0.63	2.10	3.92	4.71	4.00	8.11	9.62	6.71	2.91	1.51	3.19	1.75	0.46	0.10	0.02	0.09	0.21	0		
Q14	0.75	2.31	3.82	5.37	6.94	8.39	10.01	10.68	9.37	6.36	2.34	2.94	2.21	1.45	0.93	0.63	0.62	0.32	0.12	0.11
Q15	0.76	2.07	3.91	5.46	7.07	8.32	9.88	10.87	10.01	11.79	10.65	9.43	3.87	4.32	2.39	0.50	0.02	0	0	
Q16	0.79	2.36	3.72	4.63	4.07	8.12	8.34	8.86	12.04	7.23	3.04	1.13	0.13	0.01	0.02					

Table 4. 20: Built-up Area Coverage per Buffer per Direction in GAMA in 2023

Distance (km)	**Area_built-up**																			
	2	**4**	**6**	**8**	**10**	**12**	**14**	**16**	**18**	**20**	**22**	**24**	**26**	**28**	**30**	**32**	**34**	**36**	**38**	**40**
Q1	0.68	2.31	3.91	4.53	2.99	3.20	5.49	11.75	12.62	13.99	15.02	15.68	11.70	11.23	7.69	5.91	3.72	3.31	1.15	
Q2	0.68	1.43	2.88	4.19	5.32	8.49	10.04	11.67	12.28	11.54	16.16	13.59	13.14	18.28	19.55	14.97	3.31	0.68	0.05	
Q3	0.68	2.10	3.62	3.99	6.53	8.60	10.20	11.78	13.20	14.35	13.35	14.74	19.17	20.46	19.61	18.68	13.16	7.41	0.24	
Q12	0.72	2.02	3.93	4.91	3.51	3.70	5.51	9.33	10.59	11.91	13.70	3.57								
Q13	0.74	2.28	3.93	5.33	5.19	8.36	10.08	7.54	3.20	3.75	12.82	8.89	4.47	2.75	1.94	1.12	0.83	0.02		
Q14	0.76	2.36	3.89	5.45	6.99	8.49	10.18	11.13	10.23	8.21	7.28	11.78	12.00	11.53	10.01	7.83	2.72	0.99	0.41	0.30
Q15	0.79	2.16	3.93	5.48	7.08	8.38	9.94	11.31	12.79	13.91	15.79	15.67	10.47	12.44	7.57	2.85	0.57	0.04	0.04	
Q16	0.79	2.36	3.90	5.07	4.44	8.40	9.14	10.06	13.32	12.35	9.78	4.12	0.91	0.21	0.16					

4.1.2 Distribution and variation in the provision of selected ecosystem services in DAGL and GAMA.

4.1.2.1 Carbon storage and sequestration

Changes in Land Use and Land Cover have a significant impact on terrestrial ecosystems and the services they offer. These services include the ability to store carbon, whose changes may affect climate change worldwide. Using the InVEST (Integrated Valuation of Ecosystem Services and Trade-offs) model, this study analyses spatially the carbon storage capacity in two West African metropolitan areas, the DAGL and GAMA from 1986 to 2023 and 1991 to 2023 respectively. The results of the model, as shown in Figure 4.7, indicate that in DAGL, high carbon storage was historically concentrated in the eastern districts of Baguida, Adetikope, Legbassito Togble, and Be_Est during the 1986 baseline period, driven by dense vegetation cover in these areas. However, this capacity has declined significantly from 2001 to 2023 due to the expansion of built-up areas towards the city's periphery, which has fragmented natural habitats and reduced vegetative biomass. In contrast, In GAMA, elevated carbon storage was observed in 1991, primarily in the western districts (GA South, GA West, GA North) and Weija-Gbawe, as well as in the northern part of Accra metropolis, where Achimota Forest serves as a critical carbon sink. While these regions retained some carbon through 2023, their carbon stocks have diminished due to vegetation loss and urban expansion, particularly in peri-urban zones where agricultural and forested lands are being converted into residential and commercial developments.

In the metropolitan area of DAGL, the result in Table 4.21 indicates a significant decline in total carbon storage from 3,604,852 Mg of C in 1986 to 1,955,549 Mg of C by 2015, and to 1,367,113 Mg of C by 2023.

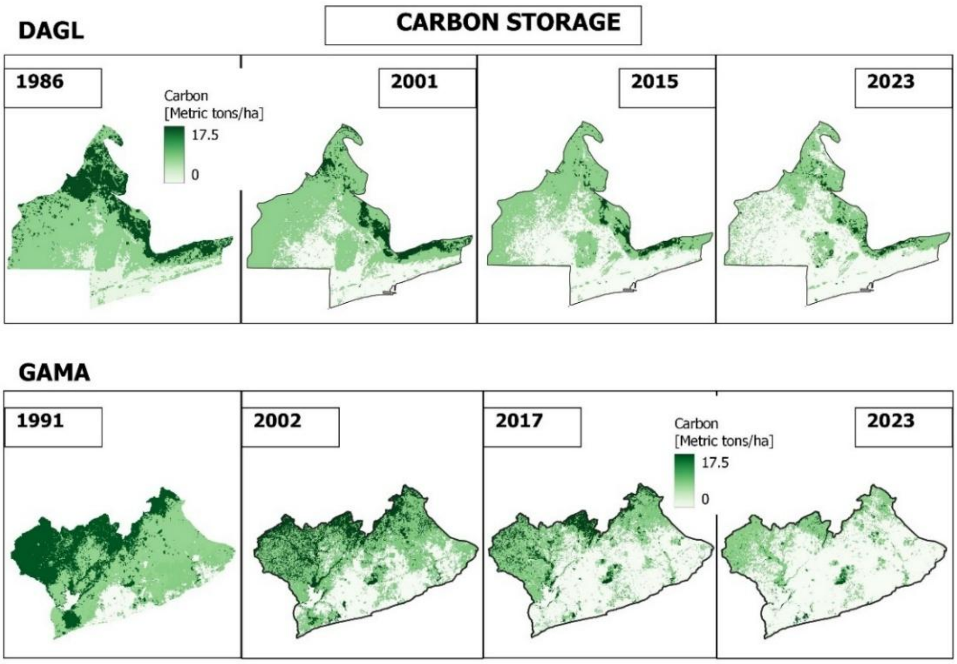

Figure 4.7: Carbon storage map in DAGL and GAMA

Initially carbon storage was heavily influenced by forested areas (1,751,758 Mg of C) and agricultural lands (1,140,615 Mg of C), which contributed substantially to the total carbon stock. However, in 2001, there was a notable reduction in carbon storage across all categories. This suggests an urbanisation trend that may have replaced natural landscapes with built structures. The most alarming decline occurred between 2001 and 2015, where carbon storage dropped sharply due to the loss of forest and grassland carbon stocks. The negative values in indicate that carbon storage per square unit has decreased significantly over time, reflecting potential land degradation or unsustainable land use practises.

In contrast, the GAMA area shows an initially high total carbon storage of 16,574,522 Mg of C in 1991 (Table 4.21), primarily driven by significant forest carbon stocks (9,721,759 Mg of C) and grassland contributions (5,236,995 Mg of C). However, this figure declined dramatically over the years, reaching only 4,120,702 Mg of C by 2023. The substantial drop in total carbon storage is particularly evident between 2002 and 2017, where total carbon storage fell from 11,974,261 Mg of

C to 7,513,407 Mg of C, indicating severe losses likely due to land use changes or deforestation. Similar to DAGL, GAMA also exhibits negative values in carbon value suggesting that the area is experiencing a net loss of carbon stocks per square unit over time.

The result on carbon storage and sequestration across different LULC types from 1986 to 2023 over DAGL reveals significant trends and changes (Figure 4.8, Figure 4.9). In particular, forests have experienced a dramatic decline in carbon storage, dropping from approximately 1,751.758 Mg of C in 1986 to 251.673 Mg of C in 2023. Grasslands initially increased their carbon storage from 712.477 Mg of C in 1986 to 894.521 Mg of C in 2001 but then faced a significant decline to 238.276 Mg of C by 2023. Agricultural land shows fluctuations as well; while it decreased slightly from 1,140.615 Mg of C in 1986 to 1,053,123 Mg of C in 2001, it then increased to 1,370.690 Mg of C by 2015 before dropping again to 877.164 Mg of C in 2023.

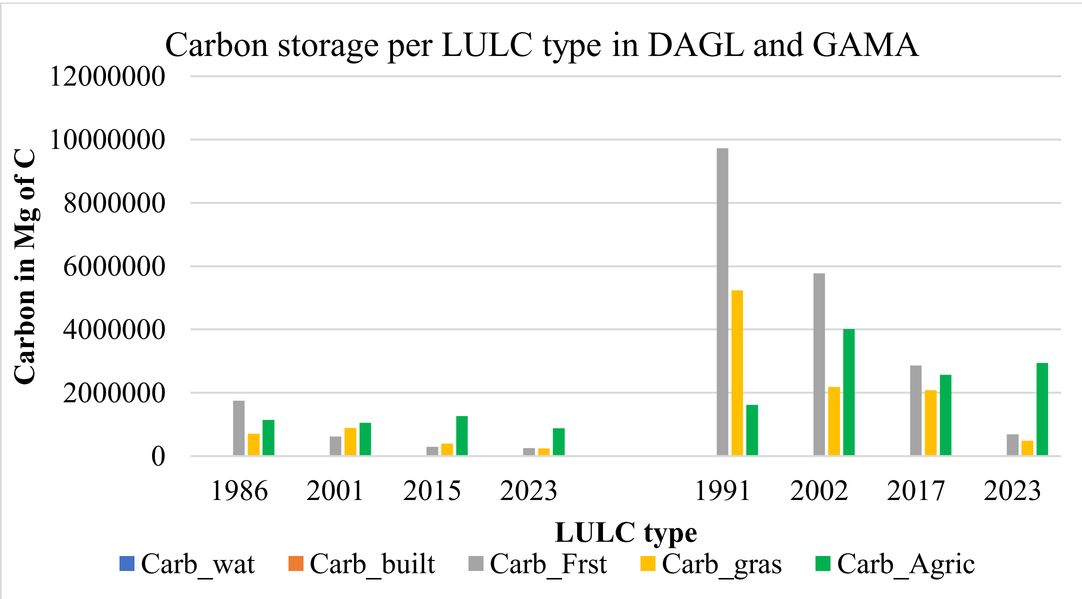

Figure 4.8: Carbon storage per LULC type over DAGL (1986 to 2023) and GAMA (1991 to 2023)

Table 4. 21: Carbon Stored and Sequestered in DAGL and GAMA and Carbon Stored per LULC Type

Area	Year	Carb_wat (Mg of C)	Carb_blt (Mg of C)	Carb_Frst (Mg of C)	Carb_gras (Mg of C)	Carb_Agric (Mg of C)	Tot Carb stor (Mg of C)	Tot Carb sqs (Mg of C)
DAGL	1986	1.35	0	1,751,758	712,477	1,140,615	3,604,852	
	2001	1.35	0	615,259	894,521	1,053,123	2,562,906	-1,041,945
	2015	0	0	293,604	398,911	1,263,034	1,955,549	-607,357
	2023	0	0	251,673	238,276	877,164	1,367,113	-588,436
GAMA	1991	0	0	9,721,759	5,236,995	1,615,769	16,574,522	
	2002	0	8	5,776,686	2,185,372	4,012,195	11,974,261	-4,600,261
	2017	0	7.42	2,863,565	2,082,909	2,566,925	7,513,407	-4,460,854
	2023	0	0	692,181	489,386	2,939,135	4,120,702	-3,392,704

Carb_wat carbon stored in water, **Carb_blt** carbon stored in built-up, **Carb_Frst** carbon stored in forest, **Carb_gras** carbon stored in grassland, **Carb_Agric** carbon stored in agricultural land, **Tot Carb stor** total of carbon stored, **Tot Carb sqs** total of carbon sequestered

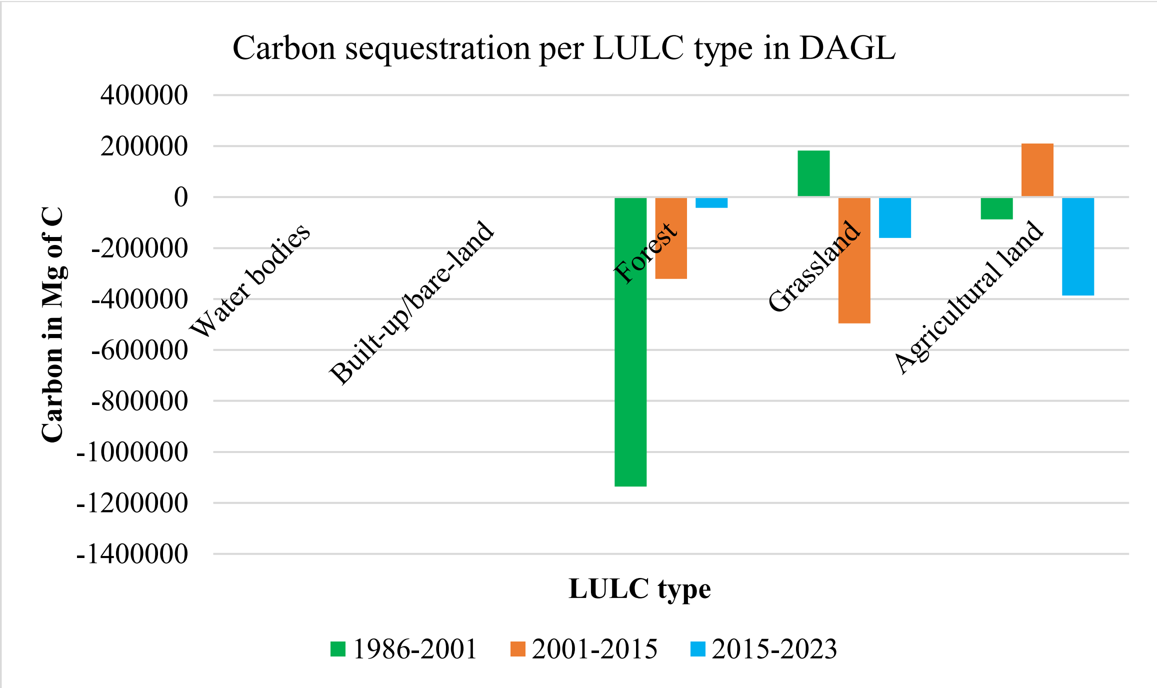

Figure 4.9: Carbon sequestration per LULC type over DAGL

The result on carbon storage and sequestration across different LULC types in GAMA reveal significant trends from 1991 to 2023 (Figure 4.8, Figure 4.10). Forest areas experienced a dramatic decline in carbon storage from 9,721,759 Mg of C in 1991 to 692,181 Mg of C in 2023, with total losses amounting to approximately 3,945,072 Mg of C between 1991 and 2002 and continued losses in subsequent years. Similarly, grasslands saw a decrease from 5,236,994 Mg of C in 1991 to 489,386 Mg of C by 2023, with total losses of about 3,051,623 Mg of C from 1991 to 2002 and further declines thereafter. In contrast, agricultural land showed an increase in carbon storage from 1,615,769 Mg of C in 1991 to 2,939,1345 Mg of C by 2023, indicating a net gain despite fluctuations.

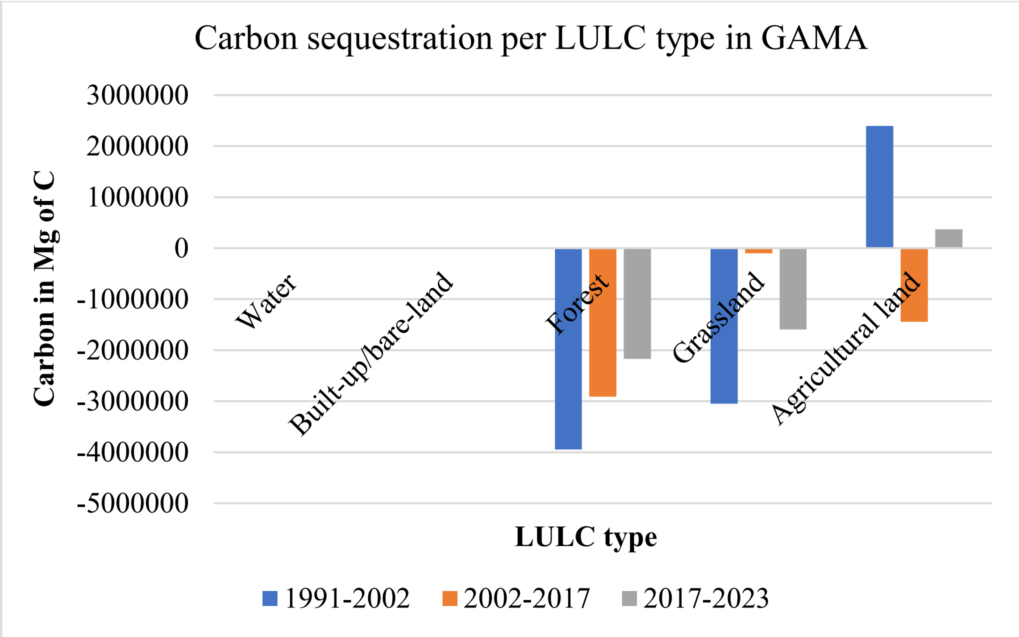

Figure 4.10: Carbon sequestration per LULC type over GAMA

4.1.2.2 Urban cooling and heat mitigation

Figure 4.11 illustrates the change in Heat Mitigation Index from 2001 to 2023 in DAGL and from 2002 to 2023 in GAMA.

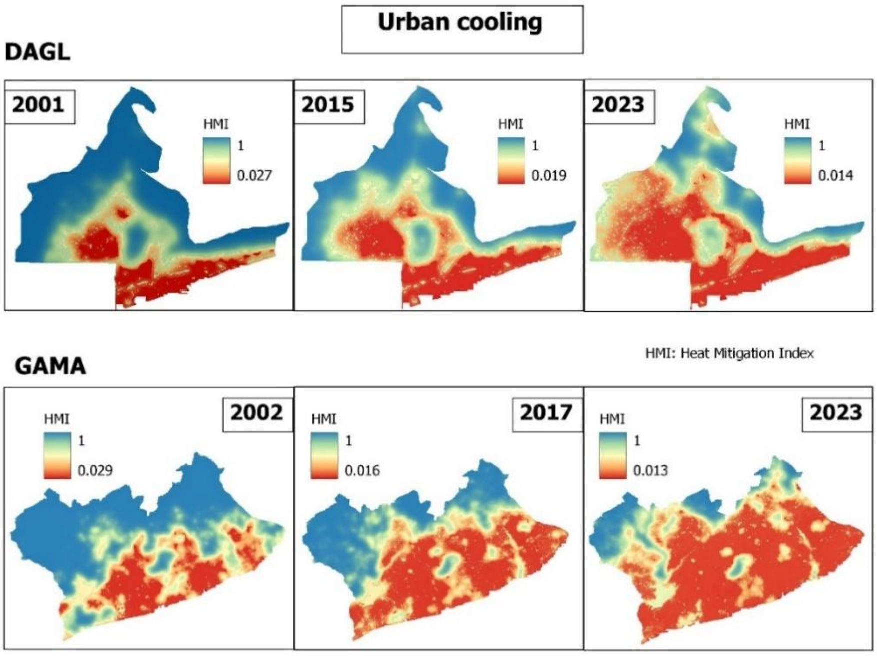

Figure 4. 11: Heat mitigation index in DAGL and GAMA

The heat mitigation index (HMI) showed a decreasing pattern, indicating a gradual decline in the heat-mitigation capacity of both regions. Spatially, low-HMI areas increased, clustering around built-up zones, while high-HMI areas diminished over time in both DAGL and GAMA. Consistent with the HMI trends, the cooling capacity also decreased in both regions, dropping from 0.60 in 2001 to 0.30 in 2023 in DAGL and from 0.65 in 2002 to 0.25 in 2023 in GAMA (Table 4.13). In parallel, the average temperature rose from 26°C in 2001 to 29.5°C in 2023 in both DAGL and GAMA (Table 4.22). The increase in average temperature is directly correlated with the decline in cooling capacity.

Table 4.22: Average Cooling Capacity and Average Temperature over DAGL and GAMA

Area	Year	Average cooling capacity (cc)	Average Temperature
DAGL	2001	0.6	26.5
	2015	0.45	28
	2023	0.3	29.5
GAMA	2002	0.65	25.5
	2017	0.4	27.5
	2023	0.25	29

In DAGL, the coolest areas in 2001 were located in the peripheral districts of Aflao-Sagbado, Zanguera, Legbassito, Adetikope, Togble, Be-Est, Be-Ouest, and Baguida, primarily due to the dense vegetation in these areas. However, this cooling capacity has significantly declined from 2015 to 2023, with the most notable reductions observed in Aflao-Gakli, Zanguera, and Legbassito. This decline correlates with the loss of vegetation and the expansion of built-up areas, which inherently have low cooling capacity. In GAMA, the coolest areas in 2002 were similarly located in the peripheral regions, including the GA districts (GA South, GA West, GA North), as well as parts of the northern Tema municipality, such as Kpone-Katamanso and Lankwantanang-Madina, and the northern Accra metropolis, where the Achimota Forest served as a key

cooling zone. From 2017 to 2023, these areas have experienced a reduction in cooling capacity due to increased residential and commercial construction, leading to significant vegetation loss. The patterns observed in both regions highlight a strong link between urbanisation and reduced cooling effects. The expansion of built-up areas at the expense of green spaces diminishes natural cooling capacities, exacerbating urban heat island effects.

4.1.2.3 Flood Risk Mitigation

Figure 4.12 provides a spatial distribution of runoff retention volum in cubic metres (m^3) in DAGL and GAMA.

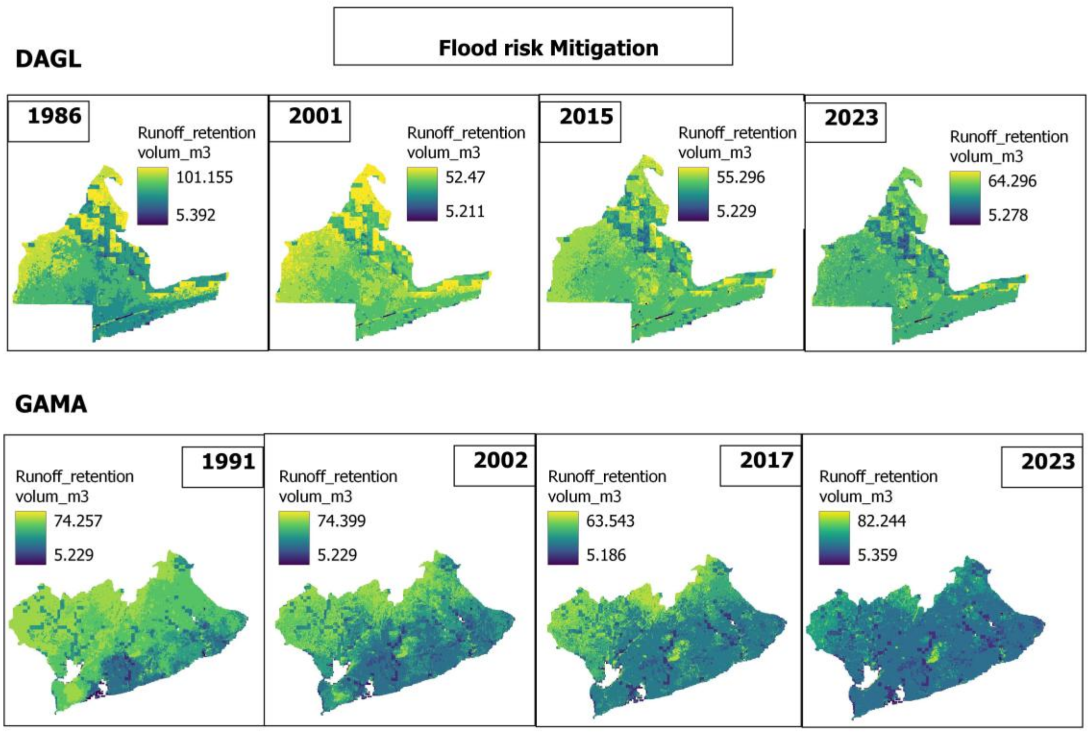

Figure 4.12: Runoff retention in DAGL and GAMA

In DAGL, from 1986 to 2023, the lowest runoff retention capacity was observed in densely built-up areas and the marshy zones of Zio Valley, encompassing parts of Togble, Adetikope, and Be-Est. These areas experienced reduced infiltration due to impervious surfaces and waterlogged soils. Conversely, regions with vegetative cover exhibited the highest runoff retention capacity, demonstrating the critical role of green spaces in mitigating surface runoff through enhanced infiltration and evapotranspiration.

Similarly, in GAMA, densely constructed areas showed the least runoff retention from 1991 to 2023, driven by impervious surfaces that limit soil permeability and accelerate runoff generation. The highest retention capacity was historically observed in the GA districts (GA South, GA West, GA North) and the northern Accra metropolis, where the Achimota Forest acted as a natural retention buffer. However, this capacity has diminished over time, likely due to urban expansion into vegetated and forested zones, which reduced permeable surfaces and disrupted natural hydrological pathways

Table 4.23 provide the model output for the two metropolitan areas including the runoff retention indices (in percentage) and the runoff retention volum in cubic metres.

Table 4.23: Runoff Retention Value in DAGL and GAMA

Area	Year	Runoff retention index (Ri) (%)	Runoff retention (m^3)
DAGL	1986	2.00	29,098,483
	2001	2.42	17,808,795
	2015	2.24	17,287,791
	2023	2.01	17,908,270
GAMA	1991	14.74	85,027,128
	2002	12.52	71,504,417
	2017	12.76	58,952,304
	2023	9.66	57,500,096

In the metropolitan area of the DAGL, like shown in table 4.23, the runoff retention index has remained relatively low, fluctuating between 2.00 % in 1986 and 2.42 % in 2001, before decreasing to 2.01 % by 2023. The total volume of runoff retained showed a significant decline from 29,098,483 m^3 in 1986 to around 17,908,270 m^3 in 2023. A similar pattern is observed in GAMA, where the Ri decreases from 14.74 % in 1991 to 9.66 % in 2023, and Runoff Retention declines from 85,027,128 m^3 to 57,500,096 m^3 during the same period.

4.1.3 Relationship between urban expansion and ecosystem service provision in the selected metropolitan areas DAGL and GAMA.

4.1.3.1 Pearson correlation analysis

The correlation matrix (Figure 4.13) for DAGL reveals significant relationships between urban expansion metrics and ecosystem services. A strong positive correlation (0.97) exists between Urban Area and Population Density, indicating that larger urban areas tend to have higher population density. Conversely, both Urban Area and Population Density show strong negative correlations with Carbon Storage (-0.97 and -0.92, respectively), suggesting that increased urbanisation is associated with a decrease in carbon storage capacity, likely due to habitat loss and reduced vegetation. Additionally, there is a very strong negative correlation between Urban Area and Urban Cooling (-0.99), indicating that larger urban areas experience less cooling effect, potentially exacerbating urban heat island effects. The correlation between Urban Cooling and Carbon Storage is notably high (0.99), highlighting the role of vegetation in providing both cooling benefits and carbon sequestration. In contrast, Flood Risk Control shows weak correlations with the other variables, suggesting that it may not be directly influenced by urban expansion or population density.

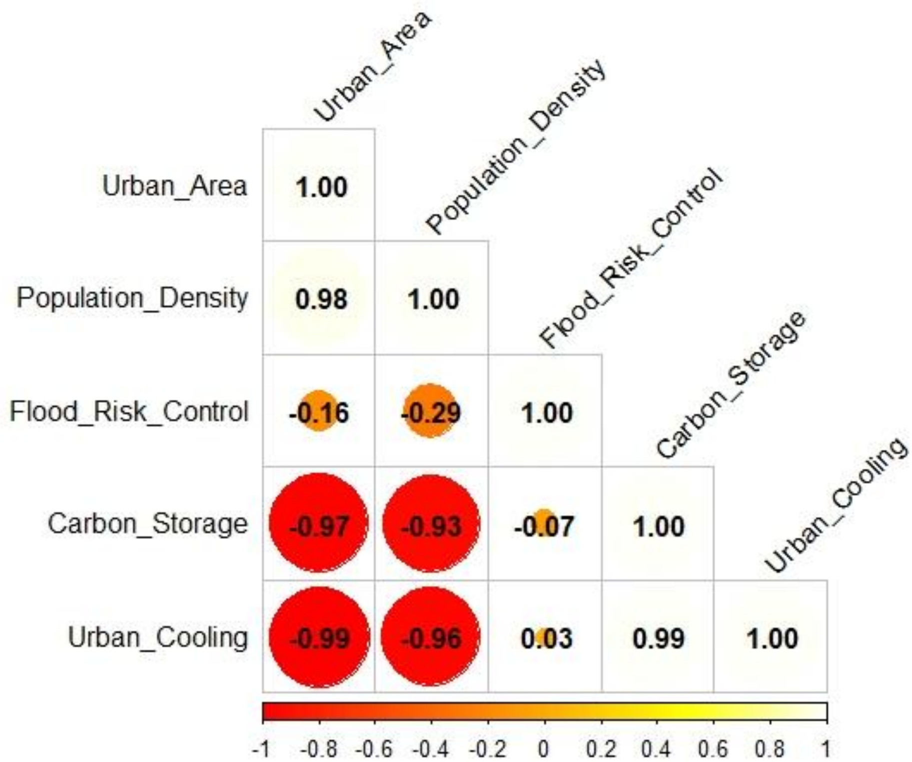

Figure 4. 13: The correlation matrix for DAGL

The correlation matrix (Figure 4.14) for GAMA illustrates strong correlation among urban expansion metrics and ecosystem services. A very highly positive correlation (0.9742) between Urban Area and Population Density indicates that larger urban areas are associated with higher population density. Conversely, both Urban Area and Population Density exhibit strong negative correlations with Carbon Storage (-0.99 and -0.96, respectively), suggesting that as urbanisation increases, the capacity for carbon storage significantly decreases, likely due to the loss of green spaces and vegetation. Additionally, there is a substantial negative correlation between Urban Cooling and both Urban Area (-0.99) and Population Density (-0.96), indicating that denser and larger urban environments tend to experience reduced cooling effects, which can exacerbate heat island effects. The relationship between Carbon Storage and Urban Cooling is notably strong and positive (0.99), emphasising the role of vegetation in providing both carbon sequestration benefits and cooling effects. Furthermore, Flood Risk Control shows strong negative correlations with urbanisation metrics, indicating a potential trade-off where increased urbanisation may lead to challenges in managing flood risks effectively. Overall, these results highlight the complex dynamics between urban development and ecosystem services.

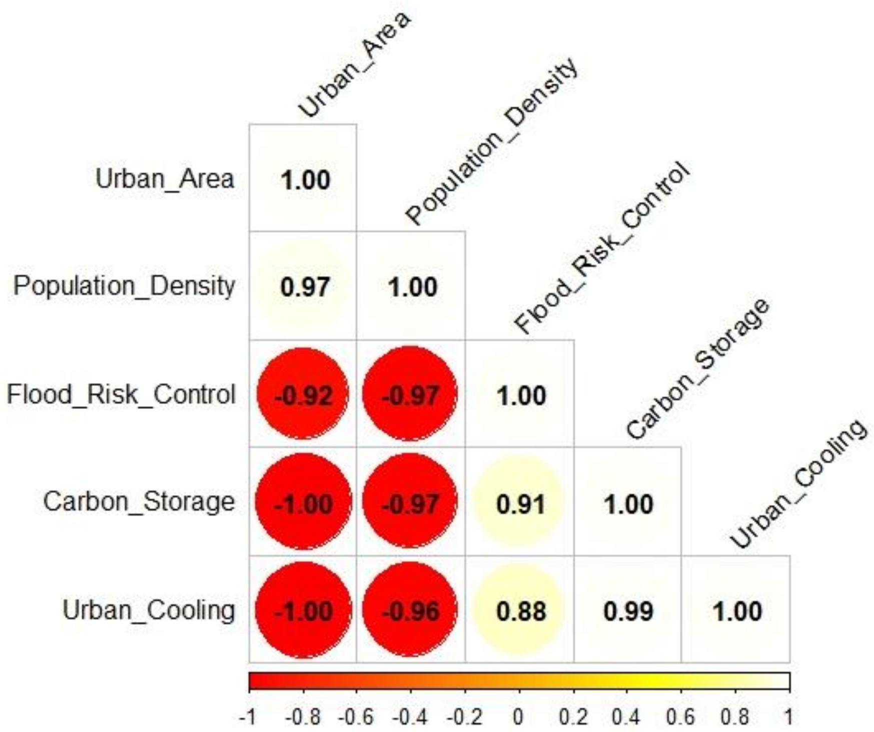

Figure 4. 14: The correlation matrix for GAMA

4.1.3.2 Geographically Weighted Regression (GWR)

The model provides valuable insights into the spatial relationships between urban expansion and environmental factors like carbon storage and heat mitigation index, using NDVI and NDBI as a predictor in DAGL (Table 4.24), and GAMA (Table 4.25). The spatial correlation between urban expansion and ecosystem services in DAGL, as revealed by the GWR model, highlights several key trends and implications for ecological management. For carbon storage, the correlation with NDVI increased significantly over time, from 0.41 in 1986 to 0.92 in 2023, indicating that vegetation cover became a stronger predictor of carbon storage. Similarly, the correlation with NDBI surged from 0.14 in 1986 to 0.91 in 2023, suggesting that urban expansion gradually became as influential as vegetation in explaining carbon storage patterns. This implies that built-up areas replaced high-capacity carbon storage ecosystems over time, contributing to their degradation.

In the case of urban cooling capacity, NDVI remained a strong predictor, peaking at 0.96 in 2023, confirming vegetation's critical role in cooling. The correlation with NDBI also increased dramatically from 0.18 in 2001 to 0.92 in 2023, indicating that urban infrastructure may have contributed to reduced cooling capacity. However, for runoff retention capacity (flood risk mitigation), initially strong correlations in 1986 decreased over time. By 2023, R^2 values for NDVI increased slightly to 0.36, and for NDBI to 0.32, suggesting that the predictors (vegetation and urban area) lost explanatory power over time, and other factors may dominate runoff retention capacity. These trends highlight that urban expansion's ecological impact is service-specific: while vegetation loss and built-up growth jointly explain carbon storage and urban cooling degradation patterns, runoff retention appears less directly linked to these factors in the DAGL.

The AICc (corrected Akaike Information Criterion) values in the table evaluate the performance of Geographically Weighted Regression (GWR) models for different ecosystem services. Lower AICc values indicate better model fit. For carbon storage, NDVI models show improving fit over time, with lower AICc values than NDBI models. In the reduction of urban cooling capacity, NDVI models have exceptionally good fits, especially in 2023, while NDBI models are less effective. For runoff retention capacity, NDVI models generally perform better than NDBI models, though with less strong fits compared to other services. Overall, NDVI tends to be a more effective predictor than NDBI across these services.

Table 4.24: GWR Analysis Results for DAGL

Ecosystem services	Year	Indices	AICc	R^2 (adjusted)
Carbon storage	1986	NDVI	69.39	0.41
		NDBI	73.17	0.14
	2001	NDVI	45.53	0.77
		NDBI	58.69	0.36
	2015	NDVI	30.35	0.92
		NDBI	40.31	0.84
	2023	NDVI	29.51	0.92
		NDBI	26.50	0.91
Urban cooling	2001	NDVI	-13.35	0.64
		NDBI	7.72	0.18
	2015	NDVI	-16.81	0.88
		NDBI	-4.52	0.75
	2023	NDVI	-29.45	0.96
		NDBI	-24.96	0.92
Flood risk mitigation (Runoff retention)	1986	NDVI	82.80	0.84
		NDBI	93.91	0.84
	2001	NDVI	58.27	0.56
		NDBI	67.42	0.16
	2015	NDVI	58.71	0.30
		NDBI	62.57	0.28
	2023	NDVI	59.75	0.36
		NDBI	60.04	0.32

AICc (corrected Akaike Information Criterion)

In GAMA (Table 4.16), for carbon storage capacity, the correlation with NDVI remained high, ranging from 0.95 in 1991 to 0.76 in 2023, indicating that vegetation cover was a strong predictor of carbon storage. Similarly, the correlation with NDBI was also high, from 0.93 in 1991 to 0.78 in 2023, suggesting that urban expansion played a significant role in explaining carbon storage degradation patterns. The NDVI was a strong predictor, with a pick at 0.96 in 2023, confirming vegetation's critical role in cooling. The correlation with NDBI also increased dramatically from 0.43 in 2001 to 0.90 in 2023, indicating that urban infrastructure may also have contributed to reducing cooling capacity over time. However, for runoff retention capacity, the correlations with both indices decreased over time, with R^2 values for NDVI dropping to 0.59 and for NDBI to 0.72 by 2023. This suggests that traditional predictors (vegetation and urban areas) lost explanatory power over time, and other factors may dominate runoff retention degradation dynamics. These trends highlight that urban expansion’s ecological impact is service-specific: while vegetation loss and built-up growth jointly explain carbon and cooling degradation patterns, runoff retention (flood risk mitigation) appears less directly linked to these factors in GAMA.

The AICc (corrected Akaike Information Criterion) values in the table evaluate the performance of Geographically Weighted Regression (GWR) models for different ecosystem services. Lower AICc values indicate better model fit. For carbon storage, NDVI models show improving fit over time, with lower AICc values than NDBI models. In the reduction of urban cooling capacity, NDVI models have exceptionally good fits, especially in 2023, while NDBI models are less effective. For runoff retention capacity, NDVI models generally perform better than NDBI models, though with less strong fits compared to other services. Overall, NDVI tends to be a more effective predictor than NDBI across these services.

Both DAGL and GAMA exhibit service-specific impacts of urbanisation, where vegetation loss and built-up growth jointly explain carbon storage and urban cooling degradation patterns, while runoff retention appears less directly linked to these factors. Additionally, NDVI is a strong predictor for carbon storage and urban cooling in both regions, highlighting vegetation's critical role in these services. Over time, the predictive power of NDVI and NDBI for runoff retention capacity decreases in both regions, suggesting other factors become more influential. The findings underscore the need for sustainable urban planning to mitigate ecosystem service degradation.

Table 4.25: GWR Analysis Results for GAMA

Ecosystem services	Year	Indices	AICc	R^2 (adjusted)
Carbon storage	1991	NDVI	77.72	0.95
		NDBI	96.75	0.93
	2002	NDVI	72.17	0.93
		NDBI	76.70	0.94
	2017	NDVI	73.72	0.87
		NDBI	82.71	0.87
	2023	NDVI	64.51	0.76
		NDBI	62.55	0.78
Urban cooling	2002	NDVI	-41.56	0.71
		NDBI	-36.95	0.43
	2017	NDVI	-52.13	0.82
		NDBI	-38.79	0.65
	2023	NDVI	-79.81	0.96
		NDBI	-83.37	0.90
Flood risk mitigation (Runoff retention)	1991	NDVI	119.77	0.94
		NDBI	147.21	0.87
	2002	NDVI	112.91	0.93
		NDBI	105.07	0.96
	2017	NDVI	110.39	0.86
		NDBI	112.54	0.88
	2023	NDVI	115.05	0.59
		NDBI	105.82	0.72

AICc (corrected Akaike Information Criterion)

4.2 Discussion

The results show a significant change in the landscapes of DAGL and GAMA, driven by urban expansion, population growth, and migration. These factors have collectively reshaped land use patterns in both regions. Furthermore, the rising population growth leads to an increased consumption rate of land and intensified urban expansion.

In DAGL, the verdant environment that was observed in 1986 has gradually degraded, with a huge proportion converted into construction land due to rapid urbanisation and increasing population density. This change occurred in the peripheral areas in the northern part of DAGL. As the population grew, so did the demand for housing and commercial spaces. Additionally, migration from rural areas to urban centres in search of employment intensified pressure on land resources leading to the loss of natural habitats. This observation is supported by Somadjago *et al*. (2020), who noted the absorption of hamlet and village, farming and woodland into the expanding urban area. These findings is also supported by Blakime *et al*. (2024) who revealed the increase in built-up areas due to the construction in the floodplain of Zio River to the detriment of vegetation and cultivated areas. Interestingly, despite this urban growth, agricultural land increased between 2001 and 2015 at the expense of grassland and forest. This trend reflects ongoing agriculture practises within urban settings and a rising demand for food, corroborated by Amouzoukpo (2021), who reported an increase in arable land in Agoènyivé, DAGL's second prefecture, between 2001 and 2019.

In contrast, GAMA, has experienced notable degradation of its grassland and forest landscapes since 1991 due to economic development and urbanisation. The region has seen considerable, rural-urban migration which has increased the demand for housing and industrial space, transforming previous lush green belts into built-up zones. Research by Addae and Oppelt, (2019); Asabere *et al*. (2020) and Devendran and Banon (2022) supports these findings by highlighting landscape fragmentation and the conversion of vegetated land into urban environments. Similar findings have also been reported by Osei *et al*. (2013); Toure *et al*. (2020) and Kleemann *et al*. (2017). Furthermore, Puplampu and Boafo (2021) pointed out a significant decrease in green spaces within the city. The expansion of the agricultural land from 1991 to 2002 aligns with the report from the Ghana MoFA (2018), which indicated an increase in agricultural areas over pasture and grassland due to government policies promoting urban and peri-urban agricultural development. The overall finding on the development of built up environments in DAGL and GAMA is confirmed by the research of Barman *et al*. (2024) in Jalpaiguri urban agglomeration, West Bengal, India; and the one of Tessema and Abebe, (2023) in Hawassa City in Ethiopia.

Regarding urban expansion analysis, it was observed expansion within the peri-urban zone in the cities, especially towards the northwest part of DAGL and in the northeastern and north-western parts of GAMA. Factors including high cost of rental in the urban core, affordability of land for housing production in the peripheral area, account for this expansion.

In terms of the intensity of urban expansion, over the past three decades, DAGL has experienced high-speed to very high-speed urban expansion, particularly in quadrants Q14 and Q15. This expansion is, primarily driven by the national road RN5, which connects the northwest suburbs to the city of Kpalimé. Affordable land and housing in areas like Aflao Gakli, Vakpossito, Zanguera, and some parts of Legbassito have attracted populations from the city centre. This supports Somadjago *et al*. (2020)'s hypothesis that housing accessibility is a major factor in DAGL's expansion. Additionally, Q14 includes

Sagbado, a border area between Togo and Ghana, where migration is prevalent, contributing to its significant population size in Grand Lomé (INSEED, 2022). Between 2015 and 2023, quadrants Q1 and Q16 have also experienced very high-speed expansion, with areas like Agoe-Nyive, Togblekope, and Adeticope emerging as new urban hubs due to their proximity to the national road RN1 and the establishment of commercial and industrial facilities (Hetcheli *et al*., 2017). For instance, Adeticope is viewed as a stable location for property investment and industrial development, with nearly 90% of its buildings being modern. The Industrial Platform of Adétikopé (PIA) exemplifies this trend as a major multi-sector economic development project aligned with the National Development Plan (PND, 2018–2022). This area has also become the main focus for the implementation of major public-private urban and property development projects, such as the Well-City project, which aims at improving the city's infrastructure, services, and liveability.

In contrast, quadrants Q2 and Q3 show moderate urban expansion due to the challenges posed by Zio valley in the eastern part of the city; water stagnation and seasonal flooding, making this area unsuitable for residential construction (Amouzoukpo, 2021; Blakime *et al*., 2024). Meanwhile, the coastal area of Grand Lomé in Q4, exhibits moderate urban expansion, but maintains a significant concentration of built-up areas due to Togo's major port and its location along the Abidjan-Lagos corridor, a critical transport road for trade and economic development in West Africa.

Similarly, GAMA experienced very high-speed urban expansion between 1991 and 2002 in quadrants Q2, Q3, Q5, Q12, and Q13, indicating peri-urbanisation in its peripheral areas. Major transportation roads linking the city centre to northeastern and western parts of GAMA have facilitated routine commuting while contributing to massive regional expansion (Owusu, 2013). In quadrant Q12, the very high expansion from 1991 to 2017 is attributed to the population increases in Weija-Gbawe Municipality, driven by built-up facilities and an industrialised economy (Adu-Boahen *et al*., 2023). Expansion in quadrant Q2 is largely due to the spillover effect from Tema and Ashaiman, meanwhile quadrant Q3's growth is driven by a high concentration of migrants seeking employment in industrial sectors and administrative institutions (Akubia and Bruns, 2019). The findings align with Agyemang *et al*. (2017), who noted significant built-up expansion toward Kpone-Katamanso to the east and Weija-Gbawe to the west. The low-speed urban expansion observed in quadrant Q13 from 2002 to 2017 result from flooding caused by overspills of Weija Dam (Owusu-Ansah *et al*., 2019). Quadrant Q14's very high urban development between 2017 and 2023 further emphasises Ga South as emerging urbanisation hotspot within GAMA (Agyemang *et al*., 2017).

The above findings are consistent with other studies suggesting that peri-urban development in Africa tends to follow major highways, which is usually an opportunity for residents to set up home-based and roadside businesses (Doan and Oduro, 2012). This is also confirmed by the research of Haldar *et al*. (2024) in Durgapur Municipal Corporation in West Bengal in India.

The spatial patterns of urban expansion in DAGL and GAMA reveal a growing trend towards urban sprawl, characterised by low-density development extending into peri urban areas. This is further evidenced by the rise in the relative Shannon's entropy values in both regions, which indicate increasing urban fragmentation and a more scattered distribution of built-up areas. This often results in inefficient land utilisation, with a significant conversion of natural land cover. Such sprawl patterns are not unique to DAGL and GAMA but are a common trend observed in various cities. For instance, similar patterns are experienced in the city of Kanpur in India (Aswal *et al.*, 2018) and Riyadh, the capital of Saudi Arabia (Rahman, 2016). Additionally, the Sekondi–Takoradi metropolitan assembly in Ghana has also experienced urban sprawl, with significant impacts on land use and land cover dynamics, as noted by Biney and Boakye (2021). Several factors may account for this sprawling growth, but major contributory factors are the improved transportation networks in the two cities that link them to other regions and informal growth and development, which is commonly observed in developing countries (Xu *et al*., 2019). Moreover, research indicates that informal settlements often emerge as a response to housing shortages driven by migration, leading to urban sprawl characterised by low-density growth and inadequate infrastructure (Seto *et al*., 2011). Furthermore, the spread of such action threatens natural habitats and can threaten urban food security due to reduced agricultural land. This trend is compounded by the limited effectiveness of existing laws and policies aimed at regulating urban expansion and protecting natural resources. Despite these regulatory frameworks, the pace of urbanisation continues to outstrip the capacity of governance structures to manage its impacts effectively. As a result, there is a pressing requirement for enhanced policy enforcement and innovative planning approaches that prioritise environmental sustainability alongside economic growth.

The results demonstrated that the expansion of the built-up areas exerts a demonstrably negative impact on Ecosystem Services (ESs) within both metropolitan regions, exhibiting spatial and temporal heterogeneity over the years. These findings align with a broader body of research confirming ESs losses due to urban expansion (Sun *et al*., 2018; Herrero-Jáuregui *et al*., 2019; Yuan *et al*., 2019; Yi *et al*., 2023; Hailu *et al*., 2024; Yushanjiang *et al*., 2024). This degradation stems primarily from the conversion of original ecological land, such as forests, grasslands, and agricultural areas, into construction sites. This land use transformation fundamentally compromises the capacity of these ecosystems to provide essential services.

As a direct consequence of this urban encroachment and ecological conversion, a parallel decline in carbon storage capacity is observed across both metropolitan areas. The work of Hailu *et al*. (2024) in Addis Ababa, Ethiopia, reported a significant decline in the value of climate regulation services, with key drivers in that region including rapid population growth and rural-urban migration trends that mirror the trends in DAGL and GAMA. This is further corroborated by Sun *et al*. (2018), who reported a decline in ESs, including carbon storage, in the Atlanta Metropolitan area, USA, emphasising the importance of forest management for carbon sequestration. However, it is important to note that the relationship between urban sprawl and ESs is not always straightforward. As demonstrated by Li *et al*. (2021) in Changchun, China, some ESs can increase (the example of carbon storage) despite urban sprawl due to improvements in land management practices. This highlights the importance of considering local context and specific management strategies when assessing the impacts of urban expansion on ESs.

The observed decline in both Heat Mitigation Index (HMI) and the cooling capacity within both regions indicate a diminishing ability of the landscape to provide cooling benefits over time, likely driven by increased urbanisation and vegetation loss. This suggests that as built environments expand, the cooling effects from green spaces become less effective. This trend aligns with the findings of Wu *et al*. (2024) in Yangzhou City, China, who also revealed a downward trend in HMI and cooling capacity, with low-value zones clustered around central urban areas coinciding with rapid urbanisation. This is further corroborated by Hu *et al*. (2023), who found that HMI was significantly higher in suburban areas than in urban centres due to differences in surface features (for example, albedo and heat capacity) population and building density. The correlation between the increase in average temperature and the decline in cooling capacity demonstrates how urbanisation contributes to higher temperatures in urban areas. This trend reflects the urban heat island effect, where cities experience significantly warmer temperatures than their rural surroundings due to human activities and land cover changes.

The overall decline in runoff retention capacity in both DAGL and GAMA likely reflects the loss of vegetated areas and the expansion of impervious surfaces due to urbanisation. As vegetation is replaced by buildings and roads, the land's ability to intercept rainfall, promote infiltration, and reduce runoff is compromised, thereby increasing the potential for surface water accumulation and flooding. This finding is corroborated by several studies. Li *et al*. (2018) revealed that urbanisation in Shenyang, China, led to increased runoff volume due to a reduction in runoff retention capacity in the inner urban area. Similarly, Bose and Mazumdar (2023) revealed a reduction in the average runoff retention capacity in the densely urbanised Kolkata City, West Bengal state (India), making the area extremely vulnerable to flooding. In North America, Sun *et al*. (2018) showed that the expansion of impervious surfaces in Atlanta metropolitan areas increased flood risk due to the fragmentation of green space and biodiversity loss. Conversely, studies in Hanoi City by Kefi *et al*. (2018) accentuated that increased green infrastructure substantially reduced flood damage. These trends are consistent with findings indicating a significant negative correlation between carbon density and urbanisation, particularly in developing areas, where substantial increases in urban land significantly impact carbon storage (Li *et al*., 2021).

Moreover, the spatial correlation between urban expansion and ecosystem services highlights the complex impacts of urbanisation on natural environments. Urban expansion often leads to the replacement of high-capacity carbon storage ecosystems with built-up areas, contributing to reduced carbon sequestration capabilities (Chen *et al*., 2023). This trend is also consistent with broader research indicating that urbanisation compromises ecosystem services, particularly through soil sealing and the expansion of impervious surfaces, which disrupt regulating services like temperature regulation and water runoff management (Eigenbrod., 2011; Tobias, 2012). For urban cooling capacity, both vegetation loss and urban infrastructure growth are critical predictors, emphasising the role of green spaces in mitigating heat island effects (Tobias, 2013; Yuan *et al*., 2019). However, for runoff retention, the influence of urban expansion and vegetation loss appears less direct, suggesting other factors such as drainage infrastructure potentially dominating. This is supported by Razaei *et al.* (2019) who highlighted the significant impact of urbanisation on runoff generation, emphasising that changes in land use and impervious surfaces alter hydrological processes. However, they also noted that urban catchment characteristics, such as drainage infrastructure, play a crucial role in runoff response. This suggests that while urban expansion affects runoff, the specific design and functionality of drainage systems can significantly influence runoff retention and management.

4.3 Major Findings

The following summarises the key findings of this study;

The study finds out that there is a significant change in the LULC of the two metropolitan areas DAGL and GAMA, characterised by a decline in forest, grassland and agricultural land over the study period, while the built environment expanded significantly from 18 % to 62 % in DAGL (1986 to 2023) and from 10 % to 70 % in GAMA (1991 to 2023), indicating substantial urban expansion. The urban expansion occurred predominantly towards the northwest in DAGL and in both north-east and north-west in GAMA of which the fragmented development is supported by a relative Shannon's entropy value close to 1.

In terms of ecosystem services, the study also finds out that the urban sprawling activities, has significantly diminished the distribution of ecosystem services in both regions over the study period, resulting in a decline in carbon storage capacity, Heat Mitigation Index (HMI), cooling capacity, and runoff retention capacity.

More so, the study finds out a strong correlation between urban expansion metrics and ecosystem services in both DAGL and GAMA. However, it's also noted that the runoff retention service in GAMA may be influenced by factors beyond urbanisation metrics.

Additionally, based on the GWR results, NDVI is a strong predictor for carbon storage and urban cooling in both regions, highlighting vegetation's critical role in these services. However, the predictive power of NDVI and NDBI for runoff retention capacity decreases in both regions over time, suggesting other factors become more influential.

CHAPTER FIVE

5.0 CONCLUSION AND RECOMMENDATIONS

5.1 Conclusion

This study investigates the implications of urban expansion for ecosystem services provision in two metropolitan cities the District Autonome du Grand Lomé (DAGL) and Greater Accra Metropolitan Area (GAMA). It focuses on critical ecosystem services such as carbon storage, flood risk control, and urban cooling, areas that have not been thoroughly evaluated in previous studies despite their importance in mitigating climate change impacts in rapidly growing cities.

The findings indicate that both DAGL and GAMA have experienced significant urban growth over the years, from 18 % to 62 % in DAGL between 1986 and 2023 and from 10 % to 70 % in GAMA from 1991 to 2023. This urbanisation has led to a decrease in natural vegetation and green spaces within these cities. Forest cover in DAGL fell from 24 % in 1986 to 3 % by 2023, and from 34 % in 1991 to 2 % in 2023 in GAMA. Grasslands also saw significant reductions, from 22.09 % to 7.38 % in DAGL and from 42 % to 4 % in GAMA. Agricultural land decreased from 35,36 % to 27.12 % while increase from 12 % to 21 % in GAMA. Directional analyses reveal that urban expansion predominantly occurred towards the northwest in DAGL and in both northeast and northwest in GAMA.

Consequently, the identified ecosystem services, carbon storage, urban cooling, and flood risk control have been degraded. In the DAGL the total carbon storage significantly declined from 3,604,852 Mg of C in 1986 to 1,367,113 Mg of C by 2023. Similarly, in the GAMA, carbon storage dropped from 16,574,522 Mg of C in 1991 to 4,120,702 Mg of C by 2023. The cooling capacity also decreased in both regions, dropping from 0.60 in 2001 to 0.30 in 2023 in DAGL and from 0.65 in 2002 to 0.25 in 2023 in GAMA. In both

DAGL and GAMA, the runoff retention decreased from 29,098,483 m^3 in 1986 to 17,908,270 m^3 in 2023, and from 85,027,128 m^3 in 1991 to 57,500,096 m^3 in 2023. A negative correlation (Between -0.96 and -0.99) was observed between urban metrics and ecosystem services in both metropolitan areas, suggesting that as urbanisation increases, the capacity of these ecosystems to provide essential services declines. These findings align with global trends indicating that urban expansion significantly impacts ecosystem services.

5.2 Recommendations

The following are recommended based on the major findings of the study:

5.2.1 Recommendations on policy improvement

Afforestation programmes are inevitable in both cities if the two countries will not fail in their national determined contributions (NDC) COP28 to limit temperature rise to 1.5 degrees Celsius by the end of this century and avoid the worst impacts of climate change like severe droughts, heat-waves and flooding.

The Ministry of Urban Planning, Housing, and Living Environment (MUHRF) in Togo and the Land Use and Spatial Planning Authority (LUSPA) in Ghana should urgently start to adopt mixed land use and vertical development while also applying integrated environmental management.

To enhance the effectiveness of Togo's Decree 67_228 on town planning and its National Housing Strategy, as well as Ghana's Land Use and Spatial Planning Act, 2016 and its National Housing Policy, there is a need for a paradigm shift from the customary landowner's control of development that proliferate informal settlements to government agencies adopting zoning ordinances, planning, and building code regulations.

Discriminant proposal development plan approval and taxes should be adopted to discourage development in reserve areas while encouraging development in other parts of the metropolises. This will help in redirecting the urban morphology and Urban Heat Island (UHI). To key into the global crusade on climate change mitigation and adaptation, there is the need to consciously integrate climate change measures into urban planning and development (Goal 13), and promoting the sustainable use of terrestrial ecosystems, reversing land degradation and biodiversity loss (Goal 15).

The significant loss of ecosystem services calls for the governmental agencies to promote urban agriculture, networks of parks and green corridors, and integrating green infrastructure into building design. The stakeholders from the Ministry of Environment and Forest Resources (MERF) and the National Environmental Management Agency (ANGE) in Togo, as well as the Environmental Protection Agency (EPA), an arm of the Ministry of Environment, Science, Technology, and Innovation (MESTI) in Ghana, must focus on mitigating environmental degradation and adapting to climate change for urban resilience and sustainability.

5.2.2 Recommendations on performance improvement

Under business-as-usual scenario, where population continue to grow and resource consumption intensifies in both cities, there is urgent need for implementing nature-based solutions, such as reforestation and urban greening with native plant species, to enhance runoff retention and mitigate flood risk, thereby improving the cities' liveability. Furthermore, encouraging community participation in urban planning processes is essential to ensure that developments meet local needs, minimise resource depletion, and increase awareness of ecological importance. Communities should also be encouraged to adopt nature-based solutions, including education on protecting and restoring natural areas. These ecosystems offer valuable protection against heat waves, erosion, and flooding, and their preservation should be prioritised.

5.3 Contributions to Knowledge

The study reveals significant land use and land cover (LULC) changes in the two metropolitan areas, DAGL and GAMA, characterized by declines in forest, grassland, and agricultural land over the study period. Meanwhile, the built-up environment expanded substantially, increasing from 18% to 62% in DAGL (1986–2023) and from 10% to 70% in GAMA (1991–2023), reflecting pronounced urban expansion. This expansion primarily occurred toward the northwest in DAGL and in both the northeast and northwest in GAMA, with the fragmented development pattern confirmed by a Shannon's entropy value close to 1. This imply that urban sprawl has significantly diminished ecosystem services in both regions, resulting in declines in carbon storage, heat mitigation, cooling capacity, and runoff retention. For instance, carbon storage decreased from 3.6 million Mg in 1986 to 1.4 million Mg in 2023 in DAGL, and from 16.6 million Mg in 1991 to 4.1 million Mg in 2023 in GAMA. Runoff retention indices also dropped considerably, alongside a halving of cooling capacity from 2000 to 2023, correlating with rising average temperatures. Furthermore, a strong negative correlation was found between urban expansion metrics and ecosystem services in both metropolitan areas. These findings underscore the adverse impacts of urban sprawl on ecosystem functions and highlight the urgent need for coordinated land-use planning and the integration of nature-based solutions to foster sustainable urban development.

REFERENCES

Abera, W., Lulseged Tamene, A., Tibebu Kassawmar, B., Kalkidan Mulatu, A., Habtemariam Kassa, C., Louis Verchot, D., & Marcela, Q. (2021). Impacts of land use and land cover dynamics on ecosystem services in the Yayo coffee forest biosphere reserve, southwestern Ethiopia. *Ecosystem Services*, *6* (101338), 1–16. https://doi.org/10.1016/j.ecoser.2021.101338

Abdulai, I. A. & Osumanu, I. K. (2023). How urbanisation shapes availability of provisioning ecosystem services in peri-urban Ghana. *International Journal of Urban Sustainable Development*, *15* (1), 282–298. https://doi.org/10.1080/19463138.2023.2267518

Abubakari, M. & Mahama M. (2023). Sustaining the urban commons in Ghana through decentralised planning. *Heliyon*, 9, e15895, 1-13. Doi: 10.1016/j.heliyon.2023.e15895

Addae, B., & Oppelt, N. (2019). Land-Use/Land-Cover Change Analysis and Urban Growth Modelling in the Greater Accra Metropolitan Area (GAMA), Ghana. *Urban Science*, *3*(26), 20. https://doi.org/10.3390/urbansci3010026

Adjei-Darko, P. (2017). *Remote Sensing and Geographic Information Systems for Flood Risk Mapping and Near Real-time Flooding Extent Assessment in the Greater Accra Metropolitan Area*. Master Thesis, KTH Royal Institute of Technology, School of Architecture and the Built Environment, Stockholm, Sweden. Retrieved from DiVA database.

Adu-Boahen, K., Addai, M. O., Hayford, S. C., Adjovu, E. T., Yeboah, D. O., & Mensah, P. (2023). Human-environment nexus: evaluating the anthropo-geomorphology and urban expansion of the Weija Gbawe Municipality, Ghana. *Discover Environment*, *1*, 21. https://doi.org/10.1007/s44274-023-00022-0

Afidégnon, D. (1999). *Les mangroves et les formations associées du sud-est du Togo : analyse écofloristique et cartographique par télédétection spatiale.* Thèse de doctorat, Université de Lomé, Togo.

Agbemedi, Y. M. (2022). *Production de la plage dans le grand Lomé (Togo) et le Greater Accra (Ghana) : pratiques , logiques , enjeux.* Thèse de doctorat, Université de Nanterre - Paris X; Université de Lomé, Togo.

Agyapong, E. B., Ashiagbor, G., Nsor, C. A., & van Leeuwen, L. M. (2018). Urban land transformations and its implication on tree abundance distribution and richness in Kumasi, Ghana. *Journal of Urban Ecology*, *4*(1), 1–11. https://doi.org/10.1093/jue/juy019

Agyemang, F. S. K., Amedzro, K. K., & Silva, E. (2017). The emergence of city-regions and their implications for contemporary spatial governance: Evidence from Ghana. *Cities,* July, 1-29. https://doi.org/10.1016/j.cities.2017.07.009

Aholou, C. C. (2008). *Proximité spaciale, distances socio-culturelles à Cotonou (Bénin) et à Lomé (Togo) : étude comparative Etude comparative.* Thèse de doctorat, Université Paris X Nanterre, Paris.

Akpagana, K., & Bouehet, P. (1994). Etat actuel des connaissances sur la flore et la végétation du Togo. *Acta Botanica Gallica:Botany letters,* 141:3, 367-372.

https://doi.org/10.1080/12538078.1994.10515170

Akubia, J. E. K., & Bruns, A. (2019). Unravelling the frontiers of urban growth: Spatio-Temporal dynamics of land-use change and urban expansion in greater Accra metropolitan area, Ghana. *Land*, *8*(9), 1–23. https://doi.org/10.3390/land8090131

Amouzoukpo, K. (2021). *Dynamique residentielle, mutations sociospatiales et environnementales a agoenyive (peripherie nord de lome au togo).* Thèse de doctorat, Université de Lomé, Togo.

Anarfi, K., Shiel C. & Hill, R. A. (2020). Assessing How Sustainability Is Promoted in Ghana's National Urban Policy and Action Plan. *Sustainability*, 12, 7556,1-15. doi:10.3390/su12187556

Anderson, J. R. (1976). *A land use and land cover classification system for use with remote sensor data* (Vol. 964). US Government Printing Office. Retrieved from https://books.google.tg/books?hl=en&lr=&id=dEToP4UpSIC&oi=fnd&pg=PA7&dq=Anderson+(1976)&ots=sZnqV1c9C&sig=5MtFNAUSDzBclC9WmMk1jvQbDQs&redir_esc=y#v=onepage&q=Anderson%20(1976)&f=false

Andreasen, M. H., Agergaard, J., Kofie, R. Y., Møller-Jensen, L., & Oteng-Ababio, M. (2022). Urban encroachment in ecologically sensitive areas: drivers, impediments and consequences. *Buildings and Cities*, *3*(1), 920–938. https://doi.org/10.5334/bc.210

Asabere, S. B., Acheampong, R. A., Ashiagbor, G., Beckers, S. C., KecAk, M., Erasmi, S., Schanze, J., & Sauer, D. (2020). Urbanisation, land use transformation and spatio-environmental impacts: Analyses of trends and implications in major metropolitan regions of Ghana. *Land Use Policy*, *96*, 104707. https://doi.org/10.1016/j.landusepol.2020.104707

Aswal, P., Saini, R., & Ansari, M. T. (2018). Spatio Temporal Monitoring of Urban Sprawl using GIS and Remote Sensing Technique. *International Journal of Computer Applications 182*(27), 11–24. https://doi.org/10.5120/ijca2018918100

Avtar, R., Kumar, P., Oono, A., Saraswat, C., Dorji, S., & Hlaing, Z. (2017). Potential application of remote sensing in monitoring ecosystem services of forests, mangroves and urban areas. *Geocarto International*, *32*(8), 874–885. https://doi.org/10.1080/10106049.2016.1206974

Awotwi, A., Forkuo, E. K., Kumi, M., Yeboah, F., & Forkuo, E. K. (2017). Assessing the land use and land cover changes due to urban growth in Accra, Ghana. *Journal of Basic and Applied Research International*, *22*(2), 2395–3446.

Barman, S., Roy, D., Chandra Sarkar, B., Almohamad, H., & Abdo, H. G. (2024). Assessment of urban growth in relation to urban sprawl using landscape metrics and Shannon's entropy model in Jalpaiguri urban agglomeration, West Bengal, India. *Geocarto International*, *39*(1). https://doi.org/10.1080/10106049.2024.2306258

Bawa, A. (2017). *Mutations des périphéries urbaines au sud du Togo : des espaces ruraux à l ' épreuve du peuplement et de la marchandisation des terres.* Thèse de doctorat, Université de Montpellier, France.

Bawa, A., Djalna, K., Kamou, H., Batawila, K., Imbernon, J., & Akpagana, K. (2021). Role of Women in Maintaining Suburban Agricultural Land in Togo (West Africa).

Open Access Library Journal, 8, 1-11. doi: 10.4236/oalib.1108182.

Belgiu, M., & Dragut, L. (2016). Random forest in remote sensing: A review of applications and future directions. *Photogrammetry and Remote Sensing*, *114*, 24–31. https://doi.org/10.1016/j.isprsjprs.2016.01.011

Biakouye Awussu Kodjo. (2014). *Lome au-dela de Lome: Etalement urbain et territoires dans une metropole d Afrique sud-saharienne*. Thèse de doctorat, Université de Lomé, Togo et Université Paris Ouest Nanterre La Défense, France.

Biney, E. & Boakye, E. (2021). Urban sprawl and its impact on land use land cover dynamics of Sekondi-Takoradi metropolitan assembly, Ghana. *Environmental Challenges*, 4, 100168. https://doi.org/10.1016/j.envc.2021.100168.

Blakime, T.-H., Komi, K., Adjonou, K., Hlovor, A. K. D., Gbafa, K. S., Oyedele, P. B., Botolisam, P., & Kokou, K. (2024). Derivation of a GIS-Based Flood Hazard Map in Peri-Urban Areas of Greater Lomé, Togo (West Africa). *Urban Science*, *8*(3), 96, 1-17. https://doi.org/10.3390/urbansci8030096

Blakime, T. H., Adjonou, K., Komi, K., Hlovor, A. K. D., Gbafa, K. S., Zoungrana, J. B. B., Polorigni, B., & Kokou, K. (2024). Dynamics of Built-Up Areas and Challenges of Planning and Development of Urban Zone of Greater Lomé in Togo, West Africa. *Land*, *13*(1), 1-16. https://doi.org/10.3390/land13010084

Bose, S., & Mazumdar, A. (2023). Correction to: Urban flood risk assessment and mitigation with InVEST-UFRM model: a case study on Kolkata City, West Bengal state (India). *Arabian Journal of Geosciences*, *16*(6). https://doi.org/10.1007/s12517-023-11486-y

Breiman, L. (2001). Random Forests. *Machine Learning*, *45*, 5–32. https://doi.org/10.1023/A:1010933404324

Burgess, E. W. (1925). *The growth of a city: An introduction to a research project*. In R. Park, E. W. Burgess, & R. D. McKenzie (Eds.), *The City* (pp. 47-62). Chicago: University of Chicago Press.

Burkhard, B., Kroll, F., Nedkov, S., & Müller, F. (2012). Mapping ecosystem service supply, demand and budgets. *Ecological Indicators*, *21*, 17–29. https://doi.org/10.1016/j.ecolind.2011.06.019

Cao, H., Liu, J., Chen, J., Gao, J., Wang, G., & Zhang, W. (2019). Spatiotemporal patterns of urban land use change in typical cities in the Greater Mekong Subregion (GMS). *Remote Sensing*, *11*(7), 801, 1-28. https://doi.org/10.3390/rs11070801

Carrasco-Escobar, G., Manrique, E., Ruiz-Cabrejos, J., Saavedra, M., Alava, F., Bickersmith, S., Prussing, C., Vinetz, J. M., Conn, J. E., Moreno, M., & Gamboa, D. (2019). High-accuracy detection of malaria vector larval habitats using drone-based multispectral imagery. *PLoS Neglected Tropical Diseases*, *13*(1), 1–24. https://doi.org/10.1371/journal.pntd.0007105

Chaplin-Kramer, R., Sharp, R. P., Weil, C., Bennett, E. M., Pascual, U., Arkema, K. K., Brauman, K. A., Bryant, B. P., Guerry, A. D., Haddad, N. M., Hamann, M., Hamel, P., Johnson, J. A., Mandle, L., Pereira, H. M., Polasky, S., Ruckelshaus, M., Shaw, M. R., Silver, J. M., … Daily, G. C. (2019). Global modeling of nature's contributions to people. *Science*, *366*(6462), 255–258.

https://doi.org/10.1126/science.aaw3372.

Chen, R., Zhang, D., Nan, Y., Feng, H. & Geng, X. (2023), Assessing the impacts of future urban expansion on multiple ecosystem services in the transnational area of Changbai Mountain. Frontiers in Earth Science. 11:1163224, 1-14. doi:10.3389/feart.2023.1163224

Chow, V., Maidment, D., & Mays, L. (1988). *Applied hydrology.* McGraw Hill Inc, New York.

Cobbinah, P. B., & Darkwah, R. M. (2016). African Urbanism: the Geography of Urban Greenery. *Urban Forum*, *27*(2), 149-165. https://doi.org/10.1007/s12132-016 9274

Dabie, K. P. (2015). *Assessing the impact of urban sprawl on agricultural land use and food security in shai osudoku district.* Master's thesis, University of Ghana, Ghana.

Devendran, A. A., & Banon, F. (2022). Spatio-Temporal Land Cover Analysis and the Impact of Land Cover Variability Indices on Land Surface Temperature in Greater Accra, Ghana Using Multi-Temporal Landsat Data. *Journal of Geographic Information System*, *14*(03), 240–258. https://doi.org/10.4236/jgis.2022.143013

DeVries, B., Huang, C., Armston, J., Huang, W., Jones, J. W., & Lang, M. W. (2020). Rapid and robust monitoring of flood events using Sentinel-1 and Landsat data on the Google Earth Engine. *Remote Sensing of Environment*, *240* (August), 1-15. https://doi.org/10.1016/j.rse.2020.111664

Doan, P., & Oduro, C. Y. (2012). Patterns of population growth in peri-urban accra, Ghana. *International Journal of Urban and Regional Research*, *36*(6), 1306–1325. https://doi.org/10.1111/j.1468-2427.2011.01075.x

Duan, Q., Tan, M., Guo, Y., Wang, X., & Xin, L. (2019). Understanding the spatial distribution of urban forests in China using Sentinel-2 images with Google Earth Engine. *Forests*, *10*(9), 1–15. https://doi.org/10.3390/f10090729

Dubresson A. (1996). *Crises et peuplement des villes en Afrique au sud du Sahara in : Crise et population en Afrique. Crises économiques, politiques d'ajustement et dynamiques démographiques*. Les Etudes du CEPED*,13, Paris*.

Dupras, J., & Alam, M. (2015). Urban Sprawl and Ecosystem Services: A Half Century Perspective in the Montreal Area (Quebec, Canada). *Journal of Environmental Policy and Planning*, *17*(2), 180–200. https://doi.org/10.1080/1523908X.2014.927755

Dupras, J., Marull, J., Parcerisas, L., Coll, F., Gonzalez, A., Girard, M., & Tello, E. (2016). The impacts of urban sprawl on ecological connectivity in the Montreal Metropolitan Region. *Environmental Science and Policy*, *58*, 61–73. https://doi.org/10.1016/j.envsci.2016.01.005

ECA/AfDB, O. (2022). *Africa's Urbanisation Dynamics 2022: The Economic Power of Africa's Cities*. OECD Publishing, Paris.

Edokossi, K. A., & Bakis, R. (2019). Analysis of Urban Expansion and its Impact on Land Surface Temperature in Lomé City (Togo) Using Remote Sensing and Gis. *International Journal of Scientific & Engineering Research*, *10*(6), 1401–1409. https://doi.org/10.1016/j.ejrs.2021.03.003

Eigenbrod, F., Bell, V. A., Davies, H. N., Heinemeyer, A., Armsworth, P. R. & Gaston, K. J. (2011), The impact of projected increases in urbanisation on ecosystem services. *Proceedings of the Royal Society B* 278, 3201–3208. https://doi.org/10.1098/rspb.2010.2754

Eneogwe, I. C., & Umunake, H. c. (2021). Exploring Urban Landuse Expansion and Its Impacts on Urban Development in Abuja Nigeria, West Africa. *Journal of Environmental Pollution and Control*, *52*, 101–111.

Foucault, B., Akpagana, K., Batawila, K., & Bouchet P. (2000). Contribution à une étude phytosociologique du littoral sableux du Togo. *Acta Botanica Gallica*, 147:4, 333-344.

Frimpong, K., Atiemo, D. E., & Van Etten, E. J. (2022). Urban Sprawl and microclimate in the GA East municipality of Ghana. *Heliyon*, *8, 7, e09791*. doi: 10.1016/j.heliyon.2022.e09791

Fryd, O., Pauleit, S., & Bühler, O. (2012). The role of urban green space and trees in relation to climate change. *CABI Digital Library*, Janvier, 1–18. https://doi.org/10.1079/PAVSNNR20116053

García-Álvarez, D., Camacho Olmedo, M. T., Mas, J.-F., & Paegelow, M. (2022). Land Use Cover Mapping, Modelling and Validation: A Background. In D. García-Álvarez, M. T. Camacho Olmedo, J.-F. Mas, & M. Paegelow (Eds.), *Land Use Cover Datasets and Validation Tools*, 21-29. https://doi.org/10.1007/978-3-030-90998-7_2

García-Pardo, K. A., Moreno-Rangel, D., Domínguez-Amarillo, S., & García-Chávez, J. R. (2022). Remote sensing for the assessment of ecosystem services provided by urban vegetation: A review of the methods applied. *Urban Forestry and Urban Greening*, *74*, 127636. https://doi.org/10.1016/j.ufug.2022.127636

Gayibor, N., Marguerat, Y., & Nyassogbo, K. (Eds.). (1998). *Lomé, 100 ans de croissance démographique*. Collection “Patrimoines”, 7, 303–314). Lomé: Presses de l’Université du Bénin, Togo.

Gorelick, N., Hancher, M., Dixon, M., Ilyushchenko, S., Thau, D., & Moore, R. (2017). Google Earth Engine: Planetary-scale geospatial analysis for everyone. *Remote Sensing of Environment*, *202*(2016), 18–27. https://doi.org/10.1016/j.rse.2017.06.031

GSS, (2021). Ghana 2021 Population and Housing Census. General Report. Retrieved from:https://www.bing.com/search?q=Ghana+2021+Population+and+Housing+Census+General+Report+pdf, 10th January 2023.

Guézéré, A. (2011). L’obsession d’habiter sa propre maison à Lomé : quel impact sur la dynamique spatiale ? *Les Cahiers d’Outre-Mer*, *256, 565-590*. https://doi.org/10.4000/com.6443.

Güneralp, B., Lwasa, S., Masundire, H., Parnell, S., & Seto, K. C. (2018). Urbanisation in Africa: Challenges and opportunities for conservation. *Environmental Research Letters*, *13*(1), 1-9. https://doi.org/10.1088/1748-9326/aa94fe

Guo, J., Zhang, M. (2021). Exploring the Patterns and Drivers of Urban Expansion in the Texas Triangle Megaregion. *Land*, 10(11), 1244.

https://doi.org/10.3390/land10111244

Gyimah, R. R., kwang, C., Antwi, R. A., Morgan Attua, E., Owusu, A. B., & Doe, E. K. (2023). Trading greens for heated surfaces: Land surface temperature and perceived health risk in Greater Accra Metropolitan Area, Ghana. *Egyptian Journal of Remote Sensing and Space Science*, *26*(4), 861–880. https://doi.org/10.1016/j.ejrs.2023.09.004

Hailu, T., Assefa, E., & Zeleke, T. (2024). Urban expansion induced land use changes and its effect on ecosystem services in Addis Ababa, Ethiopia. *Frontiers in Environmental Science*, *12*(November), 1–21. https://doi.org/10.3389/fenvs.2024.1454556

Haines-Young, R., & Potschin, M. (2018). *Common International Classification of Ecosystem Services (CICES) V5.2: Guidance on the application of the revised structure* (Vol. 5.1, January). Retrieved from: www.cices.eu

Haldar, S., Chatterjee, U., Bhattacharya, S., Paul, S., Bindajam, A. A., Mallick, J., & Abdo, H. G. (2024). Peri-urban dynamics: assessing expansion patterns and influencing factors. *Ecological Processes*, *13, 58*. https://doi.org/10.1186/s13717-024-00533-5

Hameed, A. A. S. (2021). Urban and Regional Planning Strategies to Achieve Sustainable Urban Development: (Subject review). *International Journal of Advances in Scientific Research and Engineering (ijasre)*, 7(3), 22-27. doi: 10.31695/IJASRE.2021.33980

Hamel, P., & Remme, R. (2021). A spatially explicit approach to simulate urban heat mitigation with InVEST (v3.8.0). *Geoscientific Model Development*, 14(6), *3521–3537*. https://doi.org/10.5194/gmd-14-3521-2021

Han, J., Zhang, Z., Cao, J., Luo, Y., Zhang, L., Li, Z., & Zhang, J. (2020). Prediction of winter wheat yield based on multi-source data and machine learning in China. *Remote Sensing*, *12*(2), 1-22. https://doi.org/10.3390/rs12020236

Hengl, T., Heuvelink, G. B. M., Kempen, B., Leenaars, J. G. B., Walsh, M. G., Shepherd, K. D., Sila, A., MacMillan, R. A., De Jesus, J. M., Tamene, L., & Tondoh, J. E. (2015). Mapping soil properties of Africa at 250 m resolution: Random forests significantly improve current predictions. *PLoS ONE*, *10*(6), 1–26. https://doi.org/10.1371/journal.pone.0125814

Herrero-Jáuregui, C., Arnaiz-Schmitz, C., Herrera, L., Smart, S. M., Montes, C., Pineda, F. D., Schmitz, M. F. (2019). Aligning landscape structure with ecosystem services along an urban–rural gradient. Trade-offs and transitions towards cultural services. *Landscape Ecology*, 34, 1525–1545. https://doi.org/10.1007/s10980-018-0756-3

Hetcheli, F., Dandonougbo, I., & Biakouye, awussu kodjo. (2017). Du village a l'espace periurbain : mutations socio-economiques du canton d'adetikope, un territoire sous influence de lome (togo). *Homme et Societe*, 2409–9791. https://www.researchgate.net/publication/332298960

Hope, K. R. (1998). Urbanisation and Urban Growth in Africa. *Journal of African and Asian Studies*, 33(4), 345–358. https://doi.org/10.1163/156852198X00104

Hou, Y., Huang, Q., Ren, Q., Gu, T., Zhou, Y., Wu, P., Fan, Y., & Zhu, G. (2024).

Spatiotemporal dynamics of urban sprawl in China from 2000 to 2020. *GIScience and Remote Sensing*, *61*(1), 1-25. https://doi.org/10.1080/15481603.2024.2351262

Hu, Y., Wang, C., & Li, J. (2023). Assessment of Heat Mitigation Services Provided by Blue and Green Spaces: An Application of the InVEST Urban Cooling Model withScenario Analysis in Wuhan, China. *Land*, *12*(5), 1-21. https://doi.org/10.3390/land12050963

Iddrisu, S., Siiba, A., Alhassan, J., & Abass, K. (2023). Land-use and land cover change dynamics in urban Ghana: implications for peri-urban livelihoods. *International Journal of Urban Sustainable Development*, *15*(1), 80–96. https://doi.org/10.1080/19463138.2023.2184822

Ingwani, E., Thynell, M., Gurure, L. R., Ekelund, N. G. A., Gumbo, T., Schubert, P., & Nel, V. (2024). The Impacts of Peri-Urban Expansion on Municipal and Ecosystem Services: Experiences from Makhado Biaba Town, South Africa. *Urban Forum*. 35 (2), 297-327. https://doi.org/10.1007/s12132-023-09499-7

INSEED. (2022). Résultats Definitifs du 5e Recensement Général de la Population et de l'Habitat (RGPH-5) de novembre 2022. Retrieved from : https://inseed.tg/resultats-definitifs-du-rgph-5-novembre-2022/, 7th July 2023.

IPCC. (2006). 2006 IPCC Guielines for National Greenhouse Gas Inventories, Volume 4: Agriculture, Forestry and other Land Use. Institute for Global Environmental Strategies (IGES), Japan, Retrieved from: https://www.ipcc-nggip.iges.or.jp/public/2006gl/vol4.html

IPCC. (2022). Climate Change 2022: Impacts, Adaptation, and Vulnerability. In H.-O. Pörtner, D. C. Roberts, M. Tignor, E. S. Poloczanska, & M. Mintenbeck (Eds.), Contribution of Working Group II to the Sixth Assessment Report of the Intergovernmental Panel on Climate Change. Cambridge University Press. Retrieved from https://www.ipcc.ch/report/sixth-assessment-report-working-group-ii/

Jain, M., Dawa, D., Mehta, R., Dimri, A. P., & Pandit, M. K. (2016). Monitoring land use change and its drivers in Delhi, India using multi-temporal satellite data. *Modeling Earth Systems and Environment*, *2*(1), 1–14. https://doi.org/10.1007/s40808-016

0075-0

Jin, Y., Liu, X., Chen, Y., & Liang, X. (2018). Land-cover mapping using Random Forest classification and incorporating NDVI time-series and texture: A case study of central Shandong. *International Journal of Remote Sensing*, 39, 8703–8723. https://doi.org/10.1080/01431161.2018.1490976

Kafy, A., Hasan, M. M., Muhaiminul Islam, A.-A.-F., & Rahman, M. S. (2020). Modelling future land use land cover changes and their impacts on land surface temperatures in Rajshahi, Bangladesh. *Remote Sensing Applications: Society and Environment*, 18, 100314. https://doi.org/10.1016/j.rsase.2020.100314

Kafy, A., Faisal, A. Al, Al Rakib, A., Fattah, M. A., Rahaman, Z. A., & Sattar, G. S. (2022). Impact of vegetation cover loss on surface temperature and carbon emission in a fastest-growing city, Cumilla, Bangladesh. *Building and Environment*, *208*, 108573. https://doi.org/10.1016/j.buildenv.2021.108573

Kefi, M., Mishra, B. K., Kumar, P., Masago, Y., & Fukushi, K. (2018). Assessment of tangible direct flood damage using a spatial analysis approach under the effects of climate change: Case study in an urban watershed in Hanoi, Vietnam. *ISPRS International Journal of Geo-Information*, *7*(1), 1-18. https://doi.org/10.3390/ijgi7010029

Kettunen, M., & D'Amato, D. (2013). Provisioning Services and Related Goods. In M. Kettunen & P. ten Brink (Eds.), *Social and Economic Benefits of Protected Areas: An Assessment Guide* (pp. 97–113). Routledge. https://doi.org/10.4324/9780203095348-10

Klassou, K. S. (2014). L ' influence humaine dans l ' origine et la gravite des inondations au T ogo : cas de l ' amenagement de l ' espace dans la grande banlieue nord de Lome (Togble- Adetikope). *Revue de Géographie Tropicale et d'Environnement*, *2*, 3–15. Retrived from https://www.revues-ufhb-ci.org/fichiers/FICHIR_ARTICLE_2531.pdf

Kleemann, J., Inkoom, J. N., Thiel, M., Shankar, S., Lautenbach, S., & Fürst, C. (2017). Peri-urban land use pattern and its relation to land use planning in Ghana, West Africa. *Landscape and Urban Planning*, *165*, 280–294. https://doi.org/10.1016/j.landurbplan.2017.02.004

Koko, A. F., Wu, Y., Abubakar, G. A., Alabsi, A. A. N., Hamed, R., & Bello, M. (2021). Thirty years of land use/land cover changes and their impact on urban climate: A study of kano metropolis, nigeria. *Land*, *10*(11), 1–27. https://doi.org/10.3390/land10111106

Koukou, K. (1998). *Les mosaiques forestières au sud du Togo : biodiversité , dynamique et activités humaines*. Thèse de doctorat, Université de Montpellier II, France.

Korah, A., Koch, A. M. J., & Wimberly, M. c. (2024). Understanding urban growth modeling in Africa: Dynamics, drivers, and challenges. *Cities*, 146, 104734. https://doi.org/10.1016/j.cities.2023.104734

Kotapati, N. L., Venkata, R. K., & Venkataramana, S. (2021). Analysis of Land Use and Land Cover using Machine Learning Alogarithms on Google Earth Engine for Munneru River. *Sustanability*, *13*(1), 1-15. https://doi.org/10.1016/j.ecoinf.2023.102223

Kumar, L., & Mutanga, O. (2018). Google Earth Engine applications since inception: Usage, trends, and potential. *Remote Sensing*, *10*(10), 1–15. https://doi.org/10.3390/rs10101509

OECD, (2025). Africa's Urbanisation Dynamics 2025: Planning for Urban Expansion. OECD Publishing, Paris, https://doi.org/10.1787/2a47845c-en

Leha, M. D. K., Matlocka, M. D., Cummings, E. C., & Nalley, L. L. (2013). Quantifying and mapping multiple ecosystem services change in West Africa. *Agriculture, Ecosystems and Environment*, *165*, 6-18. https://doi.org/10.1016/j.agee.2012.12.001

Li, C., Liu, M., Hu, Y., Shi, T., Zong, M., & Walter, M. T. (2018). Assessing the impact of urbanisation on direct runoff using improved composite CN method in a large urban area. *International Journal of Environmental Research and Public Health*, *15*(4), 1–14. https://doi.org/10.3390/ijerph15040775

Li, X., Suoerdahan, G., Shi, Z., Xing, Z., Ren, Y., & Yang, R. (2021). Spatial–temporal impacts of urban sprawl on ecosystem services: Implications for urban planning in the process of rapid urbanisation. *Land*, *10*(11), 1–17. https://doi.org/10.3390/land10111210

Li, & Zhao. (2019). Investigating the Spatiotemporally Varying Correlation between Urban Spatial Patterns and Ecosystem Services: A Case Study of Nansihu Lake Basin, China. *ISPRS International Journal of Geo-Information*, *8*(8), 346. https://doi.org/10.3390/ijgi8080346

Long, H., Tang, G., Li, X., Heilig, G. K. (2007). Socio-economic driving forces of land-use change in Kunshan, the Yangtze River Delta economic area of China. Environmental Management, 83, 351–364. https://doi.org/10.1016/j.jenvman.2006.04.003

Li, M., Cao, Y., Dai, J., Song, J., Liang, M. (2025). A Comprehensive Review of Urban Expansion and Its Driving Factors. *Land*, 14(8), 1534. https://doi.org/10.3390/land14081534

Lonsdorf, E. V., Nootenboom, C., Janke, B., & Horgan, B. P. (2021). Assessing urban ecosystem services provided by green infrastructure: Golf courses in the Minneapolis-St. Paul metro area. *Landscape and Urban Planning*, *208*, 104022. https://doi.org/10.1016/j.landurbplan.2020.104022

Loukika, K. N., Keesara, V. R., & Sridhar, V. (2021). Analysis of land use and land cover using machine learning algorithms on google earth engine for Munneru river basin, India. *Sustainability*, *13*(24), 13758. https://doi.org/10.3390/su132413758

Luo, Z., & Yang, X. (2024). Interrelationships between Urbanisation and Ecosystem Services in the Urban Agglomeration around Poyang Lake and Its Zoning Management at an Integrated Multi-Scale. *Sustainability*, *16*(12), 5128. https://doi.org/10.3390/su16125128

Macdicken, K. G. (1997). *A Guide to Monitoring Carbon Storage in Forestry and Agroforestry Projects*. Winrock International Institute for Agricultural Development, Forest Carbon Monitoring Program.

Malligai, M. A., & Jegankumar, R. (2018). Mapping Urban Sprawl and Measuring Urban Density using Shannon Entropy: A Case Study of Salem City and its Environ. *International Journal of Science and Research (IJSR)*, *7*(4), 1436-1440. doi: 10.21275/ART20181976

Manzanas, R., Amekudzi, L. K., Preko, K., Herrera, S., & Gutiérrez, J. M. (2014). Precipitation variability and trends in Ghana: An intercomparison of observational and reanalysis products. *Climatic Change*, *124*(4), 805–819. https://doi.org/10.1007/s10584-014-1100-9

Maxwell, A. E., Strager, M. P., Warner, T. A., Ramezan, C. A., Morgan, A. N., & Pauley, C. E. (2019). Large-Area, High Spatial Resolution Land Cover Mapping Using Random Forests, GEOBIA and NAIP Orthophotography: Findings and Recommendations. *Remote Sensing*, *11*(12), 1409. https://doi.org/10.3390/rs11121409

MEA. (2005). *Ecosystems and human well-being: Synthesis report*. Island Press, Washington, DC.

Millard, K., & Richardson, M. (2015). On the Importance of Training Data Sample Selection in Random Forest Image Classification: A Case Study in Peatland Ecosystem Mapping. *Remote Sensensing*, *7*, 8489–8515. https://doi.org/10.3390/rs70708489

MoFA. (2018). Agriculture in Ghana. In Facts and Figures. Ministry of Food and Agriculture. Retrieved from https://mofa.gov.gh/site/images/pdf/AGRIC%20IN%20GHANA%20F&F_2018.pdf, 21st February 2024.

Moisa, M. B., & Gemeda, D. O. (2021). Analysis of urban expansion and land use/land cover changes using geospatial techniques: a case of Addis Ababa City, Ethiopia. *Applied Geomatics*, *13*(4), 853–861. https://doi.org/10.1007/s12518-021-00397-w

Mosammam, M. H., Nia, J. T., Khani, H., Teymouri, A., & Kazemi, M. (2016). Monitoring land use change and measuring urban sprawl based on its spatials forms. The case of Qom City. *The Egyptian Journal of Remote Sensing and Space Sciences*, *20*(1), 103–116. https://doi.org/10.1016/j.ejrs.2016.08.002

Muchelo, R. O., Bishop, T. F. A., Ugbaje, S. U., & Akpa, S. I. C. (2024). Patterns of Urban Sprawl and Agricultural Land Loss in Sub-Saharan Africa: The Cases of the Ugandan Cities of Kampala and Mbarara. *Land*, *13*(7), 1056. https://doi.org/10.3390/land13071056

Mukhopadhyay, A., Hati, J. P., Acharyya, R., Pal, I., Tuladhar, N., & Habel, M. (2024). Global trends in using the InVEST model suite and related research: A systematic review. *Ecohydrology and Hydrobiology*, 25(2), 389-405. https://doi.org/10.1016/j.ecohyd.2024.06.002

Nasiri, V., Deljouei, A., Moradi, F., Sadeghi, S., & Borz, S. (2022). Land Use and Land Cover Mapping Using Sentinel-2 , Landsat-8 Two Composition Methods. *Remote Sensing*, *14*(9), 1977. https://doi.org/10.3390/rs14091977

Natural Capital Project. (2023). *InVEST software*. https://naturalcapitalproject.stanford.edu/software/invest

Norouzi, Y. (2023). Measuring Land Use Changes and Quantifying Urban Expansion Using Remote Sensing and Gis Techniques - a Case Study of Qom. *ISPRS Annals of the Photogrammetry, Remote Sensing and Spatial Information Sciences*, 10, 609–615. https://doi.org/10.5194/isprs-annals-X-4-W1-2022-609-2023

Obeng-Odoom, F. (2011). The informal sector in Ghana under siege. *Journal of Developing Societies*, *27*(3–4), 355–392. https://doi.org/10.1177/0169796X1102700406

Okyere, C. Y., Yacouba, Y., & Gilgenbach, D. (2012). The problem of annual occurrences of floods in Accra: An integration of hydrological, economic and political perspectives. *Theoretical and Empirical Researches in Urban Management*, 8(2), 45–79. https://www.zef.de/fileadmin/downloads/forum/docprog/Termpapers/2012_2_Gilgenbach_Okyere_Yacouba.pdf

Olofsson, P., Foody, G. M., Herold, M., Stehman, S. V., Woodcock, C. E., & M.A. Wulder. (2014). Good practices for estimating area and assessing accuracy of land change. *Remote Sensing of Environment, 148*, 42–57.

https://doi.org/10.1016/j.rse.2014.02.015

Ortega-Montoya, C. Y., & Johari, A. (2008). Urban ecological footprints in Africa. *African Journal of Ecology*, *46*(4), 463–470. https://doi.org/10.1111/j.13652028.2008.01041.x

Osei, F. E., Olutayo Balogun, B., & Afrifa, G. (2013). Identifying and Quantifying Urban Sprawl in the Greater Accra Region of Ghana from 1985 to 2014. *International*

Journal of Science and Research (IJSR) 4(1), 2793–2798.

Owoade, F. M., Adiku, S. G. K., Atkinson, C. J., Maccarthy, D. S., Kumahor, S. K., & Kolawole, G. O. (2020). Location and land use effects on soil carbon accretion and productivity in the coastal savanna agro-ecological zone of Ghana. *West African Journal of Applied Ecology*, *28*(2), 1–13.

Owusu-Ansah, J. K., Dery, J. M., & Amoako, C. (2019). Flood vulnerability and coping mechanisms around the Weija Dam near Accra, Ghana. *GeoJournal*, *84*(6), 1597–1615. https://doi.org/10.1007/s10708-018-9939-3

Owusu, G. (2013). Coping with Urban Sprawl: A Critical Discussion of the Urban Containment Strategy in a Developing Country City, Accra. *The Journal of Urbanism*, *26(1)*, 1-17. http://ugspace.ug.edu.gh/handle/123456789/6236

Owusu, K., & Obour, P. B. (2021). Urban Flooding, Adaptation Strategies, and Resilience: Case Study of Accra, Ghana. *African Handbook of Climate Change Adaptation*, 2387–2403. https://doi.org/10.1007/978-3-030-45106-6_249

Pandey, B., & Ghosh, A. (2023). Urban ecosystem services and climate change: a dynamic interplay. *Frontiers in Sustainable Cities*, *5*, 1–34. https://doi.org/10.3389/frsc.2023.1281430

Patra, S., Sahoo, S., Mishra, P., & Mahapatra, S. (2018). Impacts of urbanisation on land use/cover changes and its probable implications on local climate and groundwater level. *Journal of Urban Management*, *7* (2), 70–84. https://doi.org/10.1016/j.jum.2018.04.006

Polorigni, B., Adjonou, K., Radji, R. A., & Kokou, K. (2018). Planning and development of towns in Togo : mapping of the Thermal status of Lomé and the formation of urban heat island. *International Research Journal of Earth Sciences*, *6*(1), 12–19.

Puplampu, D. A., & Boafo, Y. A. (2021). Exploring the impacts of urban expansion on green spaces availability and delivery of ecosystem services in the Accra Metropolis. *Environmental Challenges*, 5, 100283. https://doi.org/10.1016/j.envc.2021.100283

Qian, Y., & Wu, Z. (2019). Study on urban expansion using the spatial and temporal dynamic changes in the impervious surface in Nanjing. *Sustainability*, *11*(3), 933. https://doi.org/10.3390/su11030933

Rahaman, Z. A., Kafy, A. Al, Saha, M., Rahim, A. A., Almulhim, A. I., Rahaman, S. N., Fattah, M. A., Rahman, M. T., S, K., Faisal, A. Al, & Al Rakib, A. (2022). Assessing the impacts of vegetation cover loss on surface temperature, urban heat island and carbon emission in Penang City, Malaysia. *Building and Environment*, *222*, 109335. https://doi.org/10.1016/j.buildenv.2022.109335

Rahman, M. T. (2016). Land use and land cover changes and urban sprawl in riyadh , saudi arabia : an analysis using multi-temporal landsat data and shannon ' s entropy index. *The International Archives of the Photogrammetry, Remote Sensing and Spatial Information Sciences*, XLI-B8, 1017–1021, https://doi.org/10.5194/isprs-archives-XLI-B8-1017-2016, 2016.

Rezaeia, A. R., Ismail, Z. B. & Niksok, M. H. (2019), Investigating the effective factors influencing surface runoff generation in urban catchments – A review. *Desalination and Water Treatment* 164, 276–292. https://doi.org/10.5004/dwt.2019.24359

Rijal, S., Rimal, B., Stork, N. & Sharma, P. H. (2020). Quantifying the drivers of urban expansion in Nepal. *Environonmental Monitoring Assessment* 192, 633. https://doi.org/10.1007/s10661-020-08544-3

Ross, C. W., Prihodko, L., Anchang, J. ., Kumar, S. ., Ji, W., & Hanan, N. . (2018). Global Hydrologic Soil Groups (HYSOGs250m) for Curve Number-Based Runoff Modeling. *Earth Data*, *571*(82448 MB), 1–4. Doi: 10.3334/ORNLDAAC/1566

Rudiastuti, A., Farda, N. M., & Ramdani, D. (2021). Mapping built-up land and settlements: A comparison of machine learning algorithms in Google Earth Engine. *In Proceedings of SPIE*, 12082, 47. https://doi.org/10.1117/12.2619493

Saengprachatanarug, K., Chea, C., Posom, J., Saikaew, K. (2022). A Review on Innovation of Remote Sensing Technology Based on Unmanned Aerial Vehicle for Sugarcane Production in Tropical Region. In: Ahamed, T. (eds), *Remote Sensing Application (*New Frontiers in Regional Science: Asian Perspectives, vol 59). Springer, Singapore. https://doi.org/10.1007/978-981-19-0213-0_12

Salam, R. D., Oluwatimilehin, I. A., & Ayanlade, A. (2023). Spatial analysis of urban expansion, land-use dynamics and its effects on land surface temperature in Oyo town, Southwestern Nigeria. *City and Built Environment*, *1*(1), 1–18. https://doi.org/10.1007/s44213-023-00017-w

Schatz, J., & Kucharik, C. J. (2014). Seasonality of the urban heat island effect in Madison, Wisconsin. *Journal of Applied Meteorology and Climatology*, *53*(10), 2371–2386. https://doi.org/10.1175/JAMC-D-14-0107.1

Schlüter, T. (2006). *Geological atlas of Africa: With notes on stratigraphy, tectonics, economic geology, geohazards and geosites of each country* (with contributions by M. H. Trauth). Berlin; New York: Springer.

Selmi, W., Selmi, S., Teller, J., Weber, C., Rivière, E., & Nowak, D. J. (2021). Prioritizing the provision of urban ecosystem services in deprived areas, a question of environmental justice. *Ambio*, *50*(5), 1035–1046. https://doi.org/10.1007/s13280-020-01438-1

Seto, C. K., Fragkias, M., Guneralp, B., & Reilly, M. K. (2011). A Meta-Analysis of Global Urban Land Expansion Karen. *PloS One*, *6*(8), 1–9. https://doi.org/10.1371/journal.pone.0023777

Seto, K. C., Güneralp, B., & Hutyra, L. R. (2012). Global forecasts of urban expansion to 2030 and direct impacts on biodiversity and carbon pools. *Sustainability Science,* 109(40), 16083–16088. https://doi.org/10.1073/pnas.1211658109

Sharma, S., Hussain, S., & Singh, A. N. (2023). Impact of land use and land cover on urban ecosystem service value in Chandigarh, India: a GIS-based analysis. *Journal* *of Urban Ecology*, *9*(1), 1–12. https://doi.org/10.1093/jue/juac030

Sharp, R., Chaplin-Kramer, R., Wood, S. A., & Guerry, A. (2018). *InVEST 3.7 User's Guide*. The Natural Capital Project, Stanford University, University of Minnesota, The Nature Conservancy, and World Wildlife Fund. https://doi.org/10.6084/m9.figshare.7302760.v4

Sharp, R., Tallis, H. T., Ricketts, T., Guerry, A. D., Wood, S. A., Chaplin-Kramer, R., E., N., Ennaanay, D., Wolny, S., Olwero, N., & Vigerstol, K. (2014). *InVEST user's guide.* The Natural Capital Project, Stanford, CA. Retrieved from https://naturalcapitalproject.stanford.edu/software/invest/

Shao, Y., Yuan X., Ma C., Ma R. & Ren Z. (2020). Quantifying the Spatial Association between Land Use Change and Ecosystem Services Value: A Case Study in Xi'an, China. *Sustainability*, 12, 4449, 1-20. https://doi.org/10.3390/su12114449

Sinha, S. K. (2018). Characteristics of urban sprawl: a cross-cultural analysis. *UGC Approved Journal*, *7*(11), 1–6.

Solarin, S. A., Tiwari, A., & Bello, M. O. (2019). A multi-country convergence analysis of ecological footprint and its components Sakiru. *Sustainable Cities and Society*, 46, 101422. https://doi.org/10.1016/j.scs.2019.101422

Somadjago, M., Cissokho, D., & Suka, D. K. (2020). Mutations socio-écon514omiques et demographiques des espaces ruraux phagocytés par la ville de LOMÉ. *Revue Espace Geographique et Societe Marocaine*, *36*, 27–43.

Song, X., Liu, Y., Zhu, X., Cao, G., Chen, Y., Zhang, Z., & Wu, D. (2022). The impacts of urban land expansion on ecosystem services in Wuhan, China. *Environmental Science and Pollution Research*, *29*(7), 10635–10648. https://doi.org/10.1007/s11356-021-16419-4

Sorsy, L. M., Dandonougbo, I., & Hetcheli, F. (2023). La dynamique urbaine entre fragmentation spatiale et disparité sociale, Une analyse de la périurbanisation dans les communes Nord-Ouest du Grand-Lomé. *Revue Espace Geographique et Societe Marocaine*, (*73–74)*, 31. https://doi.org/10.34874/IMIST.PRSM/EGSM/41682

Stemn, E., St, E., & Agyapong, E. (2014). Assessment of Urban Expansion in the Sekondi-Takoradi Metropolis of Ghana Using Remote-Sensing and GIS Approach Related papers Effect of Urban Growt on Urban T hermal Environment : A Case St udy of Sekondi-Takoradi M… Assessment of Urban Expansion in th. *International Journal of Science and Technology*, *3*(8), 452-460.

Sun, X., Crittenden, J. C., Li, F., Lu, Z., & Dou, X. (2018). Urban expansion simulation and the spatio-temporal changes of ecosystem services, a case study in Atlanta Metropolitan area, USA. *Science of the Total Environment*, *622–623*, 974–987. https://doi.org/10.1016/j.scitotenv.2017.12.062

Sylla, O. (2021). *Strengthen UN-Habitat Regional Representation in Sub-Saharan Africa (pp. 1–11)*. United Nations Human Settlements. Programme. https://unhabitat.org/strengthen-un-habitat-regional-representation-in-sub-saharan-africa

Tadese, S., Soromessa, T., Aneseye, A. B., Gebeyehu, G., Noszczyk, T., & Kindu, M. (2023). The impact of land cover change on the carbon stock of moist afromontane forests in the Majang Forest Biosphere Reserve. *Carbon Balance and Management*, *18*(1), 1–20. https://doi.org/10.1186/s13021-023-00243-z

Takili, M., Danvide, T. B., & Banon, F. (2020). Adétikopé , un pôle urbain émergent à Lomé : entre dynamisme de la migration résidentielle et de la masse urbaine. *REGARDSUDS*, *1*. Derived from https://regardsuds.org/adetikope-un-pole-urbain-emergent-a-lome-entre-dynamisme-de-la-migration-residentielle-et-de-la-masse-urbaine/

Tamiminia, H., Salehi, B., Mahdianpari, M., Quackenbush, L., Adeli, S., & Brisco, B. (2020). Google Earth Engine for geo-big data applications: A meta-analysis and systematic review. *ISPRS Journal of Photogrammetry and Remote Sensing*, *164*(January), 152–170. https://doi.org/10.1016/j.isprsjprs.2020.04.001

Tessema, W. M., & Abebe, G. B. (2023). Quantification of land use/land cover dynamics and urban growth in rapidly urbanised countries: The case Hawassa City, Ethiopia. *Urban, Planning and Transport Research*, *11*(1). https://doi.org/10.1080/21650020.2023.2281989

Tobias, S. (2013), Preserving Ecosystem Services in Urban Regions: Challenges for Planning and Best Practice Examples from Switzerland. *Integrated Environmental Assessment and Management*, 9, 243–251. https://doi.org/10.1002/ieam.1392

Toure, S. I., Stow, D. A., Clarke, K., & Weeks, J., (2020). Patterns of land cover and land use change within the two major metropolitan areas of Ghana. *Geocarto International,* 35:2*,* 209-223. https://doi.org/10.1080/10106049.2018.1516244

Wang, Y., P., & Kintrea, K. (2021). Urban Expansion and Land Use Changes in Asia and Africa. *Environment and Urbanization ASIA*. *Sage*, *12*(1_suppl), S13-S17. https://doi.org/10.1177/0975425321999081

Wang, K., Gao, J., Liu, C., Zhang, Y., & Wang, C. (2024). Understanding the effects of socio-ecological factors on trade-offs and synergies among ecosystem services to support urban sustainable management: A case study of Beijing, China. *Sustainable Cities and Society*, *100*, 105024. https://doi.org/10.1016/j.scs.2023.105024

Wemegah, C. S., Yamba, E. I., Aryee, J. N. A., Sam, F., & Amekudzi, L. K. (2020). Assessment of urban heat island warming in the greater accra region. *Scientific African*, 8, e00426. https://doi.org/10.1016/j.sciaf.2020.e00426

Wiafe, E. D., & Asamoah, G. (2018). Land-cover change assessment in Ejisu-Juabeng district in Ghana. *Euraian Journal of Forest Science*, *6*(1), 1–8. https://doi.org/10.31195/ejejfs.429741

World Bank. (2018). *Global Platform for Sustainable Cities, Urban Sustainability Framework (1st ed.).* Washington, DC: World Bank. https://hdl.handle.net/10986/29364

Wu, T., Wang, Z., & Xu, Q. (2024). Spatio-Temporal Heterogeneity of the Urban Heat Effect and Its Socio-Ecological Drivers in Yangzhou City, China. *Land*, *13*(1470), 16. https://doi.org/10.3390/land13091470

Xu, G., Dong, T., Cobbinah, P. B., Jiao, L., Sumari, N. S., Chai, B., & Liu, Y. (2019). Urban expansion and form Changes across African cities with a Global Outlook: Spatiotemporal Analysis of Urban Land Densities. *Journal of Cleaner Production*, 224, 802-810. https://doi.org/10.1016/j.jclepro.2019.03.276

Yang, C., Wu, G., Ding, K., Shi, T., Li, Q., & Wang, J. (2017). Improving land use/land cover classification by integrating pixel unmixing and decision tree methods. *Remote Sensing*, *9*(12), 220-230. https://doi.org/10.3390/rs9121222

Yao, X., Wang, Z., & Zhang, H. (2016). Dynamic changes of the ecological footprint and its component analysis response to land use in Wuhan, China. *Sustainability (Switzerland)*, *8*(4), 1-14. https://doi.org/10.3390/su8040329

Yi, J., Dai, S., Cheng, J., & Liu, K. (2023). How urban sprawl affects local and nearby ecosystem services in China. *Regional Environmental Change*, *23*(4). https://doi.org/10.1007/s10113-023-02124-0

Yuan, Y., Chen, D., Wu, S., Mo, L., Tong, G., & Yan, D. (2019). Urban sprawl decreases the value of ecosystem services and intensifies the supply scarcity of ecosystem services in China. *Science of the Total Environment*, 697, 1-10. https://doi.org/10.1016/j.scitotenv.2019.134170

Yuan, S., Zhu, C., Yang, L. & Xie, F., Responses of Ecosystem Services to Urbanization-Induced Land Use Changes in Ecologically Sensitive Suburban Areas in Hangzhou, China. (2019), *International Journal of Environmental Research and Public Health*, 16(7), 1124. https://doi.org/10.3390/ijerph16071124

Yushanjiang, A., Zhou, W., Wang, J., & Wang, J. (2024). Impact of urbanisation on regional ecosystem services: a case study in Guangdong-Hong Kong-Macao Greater Bay Area. *Ecological Indicators*, *159*(1), 1–14. https://doi.org/10.3390/f16010017

Yussif, K., Dompreh, E., B. & Gasparatos, A. Sustainability of urban expansion in Africa: a systematic literature review using the Drivers–Pressures–State–Impact–Responses (DPSIR) framework. (2023). *Sustainability Science,* 18, 1459–1479. https://doi.org/10.1007/s11625-022-01260-6

Zaki, M. N. A., & Abd Latif, Z. (2016). Carbon sinks and tropical forest biomass estimation: a review on role of remote sensing in aboveground-biomass modelling. *Geocarto International*, *32*(7), 701–716. https://doi.org/10.1080/10106049.2016.1178814

Zardo, L., Geneletti, D., Pérez-Soba, M., & Van Eupen, M. (2017). Estimating the cooling capacity of green infrastructures to support urban planning. *Ecosystem Services*, *26*, 225–235. https://doi.org/10.1016/j.ecoser.2017.06.016

Zhai, T., Zhang, D., & Zhao, C. (2021). How to optimize ecological compensation to alleviate environmental injustice in different cities in the Yellow River Basin? A case of integrating ecosystem service supply, demand and flow. *Sustainable Cities and Society*, *75*, 1-13. https://doi.org/10.1016/j.scs.2021.103341

Zhang, Y., Liu Y., Pan J., Zhang Y., Liu D., Wei J., Zhang Z. & Liu Y. (2020). Exploring Spatially Non-Stationary and Scale-Dependent Responses of Ecosystem Services to Urbanization in Wuhan, China. *International Journal of Environmental Research and Public Health*, 17, 2989, 1-23. doi:10.3390/ijerph17092989

Zhu, C., Zhang, X., Zhou, M., He, S., Gan, M., Yang, L., & Wang, K. (2020), Impacts of urbanisation and landscape pattern on habitat quality using OLS and GWR models in Hangzhou, China, *Ecological Indicators*, 117, 106654.

https://doi.org/10.1016/j.ecolind.2020.106654

APPENDICES

Appendix A: Ecosystem services models

Models	Bref description	Advantages	Disadvantages
Artificial Intelligence for Ecosystem Services (ARIES)	Open-source modelling framework to map ecosystem service flows; online interface and stand-alone web tools under development	Useful to quantify flows of the services to beneficiaries. Models incorporate an uncertainty measure in its estimates done through Bayesian networks and Monte Carlo simulation	Time consuming models requiring technically specialised skills. Models have a low level of generalisation (specific application at particular social-ecological contexts)
Multiscale Integrated Models of Ecosystem Services (MIMES)	Open-source dynamic modelling system for mapping and valuing ecosystem services	Integrated dynamic sand interactions among services. Values emerge from trade-offs and impacts on human well-being. Incorporate an uncertainty measure in its estimates	Time consuming models requiring technically specialised skills. Models have a low level of generalization
Social Values for Ecosystem Services (SolVES)	ArcGIS toolbar for mapping social values for ecosystem services based on survey data or value transfer	SolVES allows for the integration of spatial and nonspatial data to provide a holistic view of social values. The model incorporates public preferences It generates intuitive maps that illustrate the distribution of social values.	Data Dependency, Social values are inherently subjective, making it difficult to quantify them consistently across different contexts.
Co$tingNature	Web-accessible tool to map ecosystem services and conservation priority areas	Rapid analysis of indexed, bundled services based on global data, along with conservation priority maps. Models have a high level of generalisation	Models require high resolution biophysical and socio-economic data that is only available in few countries
The Ecosystem Service Trade-off Analysis (ESTA)	Framework including GIS tools and modelling techniques that are often available in open-source	Models developed using best available data for a region. Include direct and indirect interactions among services. Any number of services can be assessed simultaneously	Time consuming models requiring technically specialised skills and data-rich contexts

Appendix B: Ecosystem services models "continuation"

Models	Bref description	Advantages	Disadvantages
EcoServ	Geographic Information System (GIS) application designed for mapping ecosystem services at country or regional scales.	Provides detailed maps that illustrate the distribution of ecosystem services The model allows for the evaluation of multiple ecosystem services simultaneously	The model requires extensive spatial datasets It does not quantify the actual impact or value of each ecosystem service, The effectiveness of the model may vary depending on the spatial scale of application
Benefit Transfer and Use Estimating Model Toolkit	cost-benefit analyses, damage assessments, and regulatory impact evaluations	Saves time and resources by utilising existing data instead of conducting new valuation studies. It allows for rapid assessments of ecosystem service values The model can be adapted to various contexts and types of ecosystem services, making it versatile for different applications.	Accuracy Concerns, the validity of transferred values can be questionable if the study and policy sites differ significantly in ecological, social, or economic characteristics. Reliance on existing studies may lead to gaps in data or biases if the original studies are not representative of the new context.

Appendix C: Maps with ground truth for LULC classification

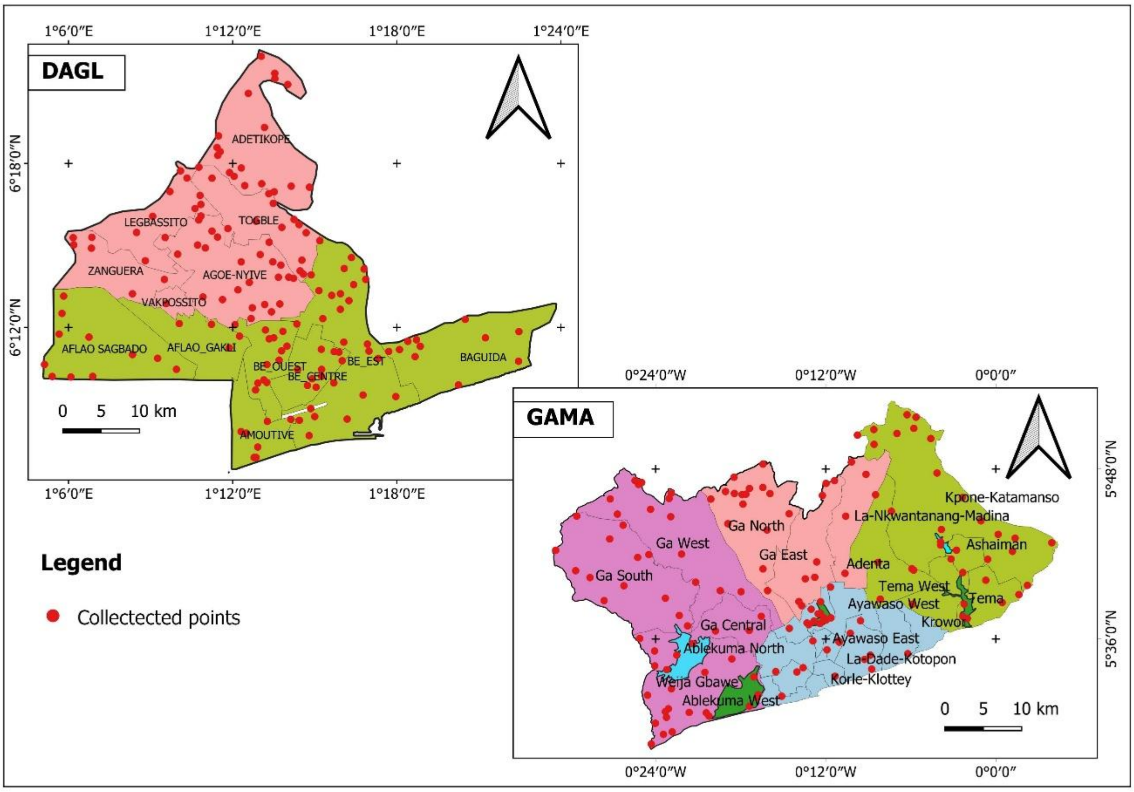

(a): Spatial locations for the reference data collection of DAGL and GAMA

Appendix D: The biophysical parameters used for the InVEST urban cooling model

lucode	LULC_name	green_area	Kc	shade	albedo
1	Water_bodies	1	1	0.1	0.1
2	Built-up/Bareland	0	0.3	0.2	0.15
3	Forest	1	1	0.9	0.3
4	Grassland	1	0.65	0.5	0.2
5	Agriculture	1	0.6	0.3	0.2

Appendix E: Additional parameters submitted to the InVEST Urban cooling model for DAGL

Parameter	Value	Reference
Reference air temperature	27 º C	Togolese Meteorological office
Magnitude of the UHI effect	3.12 º C	Global surface UHI explorer
Air blending distance	500 m	Model recommended value range from 500 m to 600 m
Maximum cooling distance	450 m	Model recommended value

Appendix F: Additional parameters submitted to the InVEST Urban cooling model for GAMA

Parameter	Value	Reference
Reference air temperature	26.8 º C	Ghana Meteorological Agency
Magnitude of the UHI effect	3.50 º C	Global surface UHI explorer
Air blending distance	500 m	Model recommended value range from 500 m to 600 m
Maximum cooling distance	450 m	Model recommended value

Appendix G: Curve numbers for a combination of LULC types and Hydrological soil group used in InVEST urban flood mitigation model.

LULC	Curve numbers for hydrological soil group			
	CN_A	CN_B	CN_C	CN_D
Forest	36	60	73	70
Grassland	49	69	79	84
Agricultural land	64	75	82	85
Water bodies	0	0	0	0
Built-up/bare-land	77	85	90	92

Appendix H: User, producer accuracies, commission and omission errors for the different classified images for DAGL

(a) Year 1986

	Frs	**Gras**	**Agric**	**Water**	**Blt/Brl**	**Total**	**CE**	**UA**
Frs	600	40	20	0	15	675	0.11	0.89
Gras	20	420	28	0	5	473	0.11	0.89
Agric	15	20	420	0	5	460	0.09	0.91
Water	0	0	0	90	0	90	0	1.00
Blt/Brl	0	5	10	0	140	155	0.10	0.90
Total	635	485	478	90	165	1853		
OE	0.06	0.13	0.12	0	0.15			
PA	0.94	0.87	0.88	1	0.85			

Blt/Brl Built-up/Bare-land, **Frs** Forest, **Gras** Grassland, **Agric** Agriculture land, **CE** commission errors, **OE** omission errors, **UA** user's accuracy, **PA** producer's accuracy

(b) Year 2001

	Frs	**Gras**	**Agric**	**Water**	**Blt/Brl**	**Total**	**CE**	**UA**
Frs	300	25	15	0	0	340	0.12	0.88
Gras	26	500	20	0	0	546	0.08	0.92
Agric	20	35	530	0	10	595	0.11	0.89
Water	1	0	0	80	2	83	0.02	0.96
Blt/Brl	0	9	10	0	420	439	0.02	0.96
Total	347	569	575	80	432	2003		
OE	0.14	0.11	0.08	0	0.03			
PA	0.86	0.88	0.92	1	0.97			

Blt/Brl Built-up/Bare-land, **Frs** Forest, **Gras** Grassland, **Agric** Agriculture land, **CE** commission errors, **OE** omission errors, **UA** user's accuracy, **PA** producer's accuracy

(c) Year 2015

	Frs	**Gras**	**Agric**	**Water**	**Blt/Brl**	**Total**	**CE**	**UA**
Frs	201	10	10	0	0	221	0.09	0.91
Gras	24	340	10	0	0	374	0.06	0.91
Agric	9	35	564	0	3	611	0.077	0.92
Water	0	0	0	75	2	77	0	0.97
Blt/Brl	0	10	5	0	650	665	0.008	0.98
Total	234	395	589	75	655	1948		
OE	0.14	0.11	0.025	0	0.005			
PA	0.86	0.86	0.96	1	0.99			

Blt/Brl Built-up/Bare-land, **Frs** Forest, **Gras** Grassland, **Agric** Agriculture land, **CE** commission errors, **OE** omission errors, **UA** user's accuracy, **PA** producer's accuracy

(d) Year 2023

	Frs	Gras	Agric	Water	Blt/Brl	Total	CE	UA
Frs	180	9	6	0	0	195	0.077	0.92
Gras	7	220	12	0	0	239	0.079	0.92
Agric	5	13	400	0	1	419	0.045	0.95
Water	1	0	0	75	0	76	0.013	0.98
Blt/Brl	0	15	10	0	840	865	0.029	0.97
Total	193	257	428	75	841	1794		
OE	0.067	0.14	0.065	0	0.001			
PA	0.93	0.86	0.93	1	1			

Blt/Brl Built-up/Bare-land, **Frs** Forest, **Gras** Grassland, **Agric** Agriculture land, **CE** commission errors, **OE** omission errors, **UA** user's accuracy, **PA** producer's accuracy

Appendix I: User, producer accuracies, commission and omission errors for the different classified images for GAMA

(a) Year 1991

	Frs	Gras	Agric	Water	Blt/Brl	Total	CE	UA
Frs	140	0	2	0	0	142	0	0.99
Gras	0	364	0	10	14	388	0.06	0.94
Agric	0	1	710	60	10	781	0.09	0.91
Water	0	10	55	962	41	1068	0.10	0.90
Blt/Brl	0	7	15	36	583	641	0.09	0.91
Total	140	382	782	1068	648	3020		
OE	0	0.05	0.09	0.10	0.10			
PA	1	0.95	0.91	0.90	0.90			

Blt/Brl Built-up/Bare-land, **Frs** Forest, **Gras** Grassland, **Agric** Agriculture land, **CE** commission errors, **OE** omission errors, **UA** user's accuracy, **PA** producer's accuracy

(b) Year 2002

	Frs	Gras	Agric	Water	Blt/Brl	Total	CE	UA
Frs	160	2	1	0	0	163	0.01	0.98
Gras	0	723	0	9	10	742	0.01	0.97
Agric	0	0	560	30	15	605	0.07	0.93
Water	0	0	24	780	12	816	0.04	0.96
Blt/Brl	0	5	20	35	960	1020	0.06	0.94
Total	160	730	605	854	997	3346		
OE	0	0.01	0.07	0.08	0.04			
PA	1	0.99	0.93	0.91	0.96			

Blt/Brl Built-up/Bare-land, **Frs** Forest, **Gras** Grassland, **Agric** Agriculture land, **CE** commission errors, **OE** omission errors, **UA** user's accuracy, **PA** producer's accuracy

(c) Year 2017

	Frs	Gras	Agric	Water	Blt/Brl	Total	CE	UA
Frs	150	0	1	0	0	150	0	1
Gras	0	1090	0	10	5	1105	0.005	0.99
Agric	0	0	349	10	5	364	0.041	0.96
Water	0	0	24	460	0	484	0.050	0.95
Blt/Brl	0	3	9	44	960	1016	0.055	0.94
Total	150	1093	382	524	970	3119		
OE	0	0.003	0.086	0.103	0.010			
PA	1	1	0.91	0.88	0.99			

Blt/Brl Built-up/Bare-land, **Frs** Forest, **Gras** Grassland, **Agric** Agriculture land, **CE** commission errors, **OE** omission errors, **UA** user's accuracy, **PA** producer's accuracy

(d) Year 2023

	Frs	Gras	Agric	Water	Blt/Brl	Total	CE	UA
Frs	141	0	1	0	0	142	0.007	0.99
Gras	0	1320	0	5	10	1335	0.011	0.99
Agric	0	0	339	9	6	254	0.059	0.94
Water	0	0	7	301	12	320	0.059	0.94
Blt/Brl	0	1	5	13	512	531	0.036	0.96
Total	141	1321	252	328	540	2582		
OE	0	0.001	0.052	0.082	0.052			
PA	1	1	0.95	0.92	0.95			

Blt/Brl Built-up/Bare-land, **Frs** Forest, **Gras** Grassland, **Agric** Agriculture land, **CE** commission errors, **OE** omission errors, **UA** user's accuracy, **PA** producer's accuracy